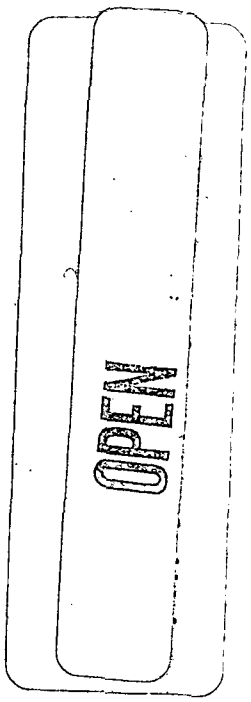

UNIVERSITY OF CALIFORNIA, BERKELEY

Department of Physics

Berkeley, California 94720

Final Report for

Contract NAS 9-9949
(August 1, 1969 to January 31, 1971)

ISOTOPIC STUDIES IN RETURNED LUNAR SAMPLES

by

E. C. Alexander, Jr.
Acting Principal Investigator
for J. H. Reynolds

W. A. Kaiser and R. S. Lewis
Co-Investigators

for

NATIONAL AERONAUTICS AND SPACE ADMINISTRATION
Manned Spacecraft Center
Lunar Receiving Laboratory
Houston, Texas

FINAL REPORT

Contract Bibliography

1. Isotopic Analysis of Rare Gases from Stepwise Heating of Lunar Fines and Rocks, J. H. Reynolds, C. M. Hohenberg, R. S. Lewis, P. K. Davis, and W. A. Kaiser, Science 167, 545-548 (1970).

2. Trapped and cosmogenic rare gases from Stepwise heating of Apollo 11 samples, C. M. Hohenberg, P. K. Davis, W. A. Kaiser, R. S. Lewis, and J. H. Reynolds, Proc. Apollo 11 Lunar Sci. Conf., Geochim. Cosmochim. Acta Suppl. 1, Vol. 2, pp 1283-1309. Pergamon (1970).

3. Rare Gases from Stepwise Heating of Lunar Rock 12013, E. C. Alexander, Jr., Earth Planet. Sci. Letters 9, 201-207 (1970).

4. Stepwise heating analyses of rare gases from pile-irradiated rocks 10044 and 10057, P. K. Davis, R. S. Lewis, and J. H. Reynolds, Proc. Second Lunar Sci. Conf., Geochim. Cosmochim. Acta Suppl. 2, Vol. 2, pp 1693-1704. M.I.T. Press (1971).

5. Rare gas measurements in three mineral separates of rock 12013,10,31, W. A. Kaiser, Proc. Second Lunar Sci. Conf., Geochim. Cosmochim. Acta Suppl. 2, Vol. 2, pp 1627-1642. M. I. T. Press (1971).

6. Spallogenic Ne, Kr, and Xe from a depth study of 12002, E. C. Alexander, Jr., Proc. Second Lunar Sci. Conf., Geochim. Cosmochim. Acta Suppl. 2, Vol. 2, pp 1643-1650. M.I.T. Press (1971).

Discussion of Results

We worked intensively during 1969-70 on lunar samples from the Apollo 11 and 12 missions. We received 11 samples of Apollo 11 material which included "fine fines," "coarse fines," rock chips and core samples totaling 30.8 grams. From Apollo 12 we received 14 samples totaling 24.4 grams. Apollo 12 samples were much better documented than samples from Apollo 11. In most if not all cases locations of our samples in the original Apollo 12 rocks were accurately specified. From at least one Apollo 12 rock we were furnished a vertically oriented slab so that depth studies could be carried out.

Paper 2 is our definitive initial report on the Apollo 11 studies; it supersedes paper 1 which was an abbreviated version prepared in great haste for the Apollo 11 conference in Houston. Isotopic studies of the rare gases from Apollo 11 samples were made by eleven groups representing five nations! There was consequently a great deal of overlap in the findings reported at Houston in January, 1970. So much so that we shall simply list here some of the more common findings in which we shared:

1. High concentrations of solar wind rare gases in the lunar soil.
2. A very good isotopic match between the solar wind gases from the moon and gas components, in certain gas-rich meteorites, which had previously been attributed to solar wind.
3. Rare gases attributable to spallation reactions induced in heavier target nuclides by cosmic ray particles. This spallation component is very marked in the crystalline lunar rocks, which are remarkably free from trapped rare gases; and much less conspicuous, although identifiable, in the soil samples.

4. General agreement, with some interesting exceptions, between the isotopic compositions of the spallation gases and those previously known from meteorites. The most interesting exception is a sometimes very striking enhancement of ^{131}Xe, which is inseparable from the spallation component but may result from resonance neutron capture on ^{130}Ba. The enhancement varies from one rock to another and is totally absent in some.
5. Surprisingly high ^{40}Ar concentrations in the lunar soil, evidently requiring that there be some mechanism for implanting in the soil radiogenic ^{40}Ar leaking out of the moon. Otherwise the lunar soil should contain mainly argon directly from the solar wind and much depleted in the 40 isotope.
6. Old but not meteoritic potassium-argon ages for the crystalline rocks. This is to say ages in excess of 3.5 billion years but still substantially less than 4.6 billion years.
7. Cosmic-ray exposure ages for the crystalline rocks, based on spallation ^{130}Xe contents and adjusted meteoritic production rates, which are generally of the order of 60 million years. These ages represent the integrated time which the sample has spent within about one meter of the lunar surface.
8. Absence of any xenon in the samples which could be attributed to decay of the extinct radioactivities ^{129}I and ^{244}Pu. This finding is thus far consistent with the absence of samples of meteoritic age.

We measured the rare gases from stepwise heating of the Apollo 11 rocks and fines, thereby obtaining some results which were unique or

at least reported less often. Among these results were:

1. The observation that for helium, neon, and argon the lower temperature fractions were enhanced in the light isotopes. The enhancement factor in the earliest temperature fractions in our work was very nearly equal to the reciprocals of the ratios of the atomic mass numbers. In our discussion we attributed this effect to two processes: (1) deeper burial of the light isotopes. (The solar wind impinges on the moon as a moving fluid; in such a case the depth of burial of isotopes will be proportional to atomic mass.) (2) more rapid diffusion of the lighter isotopes in the laboratory heating. Similar results were reported in the measurements made by Pepin and his co-workers at the University of Minnesota. They have recently proposed a different explanation, namely that a distinct component, less firmly imbedded, has resulted from implantation of rare gases from a very rarified lunar atmosphere under action of electric fields generated by the solar wind plasma. In this model the mass fractionation would be electromagnetic in origin. Such a model could also apply to certain of the gas-rich meteorites, where similar effects are seen and where the parent body would then have to be large enough for the same processes to occur. Neither our model nor the Minnesota one is presently proven in any sense.
2. By constructing correlation plots of isotope ratios we were able to show that xenon in our sample of Apollo 11 rock 57 consisted of three components: a trapped component, a spallogenic component inseparable from a high ^{131}Xe anomaly

(see above), and a fissiogenic component compatible with production by spontaneous fission of ^{238}U over the lifetime of the rock. The trapped xenon was presumably solar wind xenon from a surface patch or from lunar dust adhering to the sample. In our sample of Apollo 11 rock 44, the fissiogenic and spallogenic components (this time without a ^{131}Xe anomaly) were resolved but no trapped component was detected which could be said to be of lunar origin. Release curves with temperature of the various components of the rare gases in the lunar rocks and fines were published.

3. Radioactive ^{81}Kr was measurable by mass spectrometry in certain of the temperature fractions for the lunar rocks. Since the concentration of this 2×10^5 year isotope specifies its recent production rate on the lunar surface, the ratio of its abundance to a <u>stable</u> cosmogenic Kr isotope (e.g. ^{83}Kr) affords a precise determination of the cosmic-ray exposure age. For Apollo 11 rock 44 this age was 70 million years. Rock 44 could have had a simple history on the lunar surface: abrupt transfer from depth to its final surface location. Apollo 11 rock 57 has a Kr-Kr age of 34 million years, lower than its integrated cosmic-ray exposure age as determined from ^{130}Xe, implying a more complicated history. One can see from the interrelation of these various sorts of exposure ages how the beginnings of a "gardening history" for the lunar surface can be written. Kr-Kr ages are unusually helpful in this context.

4. Stepwise heating of the lunar fines also permitted us to identify and measure the concentration of the cosmogenic xenon in the lunar soil. The ^{130}Xe content of this soil corresponds to an exposure age of about 500 million years. The gardening effect, constantly turning over the lunar surface, would explain why this age is younger than the age of the Mare rocks.

Paper 3 describes our studies on Apollo 12 rock 13, a unique lunar rock of small size, very much enriched in the radioactive elements uranium, rubidium, and potassium. Initial measurements at Caltech of the strontium isotopic composition and rubidium content suggested that this rock might be of meteoritic age. An intense study of a 10-gram slice of the rock was collectively undertaken by a consortium of laboratories, ours included. Unfortunately as the work progressed it became evident that the rock retains a rare gas record of only 3.9 billion years. This time ago the rock was extensively recrystallized, so that in most senses 3.9 billion years is the "age" of the rock. Our study identified cosmogenic gases on the basis of which cosmic ray exposure ages (about 50 m.y.) were assigned. Radiogenic and fissiogenic gases are present in amounts consistent with the 3.9 billion year age. There appears to be some trapped xenon in rock 13. Unfortunately it is heavily masked by the cosmic-ray produced gases so that it is not possible to answer the important question of whether the trapped lunar xenon is meteoritic or terrestrial in isotopic composition. Such a determination may eventually throw light on the origin of the moon. Terrestrial xenon in lunar samples, for example, would give very strong support to theories of a terrestrial origin of the moon. There were no traces in rock 13 of xenon from the decay of extinct radionuclides.

Papers 4, 5 and 6 are the expanded versions of our report to the Apollo 12 Lunar Science Conference. Paper 4 describes our studies of neutron irradiated samples of 10044 and 10057. We obtained a ^{39}Ar-^{40}Ar age of 4.00 ± .07 x 10^9 years for 10044 and demonstrated that 10057 was not datable by the ^{39}Ar-^{40}Ar method. Auxiliary information in these experiments comes from study of the krypton and xenon released. For Apollo 11 rocks 44 and 57 we examined the heavier gases at each release temperature. Krypton in the irradiated samples is enriched in ^{80}Kr and ^{82}Kr from the (n,γ) reactions on bromine. It is also enriched in isotopes $^{83,84,85,86}Kr$ from neutron-induced fission of uranium. The krypton measurements thus yield the concentrations of bromine and uranium in sites in the lunar samples which are retentive for rare gases. The xenon measurements similarly furnish iodine, barium, and uranium concentrations. Coverage of the halogens in studies of the lunar rocks has been weak so that our results are important in fixing the contents of bromine and iodine in lunar rocks. These elements are of particular interest "geochemically" because of their volatility. Being able to differentiate between tightly and loosely bound bromine and iodine is a distinct advantage in the work.

In studying Apollo 11 rocks by this technique we noted that ^{131}Xe from the (n,γ) reaction on ^{130}Ba was more highly retained in rock 57 than in rock 44. Since the unexplained ^{131}Xe anomaly is high in rock 57 and low in rock 44 it may be that differences in the siting of barium in the two rocks is responsible for the difference in the 131 anomaly. What we are suggesting here is that ^{131}Xe is produced by resonance neutrons in the barium in all or most lunar rocks but that differences in xenon retentivity have led to differences in the magnitude of the effect as seen now in the laboratory.

A great deal of effort is going into our program for ^{39}Ar-^{40}Ar dating of lunar samples. After the two runs described above under paper 4, the "bottle" for heating the samples broke and imploded during outgassing. The system was badly overrun with molybdenum oxide as a result of this accident and required extensive repairs. Rather than run the risk of future accidents, we decided to upgrade the system by installing one of our newer systems, with a vapor-deposited tungsten crucible in a separately pumped bell-jar containing the RF coil. Outgassing from the exterior of the crucible no longer affects the sample in such systems so that we have lower blanks. And the system is highly secure against breakage: the walls of the bell jar are far removed from the heated tungsten. In the new system we have arranged valves so that the krypton and xenon can be accumulated as the temperature run proceeds and stored for total analysis after the argon measurements are over. With our newer irradiations in quartz break-off tubes we shall be able to measure as well the concentrations of lightly bound barium, bromine, iodine and uranium. While at it, we decided to renew the purification system and build a gas pipette for the system. All these improvements have consumed much time but we expect our efforts to pay off in the future.

Paper 5 describes our rare gas studies in some mineral separates from the unique Apollo 12 rock #13. We were able to separate visually three mineral fractions from a small sample of this rock and to measure all the rare gases in each fraction. From a series of control experiments on the same aluminum foil as used to wrap the samples we concluded that the mineral samples from rock #13 are essentially devoid of trapped gases. Radiogenic argon correlates as expected with the potassium content. The spallation xenon correlates well with the concentrations of

barium and other elements (rare earths) which can constitute nuclear targets for the component. In one fraction cosmogenic ^{126}Xe was, by calculation, 98.5% from Ba; in another, this percentage was 76. Thus we could make a good measurement of the cosmogenic Xe spectrum from Ba and a rough estimate of the spectrum from REE. The spectra were generally in agreement with published target data for 730 MeV protons.

Paper 6 describes a depth study for krypton and xenon in Apollo 12 rock #2. This rock has been studied by radiochemical and by nuclear track techniques and has been shown to have had a single orientation on the lunar surface. At the time we undertook this study it was still suspected that the 131 anomaly might be a surface effect i.e. that solar particles of short range in lunar material might be inducing special nuclear reactions leading to ^{131}Xe. Our results showed absolutely no depth effect in rock 12002. Samples from the top, middle, and bottom of the rock exhibited the same spectra for spallation krypton and xenon. We conclude that solar particles of short range have not played a significant role in generating krypton and xenon in this rock.

Reprinted from
30 January 1970, Volume 167, pp. 545-548

SCIENCE

Apollo 11 Lunar Science Conference

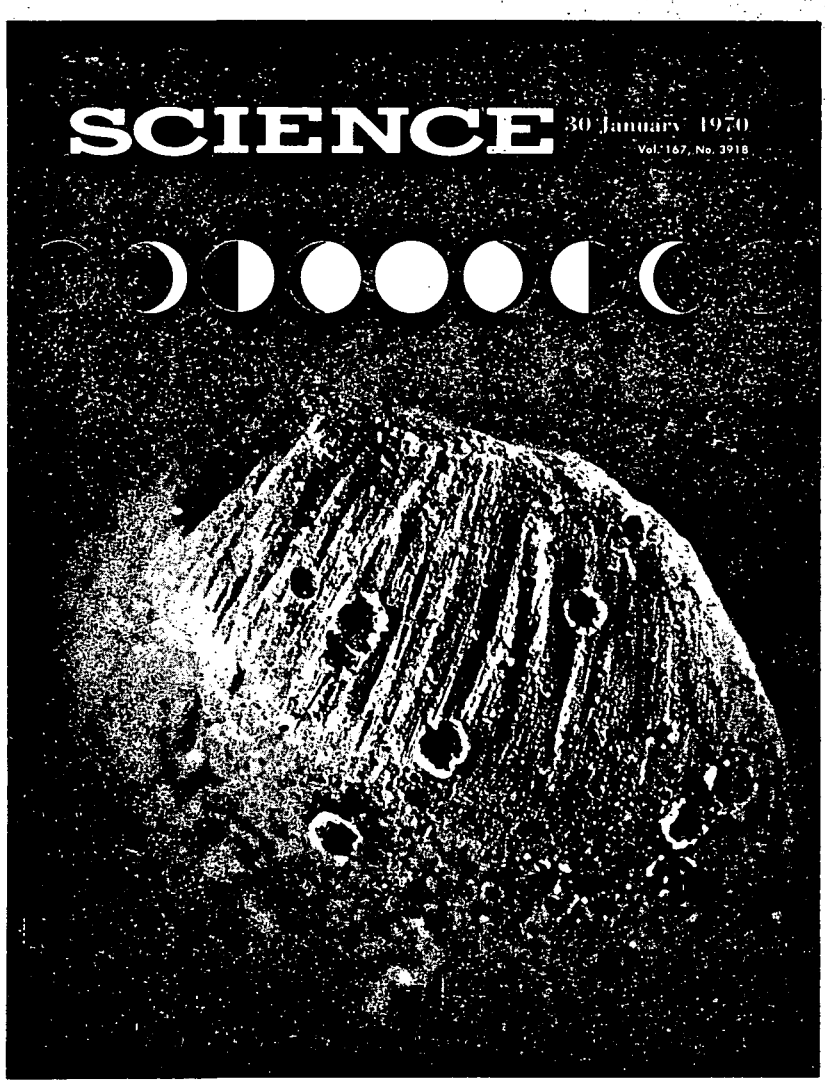

Isotopic Analysis of Rare Gases from Stepwise Heating of Lunar Fines and Rocks

J. H. Reynolds, C. M. Hohenberg, R. S. Lewis, P. K. Davis and W. A. Kaiser

Isotopic Analysis of Rare Gases from Stepwise Heating of Lunar Fines and Rocks

Abstract. *Highlights of a first effort in sorting out rare gases in lunar material are solar wind rare gases in abundance; variable $^{20}Ne/^{22}Ne$ but constant $^{21}Ne/^{22}Ne$ ratios in fractions of the trapped neon; cosmogenic rare gases similar to those found in meteorites, except for copious ^{131}Xe in one rock but not in another; at Tranquillity Base a rock 4.1 × 10^9 years old which reached the surface 35 to 65 million years ago, amid soil whose particles have typically been within a meter of the surface for 10^9 years or more.*

This paper describes the results of stepwise heating of three lunar samples. At each of a series of successively higher temperatures, all the rare gases evolved were examined in a glass mass spectrometer. The programmed heating was continued beyond the melting points of the samples until all gas had been extracted. Half-gram chips of rocks 57 (fine-grained crystalline) and 44 (coarser-grained crystalline) were studied in one system. A 0.09-g sample of lunar fines (sample 84) was studied in a second system. The lunar material was received at Berkeley in sealed, nitrogen-filled containers. All samples were handled in nitrogen; they were loaded into the vacuum systems without exposure to the atmosphere.

Attention is focused here on resolving the rare gas mass spectra into constituent components. As in meteorite studies, our basic technique has been to plot correlation diagrams for appropriate pairs of isotope ratios in the various temperature fractions from a sample. Two-component mixtures are characterized by straight lines on such a diagram, spanning end points corresponding to the two components. If the end points can somehow be inferred, relative concentrations of the two components can be deduced for each temperature fraction. Departures from a straight line indicate additional components. In particular, concentrations of additional monoisotopic components are easily deduced. The method of analysis should become clear upon discussion of examples.

Xenon in the lunar fines was detected in large concentrations and with an isotopic composition close to that predicted for solar-wind xenon by Marti (*1*) from his studies of xenon in the gas-rich achondrite Pesyanoe. The solar xenon is depleted in ^{134}Xe and ^{136}Xe relative to xenon seen in the carbonaceous chondrites. Our stepwise heating of the fines revealed an additional cosmogenic (cosmic-ray produced) xenon component, as shown in Fig. 1, which is a correlation plot of $^{124}Xe/^{130}Xe$ against $^{126}Xe/^{130}Xe$. The points define a line which spans the compositions of average-carbonaceous-chondrite (AVCC) xenon and spallation-type xenon as deduced from the 1200°C fraction from rock 57. The proximity of the most "southwesterly" points on this plot to the AVCC composition strongly suggests that the solar xenon has the AVCC ratios for the light xenon isotopes, although we have used the composition of the 820°C fraction in the fines for solar xenon in calculations in this paper. All numerical results in this paper are presented in Tables 1 and 2.

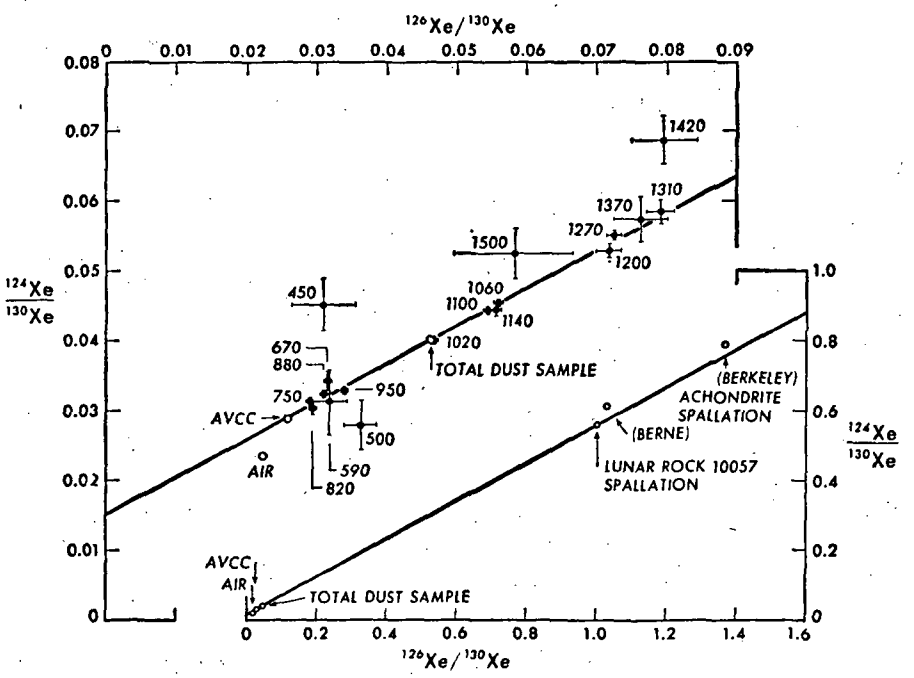

Fig. 1. Correlation of ratios $^{124}Xe/^{130}Xe$ and $^{126}Xe/^{130}Xe$ in lunar fines. The numbers are release temperatures in degrees Celsius for half-hour heatings. These isotopes belong to a two-component system. One component appears to have the AVCC ratios. The other is lunar spallation xenon as deduced from rock 10057. Note the similarity to spallation xenon in achondritic meteorites.

Neon both in the fines and in rock 57 is dominated by an abundant trapped component. Figure 2 shows the isotopic composition in the various temperature fractions. Although there is cosmogenic neon present, the spectra are dominated by neon for which the $^{21}Ne/^{22}Ne$ is relatively constant (at a value only slightly greater than the terrestrial value) but the $^{20}Ne/^{22}Ne$ is highly variable. Noncosmogenic neon in any fraction will have a composition somewhere "northwest" of the observed composition on the line joining that point with point *C*. On this basis the $^{20}Ne/^{22}Ne$ ratio for noncosmogenic neon in rock 57 varies from $\leqq 8.3$ to $\geqq 13.9$; similarly, the ratio in lunar fines ranges from $\leqq 11.3$ to $\geqq 14.3$. Effects of this type are known in stone meteorites (*2*), but have never been adequately explained. Their occurrence in lunar material is one of the most striking results of our study and places constraints upon future theories for their explanation.

Cosmogenic xenon in rock 57 presents a generally consistent picture. The 1200°C fraction is most strongly cosmogenic and has been used to deduce the spectrum. It was assumed that this fraction is a mixture of cosmogenic xenon and xenon with the composition seen at 820°C in the lunar fines. It was further assumed that there is no ^{136}Xe in the cosmogenic fraction. The cosmogenic spectrum is then easily obtained by subtraction. It fits (Fig. 3) the spallation xenon spectrum from the Stannern calcium-rich achondrite, as deduced by Marti *et al.* (*3*), more closely than it fits other published spallation spectra. The most striking difference between the spectra is at mass 131. Rock 57

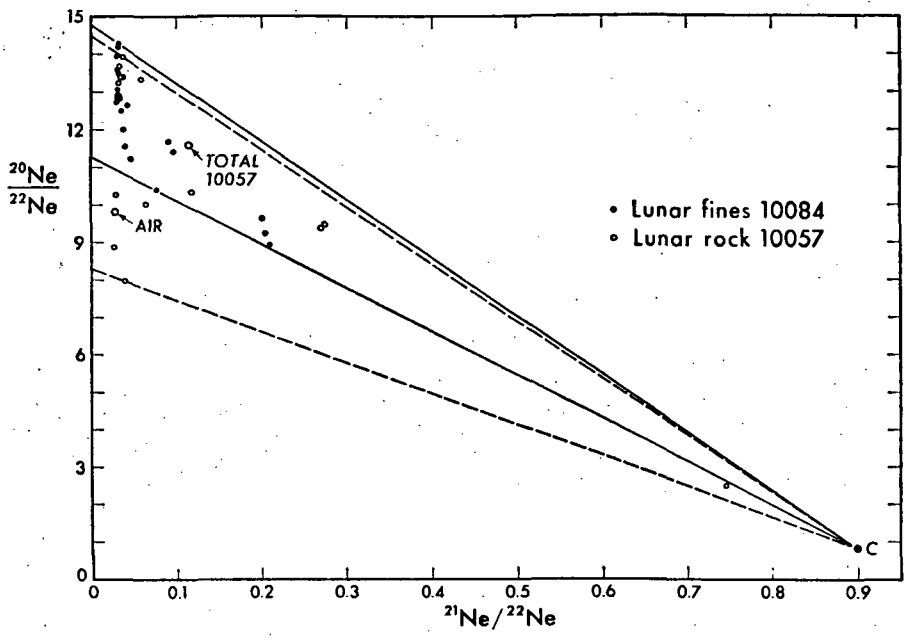

Fig. 2. Isotopic composition of neon fractions released in stepwise heating of lunar fines and rock 10057. The point *C* locates the composition of cosmogenic neon seen in a typical stone meteorite. The noncosmogenic neon composition in any fraction must lie toward the left on the line joining the observed composition with point *C*. Such lines have been drawn for the fractions of extreme composition. The trapped compositions are characterized by large variations in ratio $^{20}Ne/^{22}Ne$ but a nearly constant ratio for $^{21}Ne/^{22}Ne$.

contains an extraordinary excess of this isotope both in terms of absolute concentration and ratios! The differences at masses 132 and 134, which are small in terms of absolute gas concentration, can perhaps be attributed to fission effects in the Stannern meteorite.

A comprehensive display of the xenon isotope variations in rock 57 is given in Fig. 4, where ratios $^{M}Xe/^{130}Xe$ are plotted against $^{126}Xe/^{130}Xe$. For *M* equal to 124, 131, and 132, the points fall reasonably well on lines joining the 1200°C composition and the composition seen at 820°C in the lunar fines. Small corrections have been made for a fission contribution at masses 131 and 132 (see the following paragraph). Otherwise, these isotopes, with ^{126}Xe and ^{130}Xe, appear to belong to a two-component system of trapped and cosmogenic xenon. For *M* equal to 128 and 129, the values observed between 600° and 900°C fall above the lines containing the other points, as would occur if there were an excess of ^{128}Xe and ^{129}Xe being released at these temperatures. The correlation lines in Fig. 4 pass close to the compositions for cosmogenic xenon in calcium-rich achondrites, except at mass 131, where the correlation line observed has the opposite slope from that observed in meteorites.

Fission xenon in rock 57 was indicated, after subtraction of cosmogenic xenon, by higher values of $^{136}Xe/^{132}Xe$ and $^{134}Xe/^{132}Xe$ than in the lunar fines. The amount of fission xenon observed is approximately what should accumulate in 4.1×10^9 years (see below) of uranium decay in rock 57 (780 ppb uranium).

Argon from the samples is a mixture of radiogenic ^{40}Ar from ^{40}K decay, cosmogenic argon, and trapped argon, which can doubtless be ascribed to the solar wind. Values of the ratio $^{40}Ar/^{36}Ar$ as low as 0.82 were observed in argon fractions from the lunar fines, and provide an upper limit for this ratio in the solar wind. The much higher values of $^{40}Ar/^{36}Ar$ in gas fractions from rock 57 have to be attributed to ^{40}Ar from potassium decay. On that basis we compute a K-Ar age of

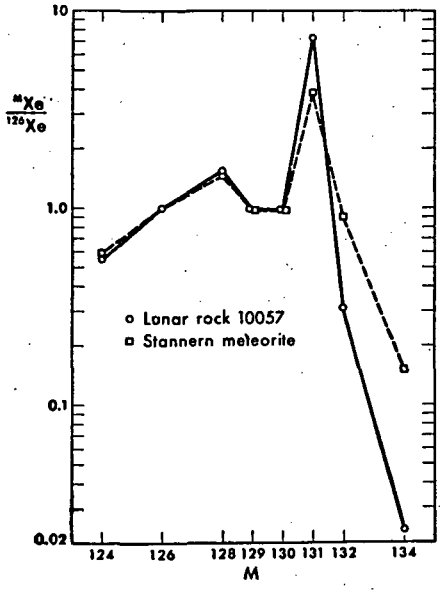

Fig. 3. Comparison of the mass spectrum of cosmogenic xenon in lunar rock 10057 with spallation xenon from the Stannern achondritic meteorite. A large and significant difference is seen for mass 131.

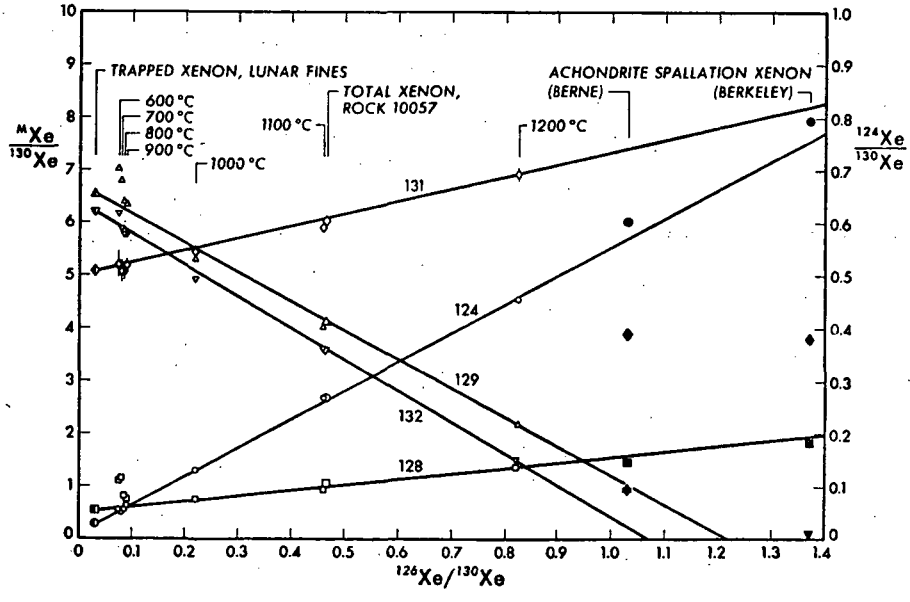

Fig. 4. Graphical analysis of the xenon released in stepwise heating of lunar rock 10057. Small corrections for fission have been made at masses 131 and 132. Isotopes 124, 126, 130, and 132 appear to belong to a simple two-component system (trapped and spallation xenon). Isotope 131 fits a two-component model but with a highly anomalous composition for the cosmogenic component. Isotopes 128 and 129 display excess amounts from 600° to 900°C inclusive.

Table 1. Rare gases from three lunar samples. The gas fractions for the stepwise heatings have been summed. All gas concentrations (boldface) are in units of 10^{-8} cm^3/g (STP). Errors in isotope ratios for total gas are about 1 percent. Errors in concentrations for total gas are about 10 percent.

Isotope	Lunar fines, sample 10084,59			Fine-grained crystalline rock, sample 10057,20					Medium-grained crystalline rock, sample 10044,20
	Total	Solar	Cosmic	Total	Trapped	Cosmic	Fission	Excess	Total
$^3He/^4He$	0.00047*			0.000545*†					
[^{4}He]	2.9×10^7			83000†					
$^{20}Ne/^{22}Ne$	12.85	12.90		11.58					3.72
$^{21}Ne/^{22}Ne$	0.0332	0.032		0.1152					0.710
[^{22}Ne]	41000	41000	>360	81	73	8.1			10.3
$^{38}Ar/^{36}Ar$	0.1925	0.183		0.237					
$^{40}Ar/^{36}Ar$	1.126	<0.82		39.1					
[^{36}Ar]	50600	50200	400	388	373	15			
$^{78}Kr/^{82}Kr$	0.0348	0.0315		0.10		0.23			0.164
$^{80}Kr/^{82}Kr$	0.2064	0.201		0.45		0.68	0.0043‡		0.486
$^{81}Kr/^{82}Kr$						0.0068			
$^{83}Kr/^{82}Kr$	1.003	0.997		1.06		1.35			1.10
$^{84}Kr/^{82}Kr$	4.91	4.91		3.57		0.47			2.91
$^{86}Kr/^{82}Kr$	1.503	1.496		1.02		0			0.786
[^{82}Kr]	7.6	7.5	0.10	0.034	0.023	≡0.011			0.027
$^{124}Xe/^{130}Xe$	0.0400	0.0302		0.265		0.57			0.59
$^{126}Xe/^{130}Xe$	0.0464	0.0293		0.465		1.03			0.94
$^{128}Xe/^{130}Xe$	0.530	0.515		1.048		1.61		0.00031‡	1.47
$^{129}Xe/^{130}Xe$	6.28	6.38		4.11		1.03		0.00027‡	2.85
$^{131}Xe/^{130}Xe$	4.98	4.98		6.05		7.50			4.55
$^{132}Xe/^{130}Xe$	5.97	6.06		3.58		0.32	0.00008‡		1.96
$^{134}Xe/^{130}Xe$	2.20	2.22		1.283		0.020	0.00012‡		
$^{136}Xe/^{130}Xe$	1.78	1.79		1.040		≡0	0.00013‡		0.439
[^{130}Xe]	0.77	0.76	0.010	0.0052	0.0029	0.0023			0.0015

*No discrimination correction was available for ^{3}He/^{4}He ratio. † Includes estimate for one gas fraction which was lost. ‡ Value is a concentration (not a ratio) for the isotope in the numerator for the row.

$4.1 \pm 0.3 \times 10^9$ years for rock 57, using the preliminary value (*5*) for the potassium content of the rock.

Krypton exhibits a cosmogenic component in all samples, and an excess of ^{80}Kr in rock 57. Radioactive ^{81}Kr was observed in the highly cosmogenic 1200°C fraction of rock 57, permitting calculation of a ^{81}Kr/^{80,82}Kr age (*6*) of 37 million years for exposure of the sample to galactic cosmic rays. Crude exposure ages (Table 2) were calculated for rock 57 and for the fines from the cosmogenic contents of ^{38}Ar, ^{82}Kr, and ^{130}Xe. We used the production rates from Munk's (*7*) study of the calcium-rich achondrite Nuevo Laredo for this purpose, assuming targets of calcium, strontium, and barium, respectively. These ages for rock 57 exceed the ^{81}Kr/^{80,82}Kr age as they should; the results would agree only if that rock was abruptly shifted to its final location from a completely shielded location. The ^{38}Ar exposure ages are older than the others. For the soil, the ages represent an average for the fine-grained material, but much of the present surface soil material at Tranquillity Base has been within a meter or so of the surface for 10^9 years or so, according to our data.

Table 2. Exposure ages of two lunar samples. Sample 10087,59 is lunar fines; sample 10057,20 is fine-grained crystalline rock.

Exposure age type	10084,59 (10^6 years)	10057,20 (10^6 years)
^{38}AR	3020	125
^{82}Kr	1600	64
^{130}Xe	720	63

Although we have not completely analyzed our results from rock 44, one important fact is immediately evident: in rock 44 the large excess of ^{131}Xe in the cosmogenic component is absent.

J. H. Reynolds
C. M. Hohenberg
R. S. Lewis, P. K. Davis
W. A. Kaiser

Department of Physics,
University of California, Berkeley

References and Notes

1. K. Marti, *Science* 166, 1263 (1969).
2. Reviewed by R. O. Pepin, *Earth Planet. Sci. Lett.* 2, 13 (1967).
3. K. Marti, P. Eberhardt, J. Geiss, *Z. Naturforsch.* 21a, 398 (1966).
4. G. W. Wetherill, *Phys. Rev.* 92, 907 (1953).
5. Lunar Sample Preliminary Examination Team, *Science* 165, 1211 (1969).
6. K. Marti, *Phys. Rev. Lett.* 18, 264 (1967); O. Eugster, P. Eberhardt, J. Geiss, *Earth Planet. Sci. Lett.* 2, 77 (1967).
7. M. N. Munk, *Earth Planet. Sci. Lett.* 3, 457 (1967).
8. We thank G. McCrory for assistance in the experimental work. Partial support from NASA and from the AEC; AEC code number UCB-34P32-71.

6 January 1970

Proceedings of the Apollo 11 Lunar Science Conference, Vol. 2, pp. 1283 to 1309.

Trapped and cosmogenic rare gases from stepwise heating of Apollo 11 samples

C. M. HOHENBERG, P. K. DAVIS, W. A. KAISER, R. S. LEWIS
and J. H. REYNOLDS
Department of Physics, University of California, Berkeley, California 94720

(*Received* 2 *February* 1970; *accepted in revised form* 10 *March* 1970)

Abstract—We examined the rare gases from stepwise heating of lunar dust and two crystalline rocks mass spectrometrically. We used isotope correlation diagrams extensively in our analysis of the data in order to identify trapped, cosmogenic, and fissiogenic components and to deduce their release curves. Cosmogenic neon, argon, krypton, and xenon have compositions similar to the cosmogenic gases in calcium-rich achondrites, although some differences occur—notably in ^{131}Xe, which is anomalously abundant in rock 10057 but not in rock 10044. Our sample of rock 10057 contains trapped solar gases, but our sample of rock 10044 does not, suggesting that production of ^{131}Xe may be depth dependent. Fissiogenic xenon in the rocks appears to originate entirely from spontaneous fission of ^{238}U. Isotopes ^{128}Xe, ^{129}Xe, ^{80}Kr and ^{82}Kr are in apparent excess in some of the temperature fractions from the rocks, but except for ^{129}Xe in rock 10044 the excesses are probably "memory" of a previous study of a neutron irradiated meteorite. A genuine excess of ^{129}Xe at two temperatures in rock 10044 is accompanied by excess ^{132}Xe and, possibly, ^{131}Xe and ^{124}Xe. There thus may be more than one cosmogenic component in rock 10044. In none of our lunar work have we seen evidence of any ^{129}Xe from decay of extinct ^{129}I. Rather large variations, with release temperature, in the isotopic composition of trapped helium, neon, and argon can probably be explained by a combination of two effects: (1) deeper burial of heavier isotopes in the solar wind; (2) diffusive separation of isotopes during thermal release. Exposure ages of rocks 10057 and 10044 by the ^{81}Kr–^{83}Kr method are 34 and 70 m.y. respectively. Exposure ages based on ^{83}Kr and ^{130}Xe and the meteoritic production rates for those isotopes, are higher than the Kr–Kr age for rock 10057 as would be expected if the rock spent time at a partially shielded depth. Rock 10044 may have had a simple irradiation history. Our average value for the average exposure age of the lunar fines is 1300 m.y.

INTRODUCTION

WE DESCRIBE the results of stepwise heating of three lunar samples. At each of a series of successively higher temperatures, we examined in a glass mass spectrometer all the rare gases evolved. We continued the programmed heating beyond the melting of the samples until all gases had been extracted. Our objective in the work was to resolve the rare gas mass spectra into the anticipated constituent components—trapped,* cosmogenic, radiogenic and fissiogenic gases—and in the process to search for possible additional components. As in meteorite studies our basic technique has been to plot correlation diagrams for appropriate pairs of isotope ratios (e.g. B/A vs. C/A) in the various temperature fractions from a sample. Two-component mixtures are straight lines on such a diagram, spanning end points corresponding to the two

* We use the term "trapped gases" to designate those gases which were not formed *in situ* by some sort of nuclear transmutation. The "trapped" component can thus include ambient gases dissolved in the minerals at time of formation, solar wind and cosmic-ray gases injected into material at the lunar surface, gases dissolved in existing minerals by diffusion and gases dissolved by shock.

components. If one can somehow infer the end points, one reads the relative concentrations of isotope A in the two components directly from the plot, using the lever rule. Departures from a straight line indicate additional components. In particular it is easy to deduce concentrations of additional monoisotopic components. The method of analysis should become clear upon discussion of examples.

EXPERIMENTAL METHODS

We opened the Houston containers at Berkeley in a nitrogen-filled glove-box and loaded the samples into the vacuum systems without exposing them to the atmosphere. One-gram rock chips of samples 10057 and 10044 were broken in half. One half was taken for the work in this paper; the other half was reserved for neutron irradiation. We shall report the analysis of gases in pile-irradiated samples elsewhere. Our ten-gram sample (10084) of lunar fines was split down to working samples of 0·09 g, using a Sepor No. 212 sample-splitter. This method of splitting may not have produced completely representative samples: we noticed that the fine material tended to clump appreciably and it is doubtful that we succeeded in dividing the clumps representatively in the splitting.

We studied half-gram samples of crystalline rocks 10057 and 10044 in "system 1," which is a completely metallic system up to and including the valve which admits the gases to the mass spectrometer, except for a small sample holder and dumper made from a glass of low permeability for helium (Corning type 1720). The "hot-blank" (1500°C heating for one hour) for helium in this system is only $0{\cdot}4 \times 10^{-8}$ cm³ STP ^{4}He. The samples were heated by radiofrequency induction in a previously outgassed crucible of vapor-deposited tungsten, which is welded to nickel tubing which is in turn welded to the demountable stainless-steel plumbing for the system. Gases released from the outside of the crucible are separately pumped to a waste vacuum. We measured temperatures with a pair of W/W–Re thermocouples attached to the outside of the crucible. In one run (sample 10057) these couples were spotwelded to the crucible, using a platinum tab as an intermediary. Thermocouples so mounted work well, but the platinum slowly sublimes. In the other run (sample 10044) the couples were bound to the crucible with tantalum wire. This scheme was only partially successful: induced currents in the tantalum wire resulted in somewhat high temperature readings. Because of the various problems encountered in the thermometry, the stated temperatures for system 1 may be in error by as much as ±50°C for rock 10057 and ±100°C for rock 10044.

We studied the 0·09 g sample of lunar fines (sample 10084) in "system 2," for which the connecting tubulations are Pyrex glass. The crucible is again vapor-deposited tungsten with a separate pumping system for the outside. The "hot blank" for helium for system 2 (1600°C heating for one half hour) is $1{\cdot}0 \times 10^{-7}$ cm³ STP ^{4}He, which is much larger than for system 1 but completely negligible in comparison with the helium released by sample 10084. In system 2, we measured the higher temperatures directly with an optical pyrometer. We measured the lower temperatures (and checked the pyrometer measurements for the higher temperatures) indirectly: immediately after the run we installed a W/W–Re thermocouple inside the crucible, without making further changes in the system, and reproduced the heating steps in vacuum at exactly the same settings on the induction heater. For the higher temperatures, determinations by the thermocouple and by the optical pyrometer were in excellent agreement. We therefore believed that the stated temperatures for system 2 are accurate within ±20°C.

In both systems, we purified gases over one or two stages of Zr–Ti alloy, supplemented by a fresh mirror in a titanium bulb. The glass mass spectrometers also carried titanium bulbs in which fresh mirrors were generated before a series of analyses. The rare gases were separated one from another with an activated charcoal trap. The sequence for separation is: liquid nitrogen on charcoal, admit He and Ne; dry ice on charcoal, admit Ar; −39°C on charcoal admit Kr; +100°C on charcoal, admit Xe. The He–Ne mixture is looked at in two stages so that each gas can be examined first in one of the two runs. Both systems contain all-metal, gas pipettes filled with pure air and ^{3}He at known pressures. Before and after each sample, several calibrations runs were made with the pipette. These runs furnish both sensitivity factors for the various gases and correction factors for mass discrimination.

We have made no corrections in any of this work for blanks. Instead, blanks were run and recorded separately in the tables. Every fraction reported here thus includes small amounts of atmospheric rare gases. These blank gases are noticeable at the lower temperatures for the runs on the rocks, expecially rock 10044. With one exception (see below) these contributions are very close in size to our hot blanks, showing that the atmospheric gases are *not* coming from the crucible, even in the hot blanks. These results testify to the excellence for rare gas extractions of vapor deposited tungsten crucibles, even though large, so long as they are separately pumped exteriorly by a waste vacuum system. The exception to which we alluded is the neon blank for rock 10057. We ran rock 10057 with a quartz chimney lining the inner surface of the nickel tube connecting with the crucible, so as to catch a fraction of the alkali metals evaporated from the sample. Even after many hours of outgassing near maximum power, small traces of dissolved atmospheric neon were still coming out of the chimney at the higher temperatures. The contribution of blank neon to the *lower* temperatures for rock 10057 can best be estimated from the blank for rock 44, where the quartz chimney was not used.

Background (i.e. "dirt") corrections were made only to ^{78}Kr, ^{80}Kr and ^{81}Kr in the rocks. Entries in the tables where there was such a correction have been flagged. We based the background correction on the 79 peak in the krypton spectrum, a procedure which is somewhat objectionable (except for corrections to ^{81}Kr) but one for which we had no good alternative. In some of the runs a correction had to be applied to $^{20}Ne^{+}$ for $^{40}Ar^{2+}$, although we usually ran neon at electron bombardment voltages which suppressed the doubly charged argon peak to insignificant levels. Again, entries in the tables where such a correction was applied are flagged.

Results for Lunar Fines (Sample 10084)

Complete results for He, Ne, Ar and Xe are set out in Table 1. The krypton data are omitted because they were not precise enough to reveal significant trends, except for an obvious cosmogenic component, which produces correlated changes in the ratios $^{78}Kr/^{82}Kr$ and $^{80}Kr/^{82}Kr$. The summed krypton data appear along with data for the other gases in our summary Table 2.

Xenon in the lunar fines was detected in large concentrations and with an isotopic composition close to that predicted for solar-wind xenon by Marti (1969) from his study of xenon in the gas-rich achondrite Pesyanoe. For the isotopes of mass 130 and below, the abundance pattern resembles the xenon in average carbonaceous chondrites (AVCC). This fact cannot be established in a total extraction or "melting" run on the sample because of the occurrence of a spallogenic xenon component. But the stepwise heating data enable one to distinguish the components. Figure 1 is a correlation plot of $^{124}Xe/^{130}Xe$ against $^{126}Xe/^{130}Xe$. The points define a line which spans the compositions of AVCC xenon and spallation-type xenon as deduced from the 1200° fraction from rock 10057. The proximity of the most "southwesterly" points on this plot to the AVCC composition, strongly suggests that the solar xenon has the AVCC ratios for the light xenon isotopes. We have used the composition of the 820°C fraction in the fines to represent solar xenon in calculations in this paper, although we recognize that "solar xenon" defined in this way may contain traces of spallation xenon. The isotopes produced abundantly in fission (^{131}Xe, ^{132}Xe, ^{134}Xe and ^{136}Xe.) are all depleted in the lunar fines relative to AVCC xenon, as was noted in the preliminary rare gas studies (LSPET, 1969). Confirmation, in results from the lunar samples, of Marti's (1969) hypothesis that solar and meteoritic xenon are one and the same—aside from possible fission effects—deepens all the more the mystery about terrestrial xenon. How can it have become so strongly fractionated in mass (almost

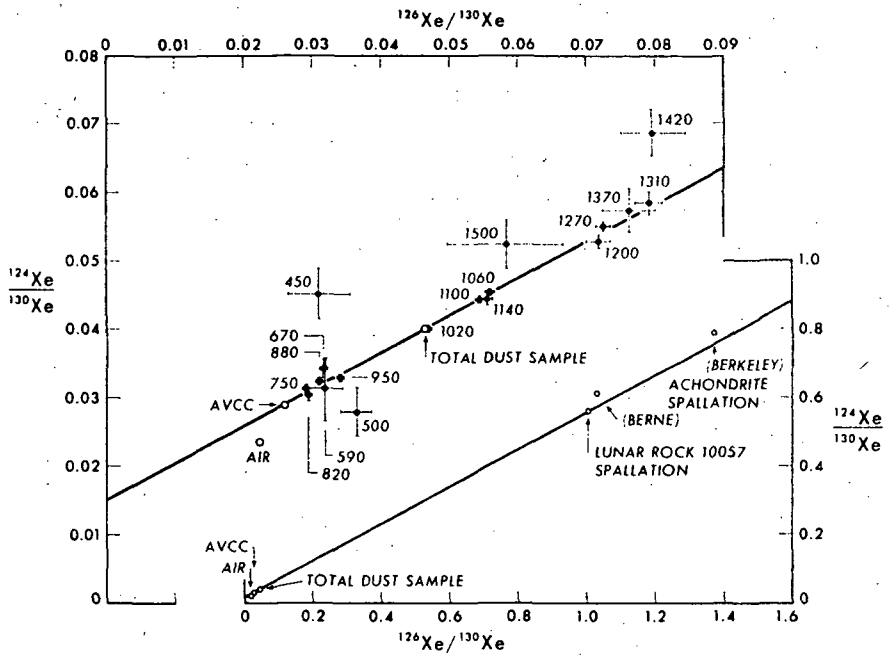

Fig. 1. Correlation of ratios $^{124}Xe/^{130}Xe$ and $^{126}Xe/^{130}Xe$ in lunar fines. The numbers are release temperatures in degrees Celsius for half-hour heatings. These isotopes belong to a two-component system. One component appears to have the AVCC ratios. The other is cosmogenic xenon as deduced from rock 10057.

4 per cent per mass unit!) relative to the xenon elsewhere in the solar system? And without similar effects occurring in argon and krypton?

Helium and neon results are of special interest. We now suspect that separations of isotopes during imbedding of the solar wind gas and in the release by heating are jointly responsible for large variations in isotope ratios. There were errors in some of our data reduction for neon at the time of our report (REYNOLDS *et al.*, 1970) to the Apollo 11 Conference. Because of a very large spread in the ratio $^{20}Ne/^{22}Ne$, without variations, except for spallation effects, in the $^{21}Ne/^{22}Ne$ ratio, we had to suppose that at least two trapped neon components were present. The corrected data no longer support this conclusion. The run of the helium isotopes during outgassing is very instructive. In Fig. 2 we plot the release curves for ^{3}He and ^{4}He for the dust sample, 10084. Both curves are normalized to 100 per cent total release. One notes that the curves are similar but displaced slightly in temperature: ^{3}He release occurs slightly earlier than ^{4}He release. The initial $^{3}He/^{4}He$ ratio of 0·000635 is 36 per cent higher than the total ratio. In a single stage diffusion process the initial enrichment in the ratio should be $(4/3)^{1/4} = 1{\cdot}074$. But we have a two stage process in this instance: ^{4}He was imbedded deeper than the ^{3}He when the solar wind struck the lunar surface, because the streaming of the solar wind is hydrodynamic, with equal velocities for the two helium isotopes. The initial burial depth for isotopes will be proportional to

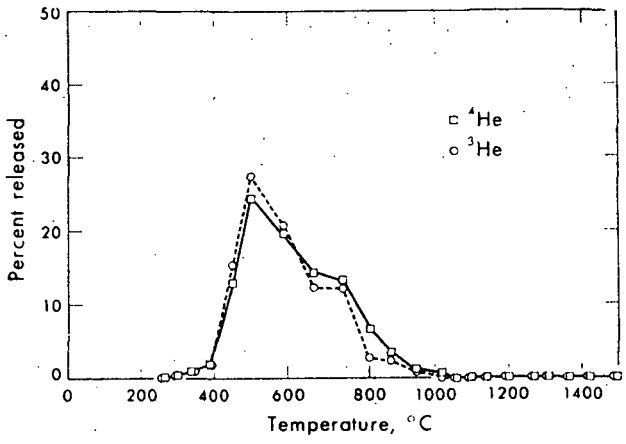

Fig. 2. Release of helium isotopes in stepwise heating of lunar dust. The curves have been normalized to 100 per cent total release.

mass.* And deeper burial of the mass 4 component, enhances the initial separative effect.

Release curves for isotopes ^{20}Ne and ^{22}Ne (not shown) exhibit a similar effect if one looks carefully at the low temperature and high temperature "tails" for the neon release, where the effect is greatest. We see an initial enrichment for $^{20}Ne/^{22}Ne$ of 11 per cent, which again exceeds the single stage enrichment of $(22/20)^{1/4} = 1{\cdot}024$ and for the same reason. Figure 3 shows the neon ratios for all three of our samples on a standard correlation plot for neon. Rock 10044, which was an interior piece, has practically no trapped gas. Because of $^{40}Ar^{2+}$ interference no precise $^{20}Ne/^{22}Ne$ ratios were obtained below 700°C where fractionation of the isotopes in the trapped component would be most visible The ratios thus fall along a line (the "rock line," PEPIN *et al.*, 1970) joining the compositions of trapped and cosmogenic neon. Point C with coordinates $^{20}Ne/^{22}Ne = 0{\cdot}82$, $^{21}Ne/^{22}Ne = 0{\cdot}90$ represents cosmogenic neon in a typical stone meteorite. In the dust sample, neon is dominated by the trapped component except at the highest temperatures where the trapped component is almost gone and the bulk of the cosmogenic component is being released. In this sample at low temperatures we thus see diffusive separation of the isotopes, trending roughly along a line of slope

$$d \ln (^{20}Ne/^{22}Ne)/d \ln (^{21}Ne/^{22}Ne) \doteq 2.$$

At later temperatures, where the last of the trapped neon is being released, an appreciable enrichment of the heavier isotopes has built up. We see from the intersections

* It is questionable to what extent the initial distributions of isotopes with depth have been preserved. There is conclusive evidence (EBERHARDT *et al.*, 1970) for saturation effects in trapped helium and neon in the bulk fines and for diffusion of trapped helium into the grains in the bulk fines to depths of about 10 μ (KIRSTEN *et al.*, 1970). Both these effects could redistribute the isotopes. But we find, surprisingly, that the distortion of the isotope ratios in the initial release is just the mass ratio of the isotopes for helium, neon, and argon alike.

Table 1. Helium, neon, argon and xenon from stepwise heating

Temperature (°C)	Ave. 1550° Blank	265	270	290	300	340	390	450	500	590	670	750	820
$^4He/^3He$‡	—	1575·0‡	1751·0‡	1678·0‡	1666·0‡	1754·0‡	1678·0‡	1754·0‡	1887·0‡	2049·0‡	2487·0‡	2299·0‡	4878·0‡
		±17·0	±34·0	±20·0	±11·0	±9·0	±8·0	±6·0	±11·0	±8·0	±37·0	±5·0	±24·0
$[^3He]$, 10^{-8} cm^{3}STP/g	<0·026*a	**79·4**	**18·1**	**21·3**	**39·1**	**128·0**	**244·0**	**2110·0**	**3690·0**	**2730·0**	**1620·0**	**1690·0**	**385·0**
$^{20}Ne/^{22}Ne$	—	14·27	13·94	14·19	13·59	12·84	12·91	13·49	12·71	13·06	12·87	12·92	12·88
		±0·06	±0·10	±0·08	±0·09	±0·04	±0·10	±0·16	±0·04	±0·10	±0·18	±0·09	±0·09
$^{21}Ne/^{22}Ne$	—	0·0323	0·0300	0·0319	0·0317	0·0313	0·0313	0·0324	0·0309	0·0319	0·0319	0·0324	0·0331
		±0·0030	±0·0010	±0·0005	±0·0003	±0·0003	±0·0003	±0·0004	±0·0002	±0·0003	±0·0006	±0·0003	±0·0004
$[^{22}Ne]$, 10^{-8} cm^{3}STP/g	0·025*	**26·8**	**4·61**	**5·76**	**13·6**	**111·0**	**244·0**	**4500·0**	**4060·0**	**6190·0**	**7300·0**	**7300·0**	**1890·0**
$^{38}Ar/^{36}Ar$	—	0·1816	0·1784	0·1807	0·1800	0·1787	0·1799	0·1810	0·1835	0·1802	0·1829	0·1897	0·1920
		±0·0007	±0·0016	±0·0011	±0·0008	±0·0013	±0·0010	±0·0010	±0·0006	±0·0010	±0·0011	±0·0009	±0·0006
$^{40}Ar/^{36}Ar$	—	38·25	34·59	30.99	25·35	14·32	11·23	5·60	3·64	2·877	2·128	0·923	0·820
		±0·09	±0·17	±0·09	±0·08	±0·07	±0·04	±0·02	±0·01	±0·010	±0·007	±0·003	±0·002
$[^{36}Ar]$, 10^{-8} cm^{3}STP/g	0·01*	**3·87**	**0·79**	**0·78**	**1·25**	**4·26**	**9·8**	**9·8**	**270·0**	**886·0**	**3780·0**	**13300·0**	**9000·0**
$^{124}Xe/^{130}Xe$	—	—	—	—	—	—	—	0·045	0·0280	0·0312	0·0342	0·0312	0·0302
								±0·004	±0·003	±0·004	±0·0013	±0·0006	±0·0008
$^{126}Xe/^{130}Xe$	—	—	—	—	—	—	—	0·0309	0·0363	0·0318	0·0316	0·0290	0·0293
								±0·0046	±0·0023	±0·0024	±0·0005	±0·0005	±0·0005
$^{128}Xe/^{130}Xe$	—	0·516	0·508	0·727	0·623	0·656	0·696	0·521	0·540	0·508	0·507	0·509	0·515
		±0·033	±0·054	±0·012	±0·058	±0·053	±0·030	±0·028	±0·010	±0·017	±0·014	±0·005	±0·004
$^{129}Xe/^{130}Xe$	—	6·32	6·92	6·91	6·49	6·74	6·91	6·58	6·57	6·30	6·31	6·31	6·38
		±0·32	±0·44	±0·11	±0·30	±0·37	±0·30	±0·20	±0·08	±0·12	±0·09	±0·03	±0·05
$^{131}Xe/^{130}Xe$	—	5·20	5·47	5·43	5·48	5·60	5·42	5·23	5·09	4·96	4·91	4·93	4·98
		±0·26	±0·35	±0·27	±0·29	±0·30	±0·34	±0·18	±0·07	±0·09	±0·08	±0·03	±0·04
$^{132}Xe/^{130}Xe$	—	6·35	7.01	7·54	6·89	6·90	6·77	6·26	6·21	6·02	5·96	5·97	6·06
		±0·31	±0·41	±0·08	±0·31	±0·37	±0·29	±0·13	±0·05	±0·08	±0·06	±0·03	±0·04
$^{134}Xe/^{130}Xe$	—	2·404	2·553	2·842	2·523	2·385	2·478	2·341	2·270	2·238	2·200	2·174	2·224
		±0·12	±0·18	±0·10	±0·11	±0·15	±0·13	±0·073	±0·032	±0·036	±0·042	±0·013	±0·019
$^{136}Xe/^{130}Xe$	—	2·086	2·374	2·434	2·225	2·138	2·105	1·942	1·840	1·817	1·790	1·763	1·793
		±0·11	±0·17	±0·037	±0·13	±0·13	±0·14	±0·07	±0·024	±0·033	±0·034	±0·013	±0·015
$[^{130}Xe]$, 10^{-12} cm^{3}STP/g	0·3*	**0·85**	**0·27**	**0·26**	**0·32**	**0·38**	**0·50**	**2·06**	**3·67**	**9·05**	**20·5**	**276·0**	**461·0**

Notes: Boldface entries are gas concentrations. Errors in gas concentrations are 10% for helium, neon, and xenon, 20% for argon. Errors are statistical only. In addition there is a fractional error in the applied mass discrimination factors as follows: Ne 20/22: 0·015; 21/22: 0·05. Ar 38/36: 0·05; 40/36: 0·04. Xe 124/130: 0·04; 126/130: 0·05; 128/130: 0·01; 129/130: 0·007; 131/130: 0·008; 132/130: 0·006; 134/130: 0·01; 136/130: 0·014.

of 0·089 g of lunar fines (10084–59). Heatings were for ½ hr.

880	950	1020	1060	1100	1140	1200	1270	1310	1370	1420	1500	1420 Blank	Total
2506.0‡	2632·0‡	26740.0‡[b]	1745·0‡	1416·0‡	1083.0‡	1923·0‡	2283·0‡	3175·0‡	2660·0‡	3270·0‡	3185·0‡	3003·0‡	2138·0‡
±13·0	±14·0	±720·0	±27·0	±14·0	±13·0	±63·0	±63·0	±170·0	±140·0	±300·0	±40·0	±126·0	±6·0
393·0	**143·0**	**5·57[b]**	**13·9**	**4·95**	**3·09**	**0·490**	**0·311**	**0·345**	**0·132**	**0·227**	**0·111**	**0·056**	**13300·0**
12·81	12·50	12·01	11·57	11·21	10·38	9·25	8·94	11·41[b]	9·64	11·67	12·64	14·01	12·85
±0·11	±0·04	±0·09	±0·03	±0·03	±0·02	±0·06	±0·05	±0·10	±0·13	±0·12	±0·09	±0·26	±0·04
0·0339	0·0355	0·0385	0·0408	0·0475	0·0781	0·205	0·211	0·097[b]	0·201	0·092	0·043	0·036	0·0332
±0·0004	±0·0002	±0·0004	±0·0002	±0·0001	±0·0004	±0·002	±0·003	±0·003	±0·004	±0·002	±0·004	±0·011	±0·0001
3050·0	**2480·0**	**1560·0**	**907·0**	**365·0**	**135·0**	**78·3**	**2·31**	**0·53[b]**	**0·33**	**0·35**	**0·13**	**0·043**	**40800·0**
0·1937	0·1950	0·1974	0·1977	0·2009	0·2070	0·2148	0·2279	0·2281	0·2295	0·2316	0·2152	0·2016	0·1925
±0·0004	±0·0009	±0·0002	±0·0003	±0·0005	±0·0008	±0·0005	±0·0005	±0·0008	±0·0005	±0·0007	±0·0008	±0·006	±0·0003
0·857	1·013	1·072	1·208	1·242	1·241	1·491	1·616	2·504	2·167	3·415	4·91	35·4	1·125
±0·001	±0·004	±0.001	±0·001	±0·002	±0·003	±0·002	0·002	±0·007	±0·003	±0·005	±0·01	±0·7	±0·001
6930·0	**3170·0**	**1950·0**	**2790·0**	**2800·0**	**1390·0**	**173·0**	**113·0**	**24·3**	**21·4**	**4·35**	**3·47**	**0·21**	**46700·0**
0.0322	0·0329	0·0401	0·0455	0·0442	0·0442	0.0529	0·0550	0·0583	0·0573	0·0686	0·0523	0·1139	0·0400†
±0·0003	±0·0002	±0·0002	±0·0004	±0·0003	±0·0009	±0·0010	±0·0007	±0·0017	0·0032	±0·0031	±0·004	±0·026	±0·0001
0·0310	0·0340	0·0469	0·0560	0.0545	0·0557	0·0719	0·0725	0·0792	0·0763	0·0796	0·0583	0·0404	0·0464†
±0·0005	±0·0003	±0·0004	±0·0008	±0·0006	±0·0009	±0·0019	±0·0011	±0·0020	±0·0038	±0·0046	±0·008	±0·007	±0·0002
0·518	0·514	0·529	0·541	0·540	0·533	0·556	0·553	0·569	0·561	0·544	0·546	0·589	0.530
±0·003	±0·003	±0·003	±0·004	±0·003	±0·004	±0.005	±0·005	±0·008	±0·015	±0·017	±0·017	±0·088	±0·001
6·33	6·31	6·28	6·26	6.27	6·23	6·18	6·17	6·19	6·18	6·05	5·93	7·10	6·28
±0·03	±0.03	±0·03	±0·04	±0·03	±0·04	±0·05	±0·04	±0·07	±0·08	±0·10	±0·14	±0·85	±0·01
4·95	4·97	4·97	5·00	5·01	5·01	4·96	5·03	5·03	5·06	4·99	4·76	5·53	4·98
±0·02	±0·02	±0·02	±0·03	±0·03	±0·03	±0·04	±0·03	±0·06	±0·06	±0·09	±0·12	±0·68	±0·01
6·01	6·01	5·97	5·94	5·95	5·92	5·82	5·87	5·88	5·87	5·81	5·76	6·30	5·97
±0·03	±0·02	±0·02	±0·03	±0·02	±0·03	±0·04	±0·03	±0·06	±0·07	±0·09	±0·10	±0·76	±0·01
2·209	2·198	2·205	2·187	2·196	2·181	2·136	2·170	2·149	2·177	2·076	2·113	2·233	2·195
±0·013	±0·009	±0·012	±0·013	±0·011	±0·016	±0·018	±0·018	±0·024	±0·032	±0·040	±0·046	±0·29	±0·005
1·785	1·795	1·790	1·776	1·787	1·773	1·741	1·768	1·741	1·773	1·757	1·701	1·707	1·783
±0·008	±0·007	±0·009	±0·010	±0·008	±0·011	±0·015	±0·012	±0·022	±0·028	±0·050	±0·056	±0·22	±0·004
936·0	**1030·0**	**1180·0**	**1700·0**	**1120·0**	**548·0**	**108·0**	**118·0**	**41·2**	**29·4**	**5·19**	**2·82**	**0·25**	**7700·0**

* Absolute blank in cm^3 STP is the tabulated blank times 0·089 g.
† Total of gas fractions where this ratio was obtained.
‡ No discrimination correction available. These ratios may be systematically in error.
[a] ^3He not measured. ^4He concentration: $\sim 10{\cdot}0 \times 10^{-8}$ cm^3 STP/g.
[b] Questionable value.

Table 2. Summary of the results for rare gases from lunar samples.

Isotope	Lunar fines Sample 10084, 59 Total	Lunar fines Sample 10084, 59 Trapped	Lunar fines Sample 10084, 59 Cosmog.	Fine-grained Sample 10057, 20 Total	Fine-grained Sample 10057, 20 Trapped	Fine-grained Sample 10057, 20 Cosmog.
$^4He/^3He$	2138·0* ±6·0	—	—	1809·3*,b ± 3·9	—	—
[^{3}He]	**13400·0 ± 1300·0**	—	—	**89·48 ± 7·2**	—	—
$^{20}Ne/^{22}Ne$	12·85 ± 0·20	12·9[a] ± 0·21	—	12·08 ± 0·15	—	—
$^{21}Ne/^{22}Ne$	0·0332 ± 0·0017	0·0324[a] ± 0·0016	≡ 0·900	0·120 ± 0·002	≡ 0·032	≡ 0·900
[^{22}Ne]	**40800·0 ± 4080·0**	**40800·0 ± 4080·0**	**40·0 + 78·0–15·0**	**76·6 ± 7·7**	**67·5 ± 6·8**	**9·2 ± 0·9**
$^{38}Ar/^{36}Ar$	0·193 ± 0·010	0·190[a] ± 0·010	—	0·237 ± 0·002	—	≡ 1·52
$^{40}Ar/^{36}Ar$	1·125 ± 0·045	—	—	39·19 ± 0·28	—	—
[^{36}Ar]	**46700·0 ± 9300·0**	**46700·0 ± 9300·0**	—	**388·0 ± 39·0**	**372·0 ± 37·0**	**15·1 ± 1·5**
$^{78}Kr/^{82}Kr$	0·0312† ± 0·0011	0·0307†,c ± 0·0013	—	0·0844† ± 0·0016	—	0·224† ± 0·0075
$^{80}Kr/^{82}Kr$	0·206 ± 0·004	0·201[c] ± 0·004	≡ 0·675	0·4420† ± 0·0066	—	0·670† ± 0·0227
$^{81}Kr/^{82}Kr$	—	—	—	—	—	0·00722† ± 0·00112
$^{83}Kr/^{82}Kr$	1·00 ± 0·01	1·00[c] ± 0·01	—	1·06 ± 0·013	—	1·35 ± 0·016
$^{84}Kr/^{82}Kr$	4·91 ± 0·05	4·91[c] ± 0·05	—	3·57 ± 0·037	—	0·45 ± 0·018
$^{86}Kr/^{82}Kr$	1·50 ± 0·01	1·50[c] ± 0·01	—	1·02 ± 0·025	—	≡ 0·000
[^{82}Kr]	**7·6 ± 1·5**	**7·5 ± 1·5**	**0·093 + 0·064–0·024**	**0·0337 ± 0·0061**	**0·0237 ± 0·0043**	**0·01 ± 0·0018**
$^{124}Xe/^{130}Xe$	0·0400 ± 0·0016	0·0302[c] ± 0·0015	—	0·265 ± 0·0037	—	0·57 ± 0·0083
$^{126}Xe/^{130}Xe$	0·0464 ± 0·0023	0·0293[c] ± 0·0016	1·03	0·465 ± 0·0097	—	1·03 ± 0·022
$^{128}Xe/^{130}Xe$	0·530 ± 0·005	0·515[c] ± 0·007	—	1·048 ± 0·053	—	1·61 ± 0·070
$^{129}Xe/^{130}Xe$	6·28 ± 0·04	6·38[c] ± 0·07	—	4·11 ± 0·072	—	1·03 ± 0·066
$^{131}Xe/^{130}Xe$	4·98 ± 0·04	4·98[c] ± 0·06	—	6·05 ± 0·040	—	7·50 ± 0·081
$^{132}Xe/^{130}Xe$	5·97 ± 0·04	6·06[c] ± 0·06	—	3·58 ± 0·023	—	0·32 ± 0·042
$^{134}Xe/^{130}Xe$	2·20 ± 0·02	2·22[c] ± 0·03	—	1·283 ± 0·0096	—	0·020 ± 0·0166
$^{136}Xe/^{130}Xe$	1·78 ± 0·03	1·79[c] ± 0·03	—	1·040 ± 0·0083	—	≡ 0·000
[^{130}Xe]	**0·77 ± 0·08**	**0·76 ± 0·08**	**0·013 ± 0·002**	**0·00517 ± 0·00031**	**0·00291 ± 0·00019**	**0·00226 ± 0·00016**

Notes: Boldface entries are gas concentrations in units of 10^{-8} cm^3 STP/g. Errors in this table are total errors.

* No discrimination correction was available.

† Correction has been made for background. Error includes uncertainty in background as well as discrimination corrections.

[a] Based on 750° fraction.

The gas fractions for the stepwise heatings have been summed

Crystalline rock		Medium-grained crystalline rock Sample 10044, 20				
Fission	Excess	Total	Trapped	Cosmog.	Fission	Excess
—	—	213·69* ± 0·15	—	—	—	—
—	—	**102·4 ± 13·3**	—	—	—	—
—	—	3·311 ± 0·043	—	—	—	—
—	—	0·719 ± 0·014	≡ 0·029	≡ 0·905	—	—
—	—	**9·5 ± 1·0**	**2·0 ± 0·2**	**7·5 ± 0·8**	—	—
—	—	0·9843 ± 0·0088	—	≡ 1·52	—	—
—	—	282·8 ± 2·0	—	—	—	—
—	—	**41·9 ± 4·2**	**16·8 ± 1·7**	**25·1 ± 2·5**	—	—
—	—	0·174† ± 0·0042	—	0·233† ± 0·0122	—	—
—	0·0039†[d,e]	0·520† ± 0·0103	—	0·617† ± 0·0265	—	0·0013†[d,e]
—	—	—	—	0·00334† ± 0·000806	—	—
—	—	1·09 ± 0·0074	—	1·27 ± 0·025	—	—
—	—	2·89 ± 0·031	—	0·51 ± 0·042	—	—
—	—	0·78 ± 0·009	—	≡ 0·000	—	—
—	0·0010[e]	**0·0311 ± 0·0093**	**0·0167 ± 0·0050**	**0·0144 ± 0·0043**	—	0·00035[e]
—	—	0·63 ± 0·01	—	0·69 ± 0·014	—	—
—	—	1·001 ± 0·022	—	1·106 ± 0·028	—	—
—	0·00028[d,e]	1·47 ± 0·075	—	1·625 ± 0·087	—	0·000047[d,e]
—	0·00040[d,e]	2·85 ± 0·052	—	1·71 ± 0·057	—	0·00052[d]
—	—	4·55 ± 0·041	—	4·28 ± 0·067	—	—
—	—	1·97 ± 0·014	—	0·77 ± 0·021	—	—
—	—	0·558 ± 0·0048	—	0·041 ± 0·0076	—	—
0·00013[d] ± 0·00006	—	0·439 ± 0·0028	—	≡ 0·000	**0·00015[d] ± 0·00005**	—
—	—	**0·00135 ± 0·000081**	**0·00021 ± 0·000029**	**0·0014 ± 0·000080**	—	—

[b] Includes estimate for one gas fraction which was lost.
[c] Based on 820° fraction.
[d] Value is a concentration (not a ratio) for the isotope with numerator for the row.
[e] Questionable effect. See text.

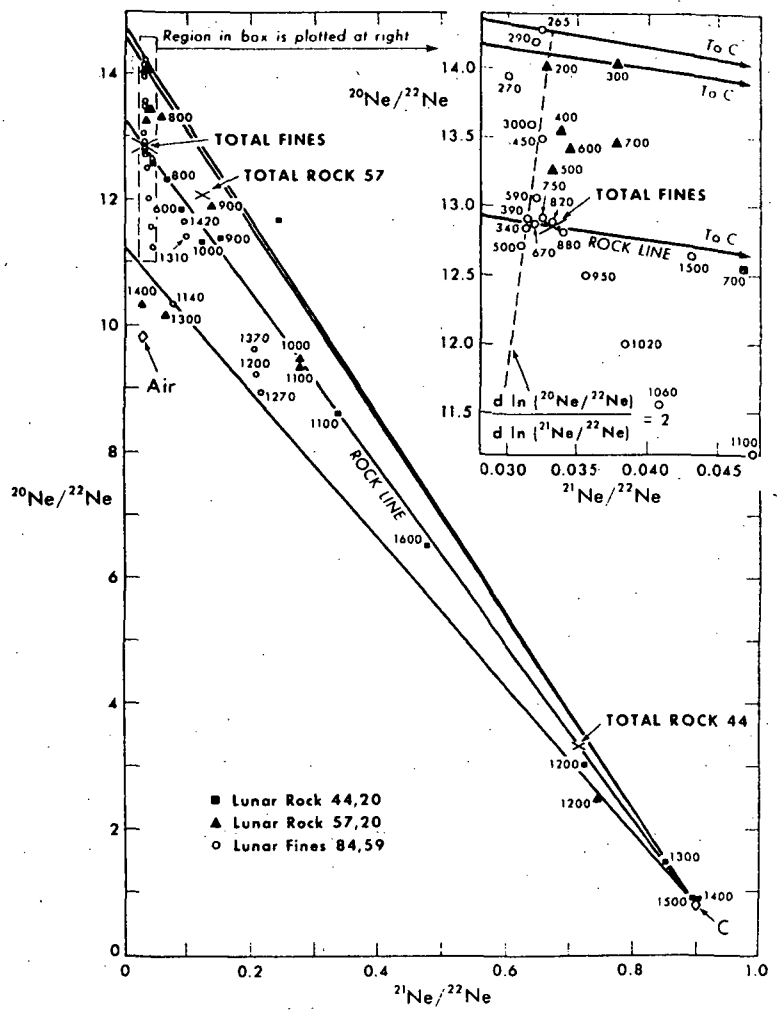

Fig. 3. Isotopic composition of neon fractions released in stepwise heating of lunar samples. The numbers are release temperatures in degrees Celsius. Mass-dependent fractionation should produce compositions on a line with d ln ($^{20}Ne/^{22}Ne$)/d ln ($^{21}Ne/^{22}Ne$) = 2. Mixing with cosmogenic neon further displaces the points toward point C. Extreme mixing lines are shown for the fines and for rock 10057. The lower mixing line for rock 10057 was omitted because of high-temperature contamination with atmospheric neon from a quartz chimney. The "rock line" should be the locus of points representing total neon from lunar samples. Rock 10044, in the temperature range plotted, essentially follows the rock line (see text).

of mixing lines through C with the diffusive trend line that in the trapped component the ratio $^{20}Ne/^{22}Ne$ varies from 14·3 to 10·9 in the course of the release. Rock 10057 is an intermediate case: it contains enough trapped gas and enough cosmogenic gas to show diffusive separation at low temperatures and strong cosmogenic features at high temperatures. At 1200°C and above, atmospheric neon from the quartz chimney

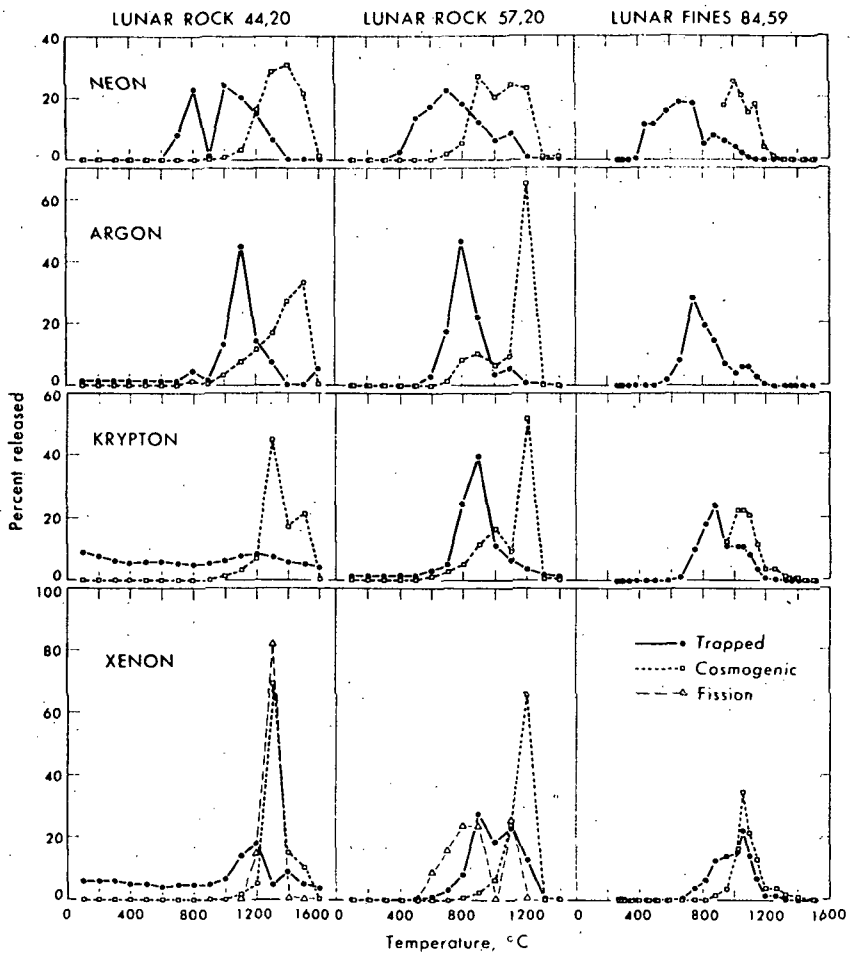

Fig. 4. Release curves for trapped, cosmogenic, and fission components from the samples. Curves are normalized to 100 per cent total release. Partial release curves are normalized to 100 per cent total for the fractions plotted. In the 900°C heating for rock 10044 there was a thermocouple malfunction; it is questionable that the temperature was actually reached.

is dominating the trapped component so that the points fall near a line joining point C with air neon.

Table 2 contains summary data on the lunar fines. For neon, krypton, and xenon we have resolved the total gas released into cosmogenic and trapped components, giving the amounts of each. For argon our estimate of the cosmogenic component would be too inaccurate (see below) to be useful and it was not included in the table. In the calculations we used the cosmogenic mass spectra for the light isotopes of Kr and Xe deduced from the highly cosmogenic gas in the 1200°C fraction from rock 10057. For neon we assumed the cosmogenic ratios corresponding to point C in Fig. 3.

Table 3. Rare gases from stepwise heating of lunar

Temperature (°C)	Ave. 1550° blank	100	200	300	400	500	600	700
$^4He/^3He$‡	—	—	1924·0‡	2157·0‡	1878·0‡	2090·0‡	1581·0‡	—[d]
	—	—	± 20·0	± 10·0	± 3·0	± 14·0	± 5·0	—
$[^3He]$, 10^{-8} cm³ STP/g	[a]	[b]	**0·149**	**0·308**	**2·594**	**12·53**	**32·74**	—[d]
$^{20}Ne/^{22}Ne$	—	11·36§	14·05§	14·04§	13·554§	13·258	13·404	13·456
	—	± 2·48	± 0·38	± 0·12	± 0·046	± 0·055	± 0·008	± 0·061
$^{21}Ne/^{22}Ne$	—	0·0274	0·0329	0·0378	0·0337	0·0331	0·0344	0·0378
	—	± 0·0025	± 0·0014	± 0·0007	± 0·0003	± 0·0003	± 0·0003	± 0·0002
$[^{22}Ne]$, 10^{-8} cm³ STP/g	**0·26***†	**0·0081**	**0·0839**	**0·2071**	**1·672**	**9·183**	**11·52**	**15·18**
$^{38}Ar/^{36}Ar$	—	0·1846	0·1802	0·1821	0·1852	0·1923	0·1924	0·1887
	—	± 0·0009	± 0·0009	± 0·0007	± 0·0009	± 0·0008	± 0·0006	± 0·0013
$^{40}Ar/^{36}Ar$	—	267·7	183·30	149·0	84·60	77·70	78·49	36·56
	—	± 0·5	± 0·40	± 0·36	± 0·09	± 0·16	± 0·07	± 0·17
$[^{36}Ar]$, 10^{-8} cm³ STP/g	**0·069***	**0·0806**	**0·1158**	**0·2084**	**0·5077**	**2·897**	**11·75**	**65·46**
$^{78}Kr/^{82}Kr$	—	—	—	—	—	—	0·0486‖	0·0453‖
	—	—	—	—	—	—	± 0·0083	± 0·0066
$^{80}Kr/^{82}Kr$	—	—	—	—	—	—	0·4253‖	0·4925‖
	—	—	—	—	—	—	± 0·0245	± 0·0225
$^{81}Kr/^{82}Kr$	—	—	—	—	—	—	—	—
	—	—	—	—	—	—	—	—
$^{83}Kr/^{82}Kr$	—	0·980	0·969	0·982	0·972	0·982	0·960	0·958
	—	± 0·019	± 0·018	± 0·022	± 0·036	± 0·039	± 0·017	± 0·012
$^{84}Kr/^{82}Kr$	—	4·642	4·541	4·627	4·649	4·291	4·198	4·198
	—	± 0·065	± 0·047	± 0·066	± 0·151	± 0·070	± 0·051	± 0·033
$^{86}Kr/^{82}Kr$	—	1·372	1·400	1·367	1·413	1·312	1·232	1·222
	—	± 0·022	± 0·019	± 0·028	± 0·047	± 0·039	± 0·023	± 0·015
$[^{82}Kr]$, 10^{-12} cm³ STP/g	**3·5***	**2·70**	**2·72**	**2·68**	**2·38**	**2·85**	**6·62**	**13·76**
$^{124}Xe/^{130}Xe$	—	—	—	—	—	—	0·0564	0·0546
	—	—	—	—	—	—	± 0·0051	± 0·0048
$^{126}Xe/^{130}Xe$	—	—	—	0·0985	—	—	0·0715	0·0795
	—	—	—	± 0·0088	—	—	± 0·0065	± 0·0038
$^{128}Xe/^{130}Xe$	—	1·257	1·110	0·912	0·839	0·976	1·099	1·142
	—	± 0·072	± 0·059	± 0·047	± 0·061	± 0·037	± 0·032	± 0·025
$^{129}Xe/^{130}Xe$	—	7·15	6·15	6·70	6·35	6·48	7·02	6·80
	—	± 0·34	± 0·27	± 0·20	± 0·27	± 0·19	± 0·22	± 0·12
$^{131}Xe/^{130}Xe$	—	5·47	4·88	5·11	4·89	5·03	5·19	5·09
	—	± 0·29	± 0·20	± 0·16	± 0·19	± 0·16	± 0·17	± 0·08
$^{132}Xe/^{130}Xe$	—	6·78	5·90	6·44	5·95	6·09	6·16	5·90
	—	± 0·28	± 0·23	± 0·19	± 0·22	± 0·17	± 0·17	± 0·087
$^{134}Xe/^{130}Xe$	—	2·75	2·38	2·431	2·467	2·363	2·393	2·258
	—	± 0·13	± 0·11	± 0·084	± 0·122	± 0·081	± 0·080	± 0·041
$^{136}Xe/^{130}Xe$	—	2·40	1·914	2·064	2·054	1·996	2·043	1·915
	—	± 0·13	± 0·082	± 0·075	± 0·092	± 0·064	± 0·062	± 0·036
$[^{130}Xe]$, 10^{-12} cm³ STP/g	**0·081***	**0·036**	**0·072**	**0·089**	**0·077**	**0·177**	**0·380**	**0·914**

Notes: Boldface entries are gas concentrations. Errors in gas concentrations are: He ± 8%; Ne ± 11% Ar ± 8%; Kr ± 18%; Xe ± 6%.

Unless otherwise specified errors are statistical only. In addition there is a fractional error in the applied mass discrimination factors as follows:

Ne 20/22: 0·01; 21/22: 0·016. Ar 38/36: 0·007; 40/36: 0·0065. Kr 78/82: 0·03; 80/82: 0·03; 83/82: 0·005; 84/82: 0·01; 86/82: 0·01. Xe 124/130: 0·013; 126/130: 0·02; 128/130: 0·05; 129/130: 0·017; 131/130: 0·005; 132/130: 0·005; 134/130: 0·005; 136/130: 0·005.

* Absolute blank in ccSTP is tabulated blank times 0·557 g.

† Total of gas fractions where this ratio was obtained.

‡ No discrimination correction available. These ratios may be systematically in error.

§ Correction has been applied for $^{40}Ar^{2+}$. Error includes uncertainty in this correction.

‖ Correction has been made for background. Error includes uncertainty in background and in discrimination correction.

rock 10057-20. Heatings were for one hour

800	900	1000	1100	1200	1300	1400	Total
2072·0‡	2138·0‡	2224·0‡	1695·0‡	1212·0‡	—	—	1809·3[e]
± 3·0	± 6·0	± 13·0	± 11·0	± 7·0	—	—	± 3·9
6·595	**3·433**	**1·002**	**0·326**	**0·402**	—	—[c]	**89·48**[e]
13·333	11·893	9·492	9·372	2·4972§	10·146§	10·350§	12·078
± 0·016	± 0·028	± 0·014	± 0·008	± 0·0088	± 0·113	± 0·088	± 0·015
0·0596	0·1362	0·2755	0·2713	0·7482	0·0666	0·0296	0·1200
± 0·0002	± 0·0005	± 0·0008	± 0·0006	± 0·0021	± 0·0011	± 0·0003	± 0·0006
12·59	**8·595**	**6·517**	**7·973**	**2·612**	**0·2211**	**0·2431**	**76·60**
0·1941	0·2085	0·2669	0·2792	1·4000	0·2405	0·1888	0·2369
± 0·0005	± 0·0006	± 0·0010	± 0·0007	± 0·0028	± 0·0017	± 0·0012	± 0·0008
18·370	34·72	146·30	43·40	212·40	154·80	235·20	39·19
± 0·037	± 0·05	± 0·28	± 0·04	± 0·33	± 0·84	± 1·00	± 0·12
176·1	**84·97**	**14·68**	**19·89**	**10·76**	**0·2153**	**0·0928**	**387·8**
0·0455‖	0·0451‖	0·0849‖	0·1084‖	0·1984‖	0·0633‖	0·0653‖	0·0844†‖
± 0·0019	± 0·0022	± 0·0036	± 0·0048	± 0·0065	± 0·0125	± 0·0155	± 0·0016
0·3285‖	0·3994‖	0·5323‖	0·3624‖	0·6086‖	0·2819‖	0·3188‖	0·4420†‖
± 0·0111	± 0·0130	± 0·0171	± 0·0129	± 0·0197	± 0·0564	± 0·0603	± 0·0066
—	—	—	—	0·0072‖	—	—	—
—	—	—	—	± 0·0012	—	—	—
0·998	0·981	1·052	1·161	1·300	0·964	0·941	1·062
± 0·011	± 0·010	± 0·010	± 0·010	± 0·012	± 0·018	± 0·030	± 0·012
4·482	4·399	3·215	3·184	1·054	4·347	4·436	3·567
± 0·026	± 0·031	± 0·016	± 0·023	± 0·007	± 0·051	± 0·118	± 0·032
1·310	1·299	0·9025	0·9200	0·1960	1·274	1·236	1·022
± 0·009	± 0·036	± 0·0083	± 0·0093	± 0·0018	± 0·025	± 0·037	± 0·023
63·05	**106·1**	**43·17**	**25·47**	**60·38**	**3·27**	**2·57**	**337·8**
0·0555	0·0632	0·1325	0·2668	0·4557	—	0·2046	0·2650†
± 0·0019	± 0·0014	± 0·0021	± 0·0035	± 0·0027	—	± 0·0137	± 0·0028
0·0792	0·0901	0·2168	0·4604	0·8235	—	0·0897	0·4647†
± 0·0023	± 0·0018	± 0·0045	± 0·0047	± 0·0064	—	± 0·0174	± 0·0050
0·800	0·7659	0·7590	0·9591	1·3770	1·457	0·878	1·048
± 0·017	± 0·0098	± 0·0075	± 0·0118	± 0·0095	± 0·135	± 0·075	± 0·013
6·381	6·288	5·289	4·033	2·152	6·53	6·39	4·107
± 0·078	± 0·071	± 0·055	± 0·037	± 0·018	± 0·49	± 0·26	± 0·058
5·099	5·176	5·456	5·919	6·976	5·91	5·38	6·048
± 0·065	± 0·066	± 0·056	± 0·058	± 0·048	± 0·36	± 0·26	± 0·062
5·780	5·763	4·906	3·614	1·523	5·56	6·13	3·579
± 0·063	± 0·060	± 0·043	± 0·029	± 0·007	± 0·30	± 0·19	± 0·046
2·164	2·110	1·780	1·303	0·4819	2·11	2·48	1·282
± 0·036	± 0·028	± 0·022	± 0·015	± 0·0050	± 0·13	± 0·11	± 0·023
1·789	1·719	1·454	1·046	0·3758	1·609	1·88	1·039
± 0·029	± 0·031	± 0·015	± 0·010	± 0·0049	± 0·093	± 0·55	± 0·027
2·506	**8·567**	**7·118**	**12·96**	**18·78**	**0·035**	**0·061**	**51·78**

[a] ^{3}He not measured. ^{4}He concentration: **0·72** × 10^{-8} cm^3 STP/g.
[b] ^{3}He not measured. ^{4}He concentration: **11·1** × 10^{-8} cm^3 STP/g.
[c] ^{3}He not measured. ^{4}He concentration: **7·2** × 10^{-8} cm^3 STP/g.
[d] Gas lost.
[e] Includes estimate for the one significant gas fraction lost.
[f] High blank (high temperature only) because of quartz chimney (see text).

In addition to amounts, Table 2 contains corrected isotopic compositions for the trapped components. These can safely be identified as the solar component for neon, krypton, and xenon, except for possible fission effects in xenon.

Argon from the fines is a complex system where a number of effects operate together in the stepwise release. The initial $^{38}Ar/^{36}Ar$ ratio of 0·18 rises to 0·19 at 750°C where the release of trapped argon reaches its peak. Judging from the release curves (see Fig. 4) for cosmogenic neon and krypton from the fines, cosmogenic argon has not yet begun to be released at this temperature so that we must again ascribe the change in the ratio to diffusive separation of the isotopes. The initial $^{38}Ar/^{36}Ar$ ratio is 5·3 per cent lower than that for the total. Again, as with helium and neon, the initial distortion in the ratio seems to be just the mass ratio for the isotopes involved. Above 750°C the cosmogenic argon begins to be released, increasing the $^{38}Ar/^{36}Ar$ ratio further. The interplay of the two independent effects on the ratio makes it difficult to compute the amount of cosmogenic argon in the fines with any precision and the computation was not attempted. It was possible, however, to ascertain that the $^{38}Ar/^{36}Ar$ ratio in the trapped component is 0·19 as reported in Table 2.

The sample certainly contains radiogenic ^{40}Ar. The difficulty in knowing how much of the ^{40}Ar is due to potassium decay in the fines themselves has been described very clearly by HEYMANN *et al.* (1970) who find that ^{40}Ar in the lunar fines is predominantly surface correlated with solar ^{36}Ar, but in proportions ($^{40}Ar/^{36}Ar = 1·056$) which greatly exceed what can reasonably be expected from the sun (BERNSTEIN *et al.*, 1963). Our concentrations for ^{36}Ar and ^{40}Ar plot near, but not precisely on, the correlation line in the paper by HEYMANN *et al.* (1970).

Our total rare gas concentrations for sample 10084 are higher than values by HEYMANN *et al.* (1970), HINTENBERGER *et al.* (1970) and MARTI *et al.* (1970) among whom there is rough consensus on the rare gas contents of this sample. For Ne, Kr and Xe our concentrations are about 100 per cent higher than those reported by MARTI *et al.*; for He and Ar, about 50 per cent higher. A possible difference in average grain size between our samples could easily produce differences in gas concentration of this magnitude, since the concentrations depend strongly on grain size.

Figure 4 includes fractional release curves against temperature for the trapped component of Ne, Ar, Kr and Xe in the dust. Cosmogenic release curves are also included, except for argon. As expected, the cosmogenic component is released at higher temperatures than the trapped component. And release of the trapped component is shifted toward higher temperatures as one progresses from helium (Fig. 2) to xenon.

RESULTS FROM FINE GRAINED CRYSTALLINE ROCK 10057

Rock 10057 is a good example of a system where a stepwise heating analysis permits us to sort out the various rare gas components with good success. The stone was heated in 100° steps. All the data are set out in Table 3. The neon results have already been discussed in the section on lunar fines.

The xenon analysis is the most complex. We know just from the uranium content and age of the rock that there is a significant xenon component from spontaneous fission of ^{238}U in addition to the cosmogenic and trapped components. We thus are dealing with at least a three component system for many of the isotopes. HOHENBERG

et al. (1967) showed in their work on stepwise heating of the Pasamonte calcium-rich achondrite that such a three component system can be unraveled without foreknowledge of the isotopic composition of the cosmogenic and fissiogenic components. An isotope ratio which was pivotal, on one correlation diagram, for subtracting a component was treated as a free parameter. "Success" of the subtraction based on an assigned value for this parameter could be judged by the fit of the residual gas, after

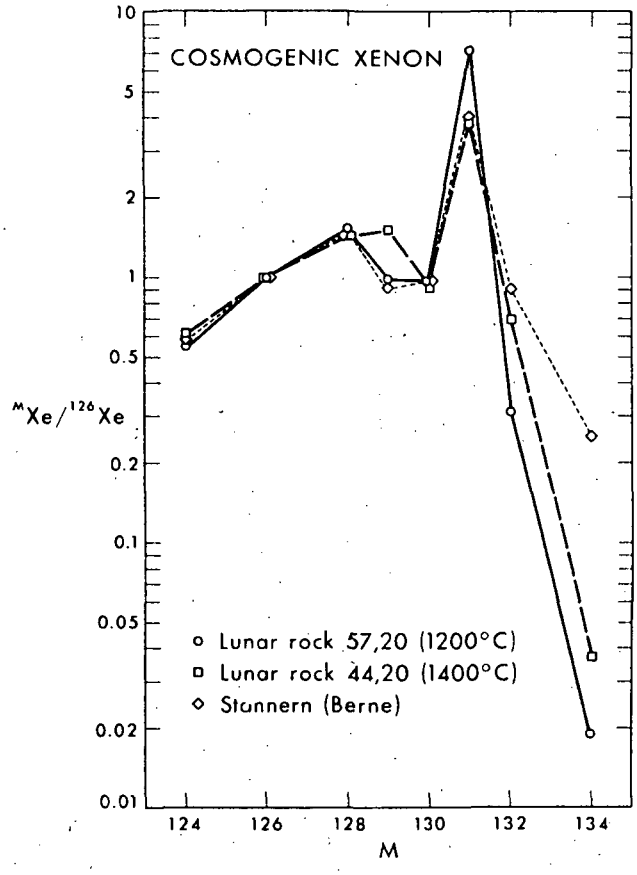

Fig. 5. Isotopic composition of cosmogenic xenon from lunar rocks. The comparison spectrum is cosmogenic xenon from the Stannern calcium-rich achondrite (MARTI *et al.*, 1966). The point for ^{128}Xe in the comparison spectrum is a value based on achondrites by ROWE (1967). Except at mass 131 the errors in the comparison spectrum and the lunar spectra overlap.

the subtraction, to a straight line on a second correlation diagram. With an electronic computer, the computational cycle was repeated rapidly and a best value for the free parameter quickly obtained.

In the present work we have made some short cuts instead of a complete analysis, but we have been able thereby to complete an adequate (if not the best possible) analysis quite quickly "by hand." In rock 10057 the successful short cut was to assume

sample, 10084) from the 1200°C fraction then immediately gave us the isotopic composition of the cosmogenic component. The end points were now known on the two-component correlation diagram (trapped and cosmogenic) for $^{124}Xe/^{130}Xe$ vs. $^{126}Xe/^{130}Xe$. This diagram could then be used to partition ^{130}Xe between trapped and cosmogenic components in the various temperature fractions. Trapped xenon was subtracted off by this technique and the residual xenon tested as a two-component system (cosmogenic and fissiogenic xenon) on the correlation diagram for $^{134}Xe/^{132}Xe$ vs. $^{136}Xe/^{132}Xe$. A straight line spanning the compositions of the cosmogenic xenon

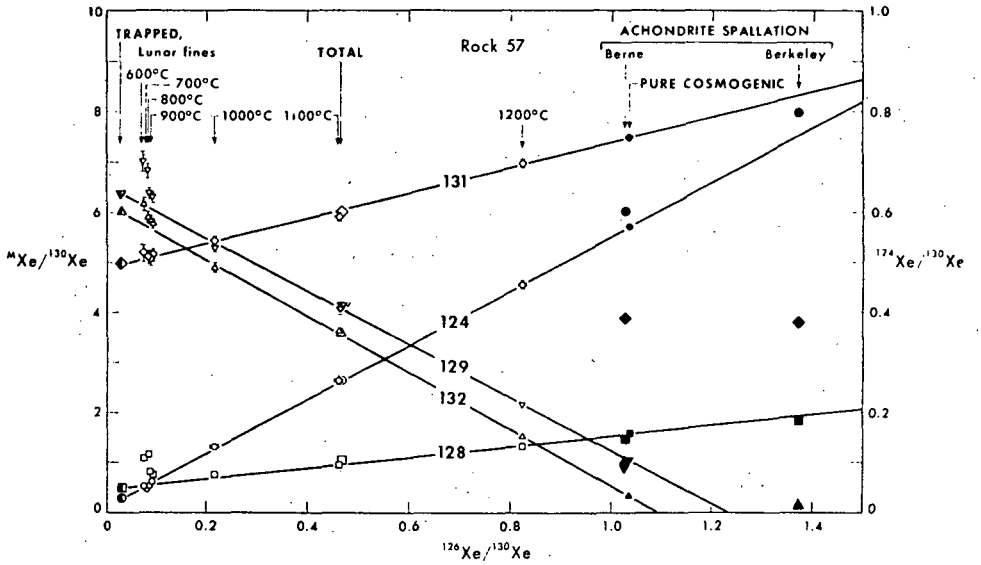

Fig. 6. Graphical analysis of the xenon released in stepwise heating of lunar rock 10057. Small corrections for fission have been made at masses 131 and 132. Isotopes 124, 126, 130 and 132 appear to belong to a simple two-component system (trapped and cosmogenic xenon). Isotope 131 fits a two-component model but with a highly anomalous composition for the cosmogenic component. Isotopes 128 and 129 display excess amounts in the temperature range 600 to 900°C inclusive but these excesses are now thought to be almost certainly due to memory of gas from a neutron-irradiated meteorite previously studied in the mass spectrometer. The errors shown are statistical only. Total errors are larger.

and xenon from spontaneous fission of ^{238}U was found. This last diagram could be used, in turn, for subtracting off fissiogenic xenon in the various temperature fractions where fission corrections were needed.

Some of the results of this analysis will now be presented. In Fig. 5 and Table 2 that the isotope ^{136}Xe in the highly cosmogenic 1200°C fraction was all trapped xenon (no fission or cosmogenic xenon). Subtraction of trapped xenon (as seen in the dust we exhibit the isotopic composition so obtained for the cosmogenic xenon. The spectrum for rock 10057 is compared with the cosmogenic spectrum for the Stannern calcium-rich achondrite. We have plotted the values obtained for this last spectrum by MARTI *et al.* (1966) at Berne simply because their values fit the lunar sample better

than other spectra do. Their spectrum has been supplemented by a meteoritic value for $(^{129}Xe/^{126}Xe)_{cosmogenic}$ obtained by ROWE (1967). Agreement between the meteoritic and lunar spectra are quite good, except at mass 131 where there is a large and conspicuous excess in the lunar sample. The discrepancies at masses 132 and 134, which are not so large in terms of absolute gas concentration, are not significant when errors are considered.

The correlation diagram for $^{124}Xe/^{130}Xe$ vs. $^{126}Xe/^{130}Xe$ is shown in Fig. 6. The

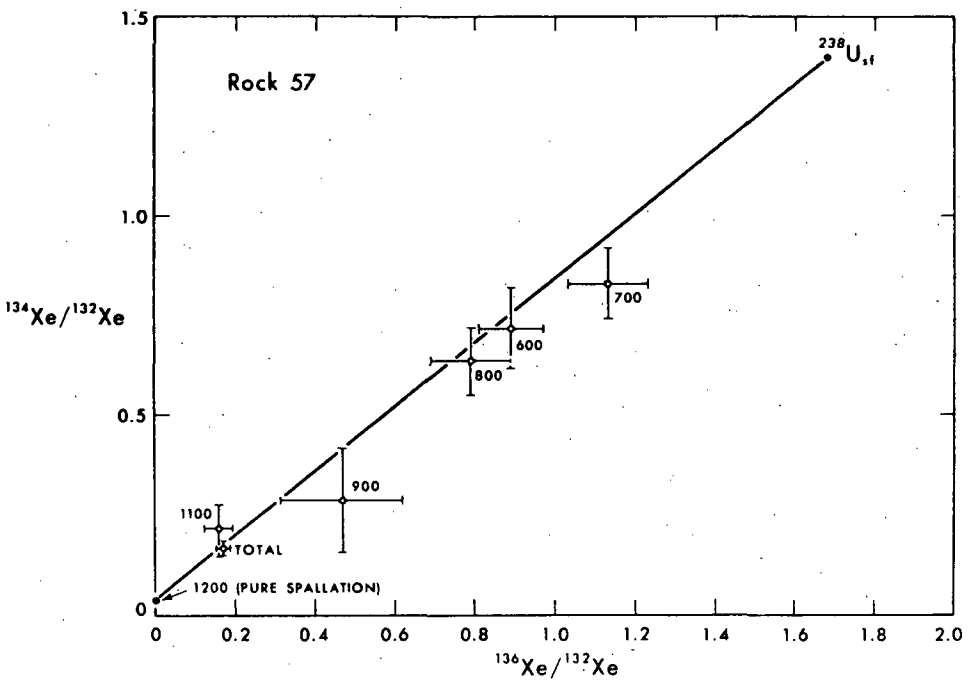

Fig. 7. Correlation of ratios $^{134}Xe/^{132}Xe$ and $^{136}Xe/^{132}Xe$ in rock 10057. Trapped xenon has been subtracted off before computing the ratios. The diagram is consistent with a two-component system of cosmogenic xenon and fissiogenic xenon from spontaneous fission of ^{238}U. The errors shown are statistical only. Total errors are larger.

experimental points fit the line very closely. For each point the amounts of $(^{130}Xe)_{cosmogenic}$ and $(^{130}Xe)_{trapped}$ are in inverse proportion to the line segments between the measured point and the cosmogenic and trapped end points. The release curves for trapped and cosmogenic xenon based on this partitioning are shown in Fig. 4. After subtraction of the trapped component, the correlation line for the heavy isotopes $^{134}Xe/^{132}Xe$ vs. $^{136}Xe/^{132}Xe$ should be a straight line. It is displayed in Fig. 7 where we see that within experimental error the points define a line between the spallation composition and the composition of xenon from the spontaneous fission of ^{238}U (WETHERILL, 1953). The release pattern for the fission component is also shown in Fig. 4. The shape is somewhat unlikely (of course the zero at 1200°C is an artifact: it was assumed so) and one wonders how, if at all, the shape would be altered by a more complete,

computerized analysis. But the total amount of fission ^{136}Xe found is in agreement with that expected after $3{\cdot}7 \times 10^9$ yr (ALBEE *et al.*, 1970) decay by spontaneous fission of 800 ppb (LSPET, 1969) uranium: $1{\cdot}3 \times 10^{-12}$ cm^3 STP/g found; $1{\cdot}5 \times 10^{-12}$ cm^3 STP/g expected. In this calculation we used $1{\cdot}0 \times 10^{16}$ yr as the half-life for spontaneous fission of ^{238}U (FLEISCHER and PRICE, 1964). The fission results were used to correct the ratios $^{131}Xe/^{130}Xe$ and $^{132}Xe/^{130}Xe$ shown in Fig. 6. The corrections are not large. Figure 6, where ratios $^{M}Xe/^{130}Xe$ are plotted against $^{126}Xe/^{130}Xe$, provides a comprehensive display of the xenon isotope variations in rock 10057. For values of M equal to 124 (already discussed), 131, and 132, the points fall reasonably well on lines joining the 1200°C fraction and the fraction seen at 820°C in the lunar fines. These isotopes, with ^{126}Xe and ^{130}Xe, appear after fission correction to belong to a two-component system of trapped and cosmogenic xenon. For values of M equal to 128 and 129, the points between 600° and 900°C fall above the lines containing the other points, as would occur if there were an excess of ^{128}Xe and ^{129}Xe being released at these temperatures. The amounts seen in excess are given in our summary Table 2. We now believe, for reasons discussed below, that the apparent excesses in ^{128}Xe and ^{129}Xe are due to memory of gas samples from a neutron irradiated meteorite studied earlier in the same mass spectrometer. One should note in Fig. 6 that the correlation lines pass close to the compositions for cosmogenic xenon in calcium-rich achondrites, except at mass 131 where the correlation line observed has the opposite slope for that observed in the Stannern meteorite.

The analysis for krypton from rock 10057 is much simpler than that for xenon because there is no appreciable fission krypton component. The assumption that krypton is the 1200°C fraction contains only trapped krypton at mass 86 should be nearly true. The cosmogenic spectrum for krypton so derived is given in Table 2 and shown in Fig. 8 along with the achondritic spectrum for Stannern as computed by MARTI *et al.* (1966). The correlations of $^{80}Kr/^{84}Kr$ and $^{82}Kr/^{84}Kr$ with $^{83}Kr/^{84}Kr$ revealed an apparent excess of ^{80}Kr and ^{82}Kr for temperatures below 1100°C. Otherwise the correlation lines for krypton were those for a two component system, leading to the release curves shown in Fig. 4. Radioactive ^{81}Kr was observed (especially in the 1200°C fraction), permitting calculation of a $^{81}Kr/^{83}Kr$ exposure age for the rock (see the section on exposure ages, below).

The ratio of the total ^{80}Kr excess to the total ^{82}Kr excess is 3·8, within 15 per cent or so error. For krypton produced by pile neutrons on bromine, the ratio is $3{\cdot}94 \pm 0{\cdot}05$ (REYNOLDS, 1950). The ratios of excess ^{80}Kr to excess ^{82}Kr in the individual temperature fractions are in good agreement, with few exceptions, with the ratio for the total excess krypton. It thus seems almost certain that we are seeing excess krypton which originated in a neutron irradiation of bromine. It is equally certain that this krypton did not originate in the sample. The highest bromine content (0·38 ppm) reported in lunar material (REED *et al.*, 1970) combined with the highest neutron exposure (17×10^{15} cm^{-2}) reported for lunar material (ALBEE *et al.*, 1970) generates only 10^{-11} cm^3 STP/g of excess ^{80}Kr. We find $3{\cdot}9 \times 10^{-11}$ cm^3 STP/g in rock 10057. The argument is even stronger in rock 10044 where REED *et al.* measured the bromine (0·22 ppm) and ALBEE *et al.* have put an upper limit of about 10^{15} cm^{-2} on the integrated neutron flux. There will be less than $0{\cdot}3 \times 10^{-12}$ cm^3 STP/g excess ^{80}Kr produced; we find

13×10^{-12} cm^3 STP/g. We did not have to look far to find a source of the excess krypton and xenon. Ten months prior to the lunar work, the mass spectrometer (but not the sample system) was used to study xenon from a heavily neutron-irradiated sample of the enstatite chondrite Abee (HOHENBERG and REYNOLDS, 1969). Krypton from the meteorite was admitted along with the xenon. The amount of excess ^{80}Kr admitted to the spectrometer from the larger of two samples studied totaled about 6×10^{-8} cm^3 STP or about 2800 times the amount of excess ^{80}Kr found in rock 10057. Such an amount of "memory" appears (in hindsight!) to be quite reasonable.

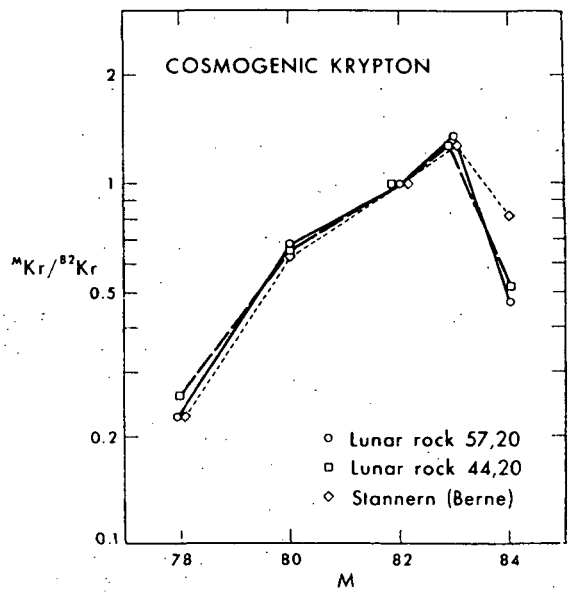

Fig. 8. Isotopic composition of cosmogenic krypton from lunar rocks. The comparison spectrum is cosmogenic krypton from the Stannern calcium-rich achondrite (MARTI *et al.*, 1966). At all masses the errors in the comparison spectrum and the lunar spectra overlap.

The excesses of ^{128}Xe and ^{129}Xe can be ascribed to the same source. In the irradiated meteorite the ratio of excess ^{129}Xe to ^{128}Xe was 1·47. In rock 10057, the ratio was the same, 1·43 (and close to that in all temperature fractions where excesses were observed). The amount of excess ^{128}Xe admitted to the mass spectrometer from the larger run with the meteorite was $0{\cdot}33 \times 10^{-8}$ cm^3 STP or 2100 times the amount of excess ^{128}Xe in rock 10057. We need say no more about excess Kr and Xe isotopes in rock 10057!

The release curves for argon and neon, also shown in Fig. 4, were computed in the same way as for the fines (see above). Looking at all the release curves for rock 10057 together, we note that the cosmogenic fraction was released similarly for all the gases, at temperatures near the melting point for the rock. Release of the trapped component takes place at lower temperatures and at temperatures which are shifted

upward progressively in going from neon to xenon. Note the agreement in temperature for each gas between the release of the trapped component in rock 10057 and in the fines. The chemical ratios (e.g. He/Ne etc.) are also very similar in rock 10057 and the fines. Our sample of 10057 is either contaminated with lunar dust or contains a surface patch in which solar wind gases have been imbedded. Other samples of rock 10057 which have been run (FUNKHOUSER *et al.*, 1970; WANLESS *et al.*, 1970; HINTENBERGER *et al.*, 1970) appear to contain much less trapped gas.

The $^{40}Ar/^{36}Ar$ ratio in rock 10057 greatly exceeds that in the fines. The excess ^{40}Ar has to be attributed to potassium decay in the rock. Curiously, our value of ^{40}Ar is more than 3 times higher than values reported by other investigators. We cannot explain this discrepancy. In rock 10044 (see below) we measured *less* ^{40}Ar than other investigators. Air argon cannot contribute appreciably to ^{40}Ar in rock 10057, judging from the release curve.

RESULTS FROM MEDIUM GRAINED CRYSTALLINE ROCK 10044

Our calculations for rock 10044 were very similar to those for rock 10057, and the same general sorts of results were obtained. The Figures and Tables contain a parallel display of results for the two rocks. In this section we mainly stress the differences encountered with rock 10044. The complete stepwise heating data are set out in Table 4.

The essential short cut for the xenon calculations in rock 10044 was the assumption that the 1400°C fraction contains only trapped ^{136}Xe. This will not be strictly true, we know, but quite consistent results were obtained with the assumption. The cosmogenic xenon spectrum so obtained is set out in Table 2 and Fig. 5. Cosmogenic xenon in rock 10044 differs markedly from rock 10057 at mass 131. The relative abundance of cosmogenic ^{131}Xe in rock 10044 is more nearly that in calcium-rich achondrites. Variability in the relative production of cosmogenic ^{131}Xe is probably some sort of depth effect. Since our sample of rock 10057 may include some lunar surface (as judged from the concentration of trapped gases) whereas rock 10044 appears (from the lack of trapped gas) to be an interior piece, we tentatively assign high production of ^{131}Xe to surface locations. Cosmogenic ^{129}Xe also differs in relative strength between rocks 10044 and 10057. As we shall see below, the amount of ^{129}Xe in the various temperature fractions is somewhat erratic in this rock, which makes it difficult to be sure about the abundance of ^{129}Xe in the cosmogenic spectrum for rock 10044.

The correlation diagram (Fig. 9) for $^{124}Xe/^{130}Xe$ vs. $^{126}Xe/^{130}Xe$ is well behaved for rock 10044 and permits us to subtract off trapped xenon and to prepare a two component correlation diagram for the heavy xenon isotopes (Fig. 10). The concentrations of trapped xenon in the various temperature fractions of rock 10044 are never greatly above the level of the xenon "hot blank," so that atmospheric values have been used for the isotopic composition of the trapped xenon. The actual trapped component is probably a blend of atmospheric and solar xenon. Figure 10 shows that the heavy isotope data are consistent with the fission xenon component originating from spontaneous fission of ^{238}U. In rock 10044 we find too much ^{136}Xe from fission. Expected from a $3{\cdot}7 \times 10^9$ yr old rock (ALBEE *et al.*, 1970; TURNER, 1970) with 280 ppb

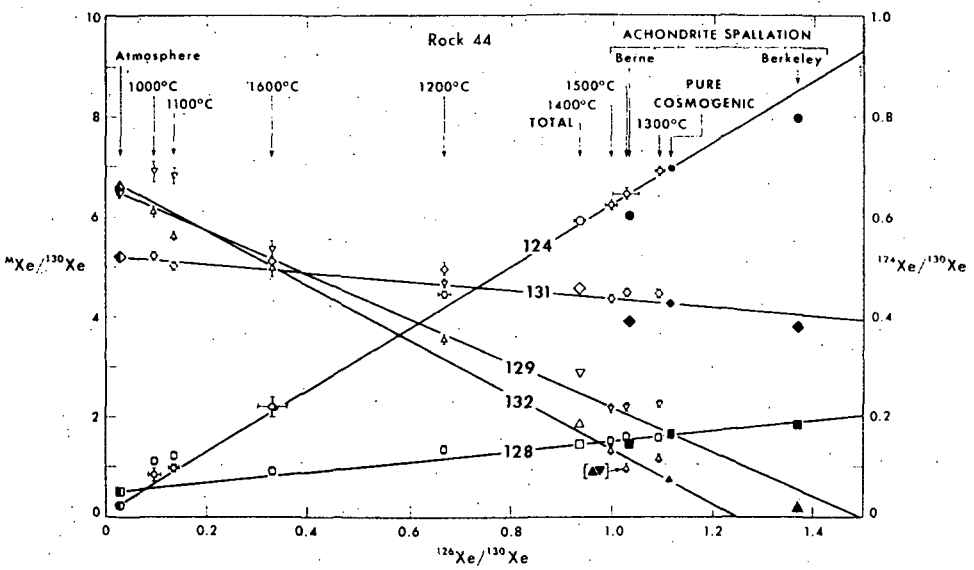

Fig. 9. Graphical analysis of the xenon released in stepwise heating of lunar rock 10044. Small corrections for fission have been made at masses 131 and 132. Isotopes 124, 126, 130, and 131 appear to belong to a simple two-component system (trapped and cosmogenic xenon). Excess ^{128}Xe and ^{129}Xe at 1000, 1100 and 1600°C is thought to be almost certainly memory of gas from an irradiated meteorite previously studied in the mass spectrometer. Isotopes 129 and 132 are in excess at 1200 and 1300°C, where the effects are *not* instrumental. Error shown are statistical only. Total errors are larger.

uranium (WÄNKE *et al.*, 1970) is $0{\cdot}5 \times 10^{-12}$ cm^3 STP/g; whereas we found $1{\cdot}5 \times 10^{-12}$ cm^3 STP/g. Possibly our sample contained more uranium than 280 ppb.

The comprehensive display of isotope abundance variations in xenon appears in Fig. 9. The isotopes ^{131}Xe and ^{132}Xe have been fission corrected. The most noteworthy feature of the diagram is the erratic behavior of ^{129}Xe. A correlation line for $^{129}Xe/^{130}Xe$ vs. $^{126}Xe/^{130}Xe$ has been drawn between trapped xenon and xenon in the 1400°C fraction. The choice leads to positive excesses of ^{129}Xe at most other temperatures, but no negative ones. Use of the cosmogenic ^{129}Xe abundance for rock 10057 would produce an even more steeply dipping correlation line and would lead to even greater excesses of ^{129}Xe in the various temperature fractions. The total excess ^{129}Xe calculated from the construction shown in Fig. 9 is $5{\cdot}2 \times 10^{-12}$ cm^3 STP/g. Only part of this is due to memory of the gas from the irradiated meteorite: we attribute the excesses at 1000, 1100 and 1600°C and part of the excess at 1200°C (totaling perhaps $0{\cdot}7 \times 10^{-12}$ cm^3 STP/g) to this source. The remainder at 1200 and the whole at 1300°C (totaling 5×10^{-12} cm^3 STP/g) is not an instrumental effect. It is accompanied at just those two temperatures by significant amounts of excess ^{132}Xe and possibly some ^{124}Xe and ^{131}Xe. It seems possible that there may be more than one cosmogenic component in rock 10044. It would be interesting to work with mineral separates of this rock as a means of exploring the question further.

Table 4. Rare gases from stepwise heating of lunar

Temperature (°C)	Ave. 1500° Blank	100	200	300	400	500	600	700	800
$^4He/^3He$	—	3817·0‡	1733·0‡	6536·0‡	2320·0‡	2041·0‡	1497·0‡	672·6‡	372·5‡
	—	±190·0	±33·0	±726·0	±151·0	±46·0	±27·0	±2·3	±0·4
[^{3}He], 10^{-8} cm^3 STP/g	a	**0·0004**	**0·0039**	**0·0002**	**0·0020**	**0·0029**	**0·0435**	**4·365**	**24·28**
$^{20}Ne/^{22}Ne$	—	9·1§	10·6§	8·4§	10·5§	11·5§	11·44§	12·55§	12·32
	—	±9·4	±6·8	±11·4	±7·0	±6·0	±0·38	±0·08	±0·05
$^{21}Ne/^{22}Ne$	—	0·0294	0·0514	0·0488	0·0374	0·0444	0·0889	0·0468	0·0678
		±0·0055	±0·0029	±0·0042	±0·0056	±0·0018	±0·0062	±0·0010	±0·0009
[^{22}Ne], 10^{-8} cm^3 STP/g	**0·0042***	**0·0021**	**0·0023**	**0·0017**	**0·0023**	**0·0025**	**0·0077**	**0·176**	**0·482**
$^{38}Ar/^{36}Ar$	—	0·1826	0·1841	0·1849	0·1879	0·1848	0·1895	0·3010	0·6101
	—	±0·0010	±0·0010	±0·0008	±0·0010	±0·0009	±0·0007	±0·0013	±0·0019
$^{40}Ar/^{36}Ar$	—	296·8	300·2	299·4	298·6	298·7	295·6	298·8	363·5
	—	±0·3	±0·7	±0·6	±0·8	±0·5	±0·4	±0·6	±0·8
[^{36}Ar], 10^{-8} cm^3 STP/g	**0·24***	**0·256**	**0·221**	**0·221**	**0·239**	**0·251**	**0·221**	**0·312**	**1·100**
$^{78}Kr/^{82}Kr$	—	—	—	—	—	—	—	—	—
	—	—	—	—	—	—	—	—	—
$^{80}Kr/^{82}Kr$	—	—	—	—	—	—	—	—	—
	—	—	—	—	—	—	—	—	—
$^{81}Kr/^{82}Kr$	—	—	—	—	—	—	—	—	—
	—	—	—	—	—	—	—	—	—
$^{83}Kr/^{82}Kr$	—	0·956	0·950	0·929	0·955	0·975	0·944	0·957	0·941
	—	±0·016	±0·016	±0·021	±0·014	±0·024	±0·020	±0·025	±0·021
$^{84}Kr/^{82}Kr$	—	4·583	4·745	4·635	4·681	4·715	4·635	4·61	4·573
	—	±0·068	±0·059	±0·091	±0·051	±0·099	±0·087	±0·10	±0·078
$^{86}Kr/^{82}Kr$	—	1·316	1·393	1·334	1·364	1·370	1·365	1·367	1·333
	—	±0·023	±0·024	±0·028	±0·020	±0·032	±0·028	±0·033	±0·025
[^{82}Kr], 10^{-12} cm^3 STP/g	**16·3***	**16·43**	**13·46**	**10·85**	**9·77**	**10·20**	**10·19**	**9·78**	**8·50**
$^{124}Xe/^{130}Xe$	—	—	—	—	—	—	—	—	—
	—	—	—	—	—	—	—	—	—
$^{126}Xe/^{130}Xe$	—	—	—	—	—	—	—	—	—
	—	—	—	—	—	—	—	—	—
$^{128}Xe/^{130}Xe$	—	0·735	0·648	0·646	0·694	0·623	0·656	0·668	0·705
	—	±0·034	±0·052	±0·038	±0·048	±0·054	±0·045	±0·049	±0·046
$^{129}Xe/^{130}Xe$	—	6·84	6·17	6·54	6·56	6·43	6·88	6·50	6·02
	—	±0·18	±0·25	±0·31	±0·22	±0·31	±0·30	±0·35	±0·26
$^{131}Xe/^{130}Xe$	—	5·28	4·98	5·18	5·23	5·04	5·35	5·05	4·95
	—	±0·14	±0·18	±0·23	±0·18	±0·23	±0·23	±0·28	±0·18
$^{132}Xe/^{130}Xe$	—	6·56	6·12	6·31	6·51	6·35	6·76	6·36	5·97
	—	±0·12	±0·22	±0·27	±0·19	±0·27	±0·23	±0·33	±0·21
$^{134}Xe/^{130}Xe$	—	2·596	2·334	2·42	2·482	2·45	2·61	2·44	2·297
	—	±0·061	±0·098	±0·12	±0·088	±0·12	±0·10	±0·13	±0·090
$^{136}Xe/^{130}Xe$	—	2·202	1·976	2·125	2·056	1·996	2·24	2·03	1·971
	—	±0·053	±0·078	±0·097	±0·072	±0·091	±0·10	0·11	±0·073
[^{130}Xe], 10^{-12} cm^3 STP/g	**0·124***	**0·116**	**0·106**	**0·101**	**0·093**	**0·103**	**0·082**	**0·094**	**0·097**

Notes: Boldface entries are gas concentrations. Errors in gas concentrations are: He ± 13%; Ne ± 10%; Ar ± 10%; Kr ± 30%; Xe ± 6%.

Unless otherwise specified errors are statistical only. In addition there is a fractional error in the applied mass discrimination factors as follows:

Ne 20/22: 0·01; 21/22: 0·016. Ar 38/36: 0·007; 40/36: 0·0065. Kr 78/82: 0·03; 80/82: 0·03; 83/82: 0·005; 84/82: 0·01; 86/82: 0·01. Xe 124/130: 0·013; 126/130: 0·02; 128/130: 0·05; 129/130: 0·017; 131/130: 0·005; 132/130: 0·005; 134/130: 0·005; 136/130: 0·005.

rock 10044-20. Heatings were for one hour

900[b]	1000	1100	1200	1300	1400	1500	1600	Total
152·72‡	100·60‡	111·00‡	210·8‡	207·0‡	92·06‡	58·46‡	2513·0‡	213·7‡
± 0·28	± 0·10	± 0·15	± 0·2	± 0·5	± 0·27	± 0·19	± 133·0	± 0·15
2·889[b]	**24·43**	**23·80**	**12·19**	**6·79**	**2·468**	**1·132**	**0·00297**	**102·4**
11·39	11·35	8·610	3·062	1·490	0·8779	0·9113§	6·53§	3·311
± 0·08	± 0·04	± 0·034	± 0·010	± 0·012	± 0·0041	± 0·0045	± 0·23	± 0·027
0·1499	0·1239	0·3364	0·7264	0·8515	0·9046	0·8955	0·477	0·7193
± 0·0034	± 0·0011	± 0·0024	± 0·0030	± 0·0087	± 0·0056	± 0·0045	± 0·021	± 0·0072
0·0273[b]	**0·522**	**0·630**	**1·503**	**2·265**	**2·267**	**1·612**	**0·0076**	**9·510**
0·3757	0·4978	0·4551	0·9091	1·191	1·516	1·521	0·4233	0·9843
± 0·0017	± 0·0010	± 0·0058	± 0·0034	± 0·003	± 0·002	± 0·003	± 0·0016	± 0·0036
396·7	352·7	316·6	720·4	346·9	103·5	51·82	249·0	282·8
± 1·4	± 0·5	± 0·4	± 1·8	± 0·7	± 0·9	± 0·07	± 0·5	± 0·8
0·241[b]	**2·842**	**9·385**	**5·100**	**5·111**	**6·907**	**8·404**	**1·099**	**41·91**
—	—	0·050‖	0·0962‖	0·2215‖	0·1739‖	0·1822‖	—	0·1740‖†
—	—	± 0·018	± 0·0098	± 0·0075	± 0·0086	± 0·0086	—	± 0·0043
—	0·286‖	0·448‖	0·513‖	0·619‖	0·493‖	0·536‖	0·137‖	0·522‖†
—	± 0·057	± 0·036	± 0·024	± 0·020	± 0·019	± 0·020	± 0·040	± 0·010
—	—	—	—	0·00236‖	—	—	—	—
—	—	—	—	± 0·00057	—	—	—	—
0·926	0·948	0·944	1·062	1·235	1·192	1·233	0·983	1·0928
± 0·016	± 0·024	± 0·015	± 0·018	± 0·012	± 0·016	± 0·017	± 0·027	± 0·0049
4·547	4·376	3·860	2·967	1·176	1·800	1·560	4·74	2·886
± 0·071	± 0·099	± 0·051	± 0·023	± 0·005	± 0·014	± 0·012	± 0·12	± 0·010
1·314	1·257	1·108	0·808	0·2359	0·4261	0·3275	1·353	0·7802
± 0·022	± 0·032	± 0·018	± 0·010	± 0·0045	± 0·0060	± 0·0036	± 0·038	± 0·0037
10·03	**11·81**	**17·05**	**24·34**	**77·48**	**35·52**	**39·26**	**7·07**	**311·8**
—	0·0845	0·0973	0·444	0·6896	0·6206	0·643	0·222	0·6307†
—	± 0·0091	± 0·0057	± 0·014	± 0·0074	± 0·0093	± 0·016	± 0·019	± 0·0053
—	0·097	0·1379	0·669	1·096	0·998	1·029	0·331	1·001†
—	± 0·012	± 0·0076	± 0·014	± 0·017	± 0·015	± 0·025	± 0·029	± 0·011
0·655	1·102	1·226	1·355	1·579	1·510	1·516	0·914	1·471
± 0·050	± 0·036	± 0·042	± 0·025	± 0·022	± 0·021	± 0·028	± 0·039	± 0·014
6·21	6·91	6·83	4·688	2·252	2·185	2·174	5·34	2·848
± 0·33	± 0·19	± 0·12	± 0·074	± 0·027	± 0·035	± 0·056	± 0·21	± 0·020
4·84	5·24	5·040	4·964	4·463	4·369	4·430	5·10	4·548
± 0·26	± 0·15	± 0·095	± 0·093	± 0·052	± 0·056	± 0·083	± 0·21	± 0·034
6·05	6·37	5·720	3·795	1·265	1·347	1·340	5·06	1·965
± 0·30	± 0·10	± 0·075	± 0·056	± 0·012	± 0·014	± 0·021	± 0·19	± 0·010
2·21	2·452	2·240	1·325	0·2611	0·2929	0·2742	1·790	0·5583
± 0·12	± 0·071	± 0·040	± 0·026	± 0·0041	± 0·0054	± 0·0064	± 0·078	± 0·0041
1·98	2·116	1·840	1·123	0·1870	0·1959	0·1753	1·499	0·4392
± 0·11	± 0·070	± 0·032	± 0·021	± 0·0027	± 0·0031	± 0·0072	± 0·067	± 0·0031
0·071	**0·143**	**0·314**	**0·901**	**7·965**	**1·907**	**1·328**	**0·117**	**13·53**

* Absolute blank in cm³ STP is tabulated blank times 0·6121 g.
† Total of gas fractions where this ratio was obtained.
‡ No discrimination correction available. These ratios may be systematically in error.
§ Correction has been applied for $^{40}Ar^{2+}$. Error includes uncertainty in this correction.
‖ Correction has been made for background. Error includes uncertainty in background and in discrimination correction.
[a] ^{3}He not measured. Concentration of ^{4}He is **0·68** × 10^{-8} cm³ STP/g.
[b] Thermocouple problem: doubtful that 900°C was actually reached in this heating.

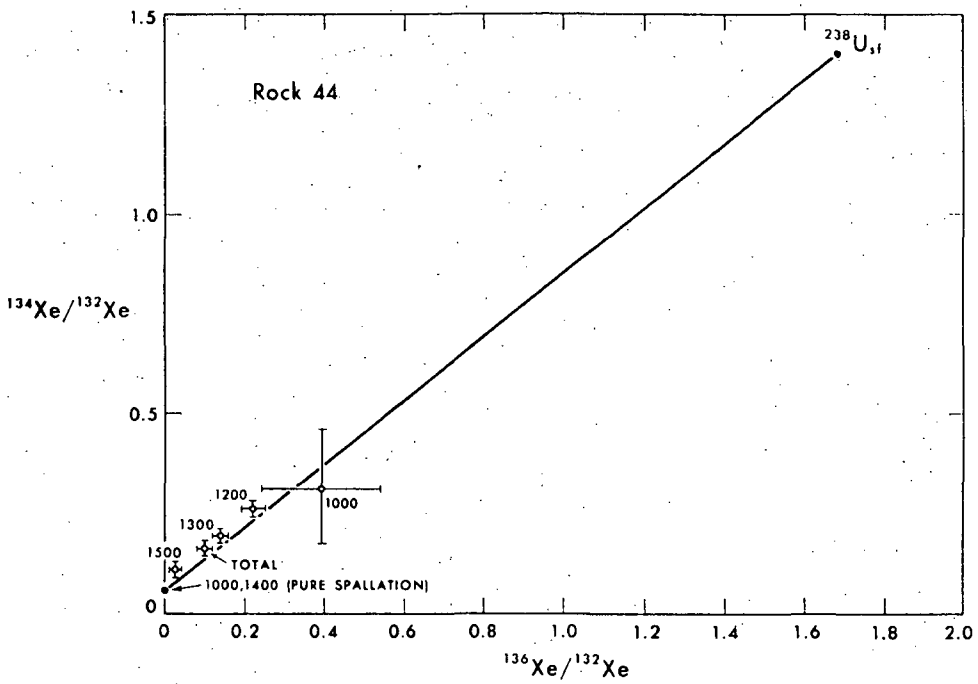

Fig. 10. Correlation of ratios $^{134}Xe/^{132}Xe$ and $^{136}Xe/^{132}Xe$ in rock 44. Trapped xenon has been subtracted off before computing the ratios. The diagram is consistent with a two-component system of cosmogenic xenon and xenon from spontaneous fission of ^{238}U. The errors shown are statistical only.

COSMIC RAY EXPOSURE AGES OF THE SAMPLES

The data obtained in this paper permit calculation in a number of ways of cosmic-ray exposure ages for the samples. We conclude this report by giving results of some of these calculations.

The most precise exposure ages which we can calculate come from our observation in both rocks of cosmogenic ^{81}Kr, a radioactive isotope with a half-life of 0·21 million years. Since decay of this isotope will be in equilibrium, at the time the rock was collected, with its production, measurement of its concentration gives us a production rate for ^{81}Kr. One of the stable cosmogenic Kr isotopes gives us a measure of the time-integrated production. If the relative production rates of the two isotopes can be specified, an exposure age which depends only on mass spectrometer krypton measurements is obtained. Errors in the sensitivity of the mass spectrometer for krypton do not affect the result, since only abundance ratios for krypton isotopes are involved.

We have carried out these calculations using the same assumptions as MARTI *et al.* (1970) who are among the originators of the method. Our results appear in Table 5. We are in fair agreement with MARTI *et al.* (1970) on rock 10057. They obtain 47 m.y. in comparison with our value of 34 m.y.

Table 5. Exposure ages of lunar samples

	$(^{83}Kr/^{81}Kr)_{cosm.}$	P_{81}[a]	P_{83}[a]	^{81}Kr–^{83}Kr age in 10^6 yr	$^{83}Kr^{b}_{cosm.}$	Sr (ppm)	Y (ppm)	Zr (ppm)	$^{83}Kr_{cosm.}$ age in 10^6 yr	$^{130}Xe^{b}_{cosm.}$	Ba (ppm)	Ce (ppm)	$^{130}Xe_{cosm.}$ age in 10^6 yr
Nuevo Laredo[c]	—	—	—	—	13 ± 0·39	84·4[d]	—	67[e]	≡ 16[f]	1·5 ± 0·45	46[g]	10·7[h]	≡16[f]
Lunar fines 10084-59	—	—	—	—	1255 + 864 − 324	200[i]	150[i]	390[i]	1130[j] + 840 − 450	130 ± 20	220[i]	50[i]	1450[j] ± 540
Lunar rock 10057-20	187·6 ± 29·3	79·3	135	34 ± 5	135 ± 24·3	130[i]	210[i]	560[i]	118[j] ± 41	22·6 ± 1·4	280[i]	88[i]	76[j] ± 23
Lunar rock 10044-20	380·2 ± 92·4	76·8	127	70 ± 17	183 ± 55	167[k]	160[i]	410[i]	176[j] ± 75	11·4 ± 0·7	285[k]	76[k]	100[j] ± 30

[a] Production rates (P) computed after MARTI *et al.* (1970) $P_{81} = 0{\cdot}95\,[(P_{80} + P_{82})/2]$; $P_{82} \equiv 100$.
[b] Gas concentration in units 10^{-12} cm³ STP/g.
[c] MUNK (1967).
[d] GAST (1962).
[e] SCHMITT *et al.* (1964).
[f] MUNK (1967); HEYMANN *et al.* (1968).
[h] HAMAGUCHI *et al.* (1957).
[h] SCHMITT *et al.* (1963).
[i] MORRISON *et al.* (1970).
[j] 2π irradiation geometry assumed.
[k] PHILPOTTS and SCHNETZLER (1970).
[l] MAXWELL *et al.* (1970); Value is for Type B Rock 10017.

An ^{81}Kr–^{83}Kr age is very meaningful if the sample has had a simple irradiation history: i.e. if it has been abruptly transferred from a completely shielded environment to its final position on the surface of the moon. If the rock came to its final position in stages, the ^{81}Kr–^{83}Kr method will overestimate its time in the final position but underestimate the integrated period when it was within a meter or so of the surface.

For this reason, it is interesting to compare the ^{81}Kr–^{83}Kr ages with exposure ages determined from various stable cosmogenic nuclides and the production rates inferred for those nuclides from stone meteorites. We have elected to compute exposure ages based on ^{83}Kr and ^{130}Xe, using the calcium-rich achondrite Nuevo Laredo as a meteorite standard. The exposure age for Nuevo Laredo has been found by more than one author to be 16 million years. MUNK (1967) has conveniently measured the ^{83}Kr and ^{130}Xe concentrations from spallation in the Nuevo Laredo stone. We can correct for chemical differences between Nuevo Laredo and the lunar rocks, using the Rudstam calculations carried out by HOHENBERG *et al.* (1967) for Kr and Xe production in the relevant target elements. In other words we take the Kr and Xe production rates from the 16 m.y. exposure in Nuevo Laredo, but we adjust these production rates (using relative yields given by the Rudstam calculations) to allow for differences in chemical composition between Nuevo Laredo and the lunar sample in question. The details, including the chemical compositions we used, appear in Table 5. The production rates found for Nuevo Laredo were halved to take into account the 2π instead of 4π irradiation geometry for samples near the lunar surface. We believe that the ^{130}Xe ages are to be preferred to the ^{83}Kr ages because we have encountered occasional severe variations in our krypton sensitivity which make Kr concentrations somewhat suspect. But in all cases the two methods agree within the

errors. In comparing the ^{81}Kr–^{83}Kr ages with the ^{130}Xe ages, we find agreement, within the errors, for rock 10044, suggesting that this rock may have had a simple irradiation history: sudden emplacement on the lunar surface from shielded depth. For rock 10057, the ^{81}Kr–^{83}Kr age of 34 m.y. is significantly less than the ^{130}Xe age of 76 m.y., as if it had spent some time at a partially shielded location. Our average value for the average exposure age of the fines is 1300 m.y. plus or minus about 500 m.y.

Acknowledgments—We thank G. MCCRORY for much help in the experimental work. This work received partial support from NASA and from the AEC and bears AEC code number UCB-34P32-72.

Note added in proof: All krypton ratios in Table 4 (of the form $^{M}Kr/^{82}Kr$) should be multiplied by the factor 1·008. None of the conclusions reached in the paper will be changed thereby.

REFERENCES

ALBEE A. L., BURNETT D. S., CHODOS A. A., EUGSTER O. J., HUNEKE J. C., PAPANASTASSIOU D. A., PODOSEK F. A., RUSS G. P., SANZ H. G. and WASSERBURG G. J. (1970) Ages, irradiation history, and chemical composition of lunar rocks from the Sea of Tranquillity. *Science* **167**, 463–466.

BERNSTEIN W., FREDRICKS R. W., VOGL J. L. and FOWLER W. A. (1963) The lunar atmosphere and the solar wind. *Icarus* **2**, 233–248.

EBERHARDT P., GEISS J., GRAF H., GRÖGLER N., KRÄHENBÜHL U., SCHWALLER H., SCHWARZMÜLLER J. and STETTLER A. (1970) Trapped solar wind noble gases, Kr^{81}/Kr exposure ages and K/Ar ages in Apollo 11 lunar materal. *Science* **167**, 558–560.

FLEISCHER R. L. and PRICE P. B. (1964) Decay constant for spontaneous fission of U^{238}. *Phys. Rev.* **133**, B63–64.

FUNKHOUSER J. G., SCHAEFFER O. A., BOGARD D. D. and ZÄHRINGER J. (1970) Gas analysis of the lunar surface. *Science* **167**, 561–563.

GAST P. W. (1962) The isotopic composition of strontium and the age of stone meteorites—I. *Geochim. Cosmochim. Acta* **26**, 927–943.

HAMAGUCHI H., REED G. W. and TURKEVICH A. (1957) Uranium and barium in stone meteorites. *Geochim. Cosmochim. Acta* **12**, 337–347.

HEYMANN D., MAZOR E. and ANDERS E. (1968) Ages of calcium-rich achondrites—I. Eucrites. *Geochim. Cosmochim. Acta* **32**, 1241–1268.

HEYMANN D., YANIV A., ADAMS J. A. S. and FRYER G. E. (1970) Inert gases in lunar samples. *Science* **167**, 555–558.

HINTENBERGER H., WEBER H. W., VOSHAGE H., WÄNKE H., BEGEMANN F., VILCSEK E. and WLOTZKA F. (1970) Rare gases, hydrogen, and nitrogen: concentrations and isotopic composition in lunar material. *Science* **167**, 543–545.

HOHENBERG C. M., MUNK M. N. and REYNOLDS J. H. (1967) Spallation and fissiogenic xenon and krypton from stepwise heating of the Pasamonte achondrite; The case for extinct plutonium 244 in meteorites; Relative ages of chondrites and achondrites. *J. Geophys. Res.* **72**, 3139–3177.

HOHENBERG C. M. and REYNOLDS J. H. (1969) Preservation of the iodine-xenon record in meteorites. *J. Geophys. Res.* **74**, 6679–6683.

KIRSTEN T., STEINBRUNN F. and ZÄHRINGER J. (1970) Rare gases in lunar samples: study of distribution and variations by a microprobe technique. *Science* **167**, 571–574.

LSPET (LUNAR SAMPLE PRELIMINARY EXAMINATION TEAM) (1969) Preliminary examination of lunar samples from Apollo 11. *Science* **165**, 1211–1227.

MARTI K. (1969) Solar-type xenon: a new isotopic composition of xenon in the Pesyanoe meteorite. *Science* **166**, 1263–1265.

MARTI K., EBERHARDT P. and GEISS J. (1966) Spallation, fission, and neutron capture anomalies in meteoritic krypton and xenon. *Z. Naturforsch.* **21a**, 398–413.

MARTI K., LUGMAIR G. W. and UREY H. C. (1970) Solar wind gases, cosmic ray spallation products, and the irradiation history. *Science* **167**, 548–550.

MAXWELL J. A., ABBEY S. and CHAMP W. H. (1970) Chemical composition of lunar material. *Science* **167**, 530–531.

MORRISON G. H., GERARD J. T., KASHUBA A. T., GANGADHARAM E. V., ROTHENBERG A. M., POTTER N. M. and MILLER G. B. (1970) Multielement analysis of lunar soil and rocks. *Science* **167**, 505–507.

MUNK M. N. (1967) Argon, krypton, and xenon in Angra dos Reis, Nuevo Laredo, and Norton County achondrites: the case for two types of fission xenon in achondrites. *Earth Planet. Sci. Lett.* **3**, 457–465.

PHILPOTTS J. A. and SCHNETZLER C. C. (1970) Potassium, rubidium, strontium, barium, and rare-earth concentrations in lunar rocks and separated phases. *Science* **167**, 493–495.

REED G. W., JR., JOVANOVIC S. and FUCHS L. H. (1970) Trace elements and accessory minerals in lunar samples. *Science* **167**, 501–503.

REYNOLDS J. H. (1950) A mass spectrometric investigation of branching in Cu^{64}, Br^{80}, Br^{82} and I^{128}. *Phys. Rev.* **79**, 789–794.

REYNOLDS J. H., HOHENBERG C. M., LEWIS R. S., DAVIS P. K. and KAISER W. A. (1970) Isotopic analysis of rare gases from stepwise heating of lunar fines and rocks. *Science* **167**, 545–548.

ROWE M. W. (1967) Cosmic ray spallation and the special anomaly in achondrites. *Earth Planet. Sci. Lett.* **2**, 92–98.

SCHMITT R. A., BINGHAM E. and CHODOS A. A. (1964) Zirconium abundances in meteorites and implications to nucleosynthesis. *Geochim. Cosmochim. Acta* **28**, 1961–1979.

SCHMITT R. A., SMITH R. H., LASCH J. E., MOSEN A. W., OLEHY D. A. and VASILEVSKIS J. (1963) Abundances of the fourteen rare-earth elements, scandium, and yttrium in meteoritic and terrestrial matter. *Geochim. Cosmochim. Acta* **27**, 577–622.

TURNER G. (1970) Argon-40/argon-39 dating of lunar rock samples. *Science* **167**, 466–468.

WÄNKE H., BEGEMANN F., VILCSEK E., RIEDER R., TESCHKE F., BORN W., QUIJANO-RICO M., VOSHAGE H. and WLOTZKA F. (1970) Major and trace elements and cosmic-ray produced radio-isotopes in lunar samples. *Science* **167**, 523–525.

WANLESS R. K., LOVERIDGE W. D. and STEVENS R. D. (1970) Age determinations and isotopic abundance measurements on lunar samples. *Science* **167**, 479–480.

WETHERILL G. W. (1953) Spontaneous fission yields from uranium and thorium. *Phys. Rev.* **92**, 907–912.

EARTH AND PLANETARY SCIENCE LETTERS 9 (1970) 201–207. NORTH-HOLLAND PUBLISHING COMPANY

RARE GASES FROM STEPWISE HEATING OF LUNAR ROCK 12013

E.C.ALEXANDER Jr.
Department of Physics
University of California, Berkeley, California 94720, USA

Received 30 July 1970

Helium, neon, argon and xenon data are presented from a seven step heating of lunar rock 12013. Helium, neon and argon contain radiogenic and spallation components with no discernible trapped component. ^{3}He and ^{21}Ne cosmic ray exposure ages are 60 ± 12 m.y. The xenon contains a well defined spallation component, a fission component and possibly a trapped component but *no* evidence for decay products of extinct ^{129}I or ^{244}Pu. Apparent solidification ages are UTh-He: 2.3 ± 0.5 by; K-Ar: 3.0 ± 0.7 by; ^{238}U-^{136}Xe: $3.6^{+1.0}_{-1.4}$ by (assuming solar wind type xenon as trapped xenon) or $2.2^{+1.6}_{-2.2}$ by (assuming atmospheric trapped xenon).

1. Introduction

Apollo rock 12013 is atypical in many respects [1]. In particular the 40-fold uranium enrichment relative to other Apollo 12 samples [1], and the report that its [2] Rb-Sr age might be as old as 4.6 billion years (by) make rock 13 the most favorable lunar sample yet encountered for possible detection of decay products of extinct ^{244}Pu and ^{129}I. In this letter I report the first results from an analysis of rare gases in rock 13. In addition to searching for the decay products of extinct ^{129}I and ^{244}Pu, I have measured the UTh-He, K-Ar and U-Xe retention ages, the ^{3}He, ^{21}Ne and ^{130}Xe cosmic ray exposure ages, and the relative spallation yields of xenon isotopes in this rock.

2. Experimental methods and data

The sample of rock 13 analyzed was a 70.0 mg aliquot of the "crushed and split light sample" prepared under sample number 12013, 10, 37+24 [3]. The rare gases were extracted in seven temperature steps in a glass extraction system which has been previously described as "System 2" [4]. The only change in the experimental procedure from that described for "System 2" was to run a smaller fraction of the helium released from the sample, in the interest of higher accuracy for the helium analysis. The temperatures of the "≈350°" and "≈700°" fractions are based on a calibration of the induction heater made during the analysis of the Apollo 11 samples. They may be in error by ±100°C due to instrumental drift in the intervening six months. The higher temperatures, accurate to ±20°C, were measured during the runs with an optical pyrometer.

The helium, neon and argon data are listed in table 1. Isotopic ratios were calculated by selecting "linearly" or "exponentially" extrapolated peak heights, according to which gave the smaller error. We refer here to calculations using a computer program which fitted the peaks of each individual isotope to both exponential and linear functions of time and extrapolated these functions to the moment when the high voltage was turned on in the mass spectrometer, after insertion of the gas sample. Peak heights were extrapolated because they were observed to change in a more regular fashion than did the isotope ratios.

No corrections have been made to these data for blanks. Data for an 1800°C blank, run immediately

Table 1
Helium, neon and argon from a stepwise heating of Apollo sample 12013

Temperature (°C)	$[^3He]$ * ($\times 10^{-8}$ cm^3/g)	4/3	$[^{22}Ne]$ * ($\times 10^{-8}$ cm^3/g)	20/22	21/22	$[^{36}Ar]$ * ($\times 10^{-8}$ cm^3/g)	40/36	38/36
≈350	6.6	7 350 ± 80	0.22	–	0.160 ± 0.008	0.19	2 360 ± 130	0.46 ± 0.03
≈700	44.9	10 000 ± 200	0.53	0.82 ± 0.51	0.737 ± 0.014	0.51	21 000 ± 9 000	1.00 ± 0.44
850	2.8	10 300 ± 100	3.14	0.89 ± 0.06	0.848 ± 0.012	0.62	25 000 ± 12000	1.52 ± 0.09
1000	3.5	8 230 ± 70	2.36	0.94 ± 0.10	0.852 ± 0.010	0.55	20 500 ± 9 600	1.36 ± 0.08
1150	2.8	5 600 ± 90	1.99	1.00 ± 0.15	0.861 ± 0.009	1.38	6 100 ± 700	1.26 ± 0.07
1300	0.4	1 100 ± 300	0.41	1.32 ± 0.41	0.809 ± 0.026	0.96	1 340 ± 50	1.21 ± 0.02
1800	–	–	0.08	4.3 ± 1.2	0.494 ± 0.032	0.60	940 ± 20	1.02 ± 0.02
Total	61.0	9 370 ± 170	8.73	0.98 ± 0.15	0.823 ± 0.012	4.81	10 000 ± 3 800	1.21 ± 0.10

* The amounts of these isotopes were determined by the "peak height" method and are only reproducible to about ±15%. An 1800° blank run immediately before the 350° fraction yielded ^{22}Ne and ^{36}Ar corresponding to 0.029×10^{-8} cm^3/g and 0.23×10^{-8} cm^3/g respectively and no detectable ^3He. No blank corrections has been applied to the above data. However, background corrections have been applied and are discussed in the text. In addition the amount of Ar is subject to a systematic error which is also discussed in the text.

Table 2
Xenon from a stepwise heating of Apollo sample 12013

Temperature (°C)	142/132	126/132	128/132	129/132	130/132	131/132	134/132	136/132	$[^{132}Xe]$ † ($\times 10^{-12}$ cm^3/g)
≈350	0.017 ± 0.002*	0.014 ± 0.003*	0.099 ± 0.007	1.009 ± 0.009	0.163 ± 0.003	0.843 ± 0.030	0.395 ± 0.008	0.328 ± 0.006	7.1
≈700	0.060 ± 0.003	0.101 ± 0.004	0.208 ± 0.012	1.052 ± 0.019	0.245 ± 0.013	1.212 ± 0.049	0.378 ± 0.010	0.314 ± 0.005	9.8
850	0.159 ± 0.004	0.296 ± 0.009	0.525 ± 0.012	1.159 ± 0.012	0.472 ± 0.011	2.167 ± 0.038	0.311 ± 0.004	0.246 ± 0.004	12.2
1000	0.297 ± 0.006	0.562 ± 0.011	0.934 ± 0.014	1.362 ± 0.014	0.755 ± 0.015	3.457 ± 0.064	0.221 ± 0.007	0.166 ± 0.003	32.9
1150	0.350 ± 0.006	0.649 ± 0.015	1.059 ± 0.016	1.357 ± 0.011	0.848 ± 0.014	3.594 ± 0.056	0.230 ± 0.003	0.177 ± 0.002	87.9
1300	0.350 ± 0.008	0.651 ± 0.003	1.061 ± 0.011	1.370 ± 0.012	0.837 ± 0.011	3.534 ± 0.034	0.250 ± 0.003	0.204 ± 0.003	60.0
1800	0.356 ± 0.007	0.643 ± 0.009	1.024 ± 0.014	1.317 ± 0.019	0.828 ± 0.009	3.490 ± 0.032	0.254 ± 0.005	0.210 ± 0.004	66.8
Total	0.318 ± 0.006	0.586 ± 0.010	0.958 ± 0.014	1.322 ± 0.014	0.774 ± 0.012	3.322 ± 0.045	0.252 ± 0.004	0.201 ± 0.003	276.7

* Average instead of extrapolated ratios.
† The amount of ^{132}Xe was calculated by "peak height" method and is only reproducible to about ±5%. An 1800°C blank measured immediately before the 350°C fraction yielded 2.0×10^{-13} cm^3 STP of ^{132}Xe (corresponding to 2.9×10^{-12} cm^{-3} STP/g for this sample).

before the sample was dropped into the crucible, appear among the notes in table 1. The data have been corrected for instrumental background. Because of the high $^{40}Ar/^{36}Ar$ and helium to neon ratios, the background corrections were sometimes quite significant (as high as 40% for some of the ^{36}Ar fractions). Where background corrections were made, an error equal to half the correction was added to the statistical error. The large errors listed for the $^{20}Ne/^{22}Ne$ and some of the $^{40}Ar/^{36}Ar$ ratios are mainly due to this background correction.

We have recently discovered an error in argon concentrations for Apollo 11 samples as measured in Berkeley [4]. The error, which affected argon concentrations but not argon isotope ratios, was caused by non-linearity of spectrometer sensitivity for the excessive amount of argon present in the calibration samples from our gas pipettes. In the present work the argon sensitivity was calculated indirectly by comparing our results from the controlled samples of Bruderheim interlaboratory standard (which were rune immediately before the rock 12013 sample) with the data of Schultz [6] and Hintenberger et al. [6].

Xenon data are set out in table 2. The reported ratios are linear extrapolations of the ratios (as opposed to the peaks for the light gases) as a function of time to the point in time when the high voltage was turned on in the mass spectrometer. The errors listed are the statistical error in the extrapolated ratios [5]. As with the light gases, the blank is tabulated separately and has not been subtracted from the data. There is no significant background in the xenon region.

The krypton peaks were comparable in all temperature fractions to our blank levels for krypton. Analysis of the krypton has for this reason been deferred.

3. Results and discussion

3.1. *Helium, neon and argon*

The rare gases in table 1 appear to be a simple mixture of spallation and radiogenic components. There is no evidence of a trapped component. In contrast the abundances of Ne and Ar (and Xe) reported by LSPET [1] for rock 12013 are uniformly larger than our data and show evidence of a trapped component. Although LSPET states "the crystalline rock samples reported here were completely interior chips ...", our sample evidently contained less trapped gas than did the sample analyzed by LSPET. This picture is somewhat confused by the He data where we observed a similar $^{4}He/^{3}He$ ratio but more ^{3}He than did LSPET.

For the spallation production rates of ^{3}He and ^{21}Ne we used the values $P^3 = 1 \times 10^{-8}$ cm^3/g-my and $P^{21} = 0.12 \times 10^{-8}$ cm^3/g-my which have commonly been used for lunar samples. Cosmic ray exposure ages calculated by dividing the observed ^{3}He and ^{21}Ne concentrations by P^3 and P^{21}, respectively are set out in table 3. Agreement between the ages calculated from the two isotopes is good.

Wakita and Schmitt [7] have determined the U, Th and K concentrations in an aliquot of our sample. Using their values for U (9.7 ppm) and Th (25 ppm) and the observed ^{4}He concentration of $(5.7 \pm 0.9) \times 10^{-3}$ cm^3/g we calculated a UTh-He age of 2.5 ± 0.5 by. This is in good agreement with the value of 2.3 by reported by LSPET [1] for rock 12013.

Combining Wakita and Schmitt's [7] value for K (1.65%) with the measured ^{40}Ar content of $(4.9 \pm 2.0) \times 10^{-4}$ cm^3/g yielded a K-Ar age of 3.0 ± 0.7 by. This can be compared with Schaeffer et al.'s [8] value of 3.6 by and with Turner's ^{40}Ar-^{39}Ar age of 3.9 ± 0.1 by [9].

3.2. *Spallation xenon*

Spallation is the major source of the xenon in the sample. The technique used to resolve the spallation spectrum is an adaptation of a technique used by Bogard et al. [10]. If a sample contains xenon which is a simple mixture of a well defined spallation component (with no ^{136}Xe) and a trapped component, and if a heating experiment releases the two components in varying relative amounts then a plot of $^{i}Xe/^{136}Xe$ versus $^{126}Xe/^{136}Xe$ for each i will give a well defined linear plot whose *slope* is the ratio of spallation $^{i}Xe/^{126}Xe$. Such an ideal case is rare in reality because xenon normally contains at least some fission ^{136}Xe (rock 13 was expected to contain a significant fission component). It is also possible that the ^{136}Xe spallation yield is not zero, Marti [11]. However, the presence of additional sources of ^{136}Xe does not destroy the method. An additional compo-

Table 3
Cosmic ray exposure ages, gas retention ages and xenon spallation yields from Apollo Sample 12013

Isotope	Concentration (cm^3/g)	Production rate (cm^3/g-my)	Exposure age (my)
^{3}He	$(61 \pm 9) \times 10^{-8}$	1×10^{-8}	61 ± 12
^{21}Ne	$(7.2 \pm 1.2) \times 10^{-8}$	0.12×10^{-8}	60 ± 12
^{130}Xe[5]	$(191 \pm 10) \times 10^{-12}$	2.5×10^{-12}	76 ± 23

Method	Parent abundance [7]	Gas abundance (cm^3/g)	Age (by)	Reference
UTh-He	U = 9.7 ppm, Th = 25 ppm	$^{4}He = (5.7 \pm 0.9) \times 10^{-3}$	2.5 ± 0.5	this work
			2.3	[1]
K-Ar	K = 1.65%	$^{40}Ar = (4.8 \pm 2.0) \times 10^{-4}$	3.0 ± 0.7	this work
			3.6	[8]
			3.9 ± 0.1	[9]
U-Xe	U = 9.7 ppm	$^{136}Xe^{f} = (13.5 \pm 6.0) \times 10^{-12}$ *	$3.6^{+1.0}_{-1.4}$ *	this work
		$^{136}Xe^{f} = (7.3 \pm 6.8) \times 10^{-12}$ †	$2.2^{+1.6}_{-2.2}$ †	this work

Trapped xenon assumed	Relative spallation yields							
	124	126	128	129	130	131	132	134
Solar wind [13]	53.2 ± 0.7	≡100	157 ± 2	135 ± 6	118 ± 2	487 ± 9	77 ± 4	3 ± 1
Atmosphere [14]	53.2 ± 0.7	≡100	157 ± 2	135 ± 6	118 ± 2	487 ± 9	77 ± 5	3 ± 2

* Assuming solar wind xenon as trapped.
† Assuming atmospheric xenon as trapped.

nent of ^{136}Xe moves the datum point directly toward the origin of the graph. If the linear plot nearly intersects the origin (as is the case for the $^{124}Xe/^{136}Xe$, $^{128}Xe/^{136}Xe$ and $^{130}Xe/^{136}Xe$ versus $^{126}Xe/^{136}Xe$ plots) the net effect is to move the data points toward the origin without making appreciable changes in the slope. Spallation yields can be determined for ^{124}Xe, ^{126}Xe, ^{128}Xe and ^{130}Xe from the slopes of the plots of the raw data and can be used to correct the data of the other isotopes for fission (or better to correct for non-trapped ^{136}Xe).

Fig. 1 is a plot of $^{128}Xe/^{136}Xe$ versus $^{126}Xe/^{136}Xe$. Solid points are the raw data, with error bars shown only where the errors are larger than the points. The data form a well defined linear array which passes near the origin. Plots of $^{124}Xe/^{136}Xe$ and $^{130}Xe/^{136}Xe$ versus $^{126}Xe/^{136}Xe$ were constructed and are very similar to fig. 1. The solid line is the

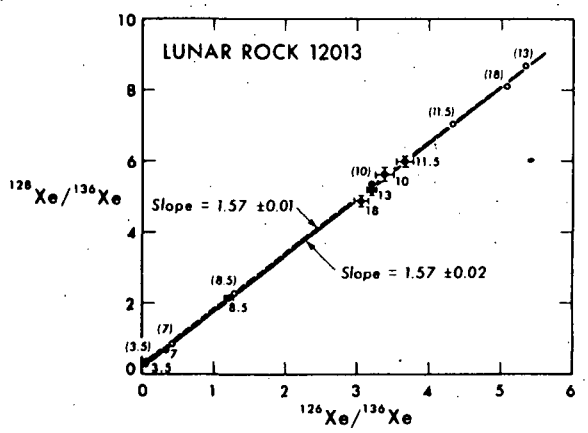

Fig. 1. Correlation of ratios $^{128}Xe/^{136}Xe$ and $^{126}Xe/^{136}Xe$ in lunar rock 12013. The numbers are release temperatures in degrees celcius for half-hour heatings. Solid points are the uncorrected data and the open circles are the fission corrected data (assuming solar wind as the trapped component). The solid line is the least-squares fit to the uncorrected data and the dashed line is the fit to the fission corrected data. Slopes of the lines are the ratio of spallation ^{128}Xe to spallation ^{126}Xe.

least-squares fit, using the method of York [12] to the uncorrected data. The spallation ratios, inferred from the slopes of fig. 1 and the two similar graphs were used to calculate the fraction of trapped ^{130}Xe in each temperature fraction:

$$^{130}Xe^{t}/^{130}Xe^{o} =$$

$$= \frac{(^{i}Xe^{s}/^{130}Xe^{s}) - (^{i}Xe^{o}/^{130}Xe^{o})}{(^{i}Xe^{s}/^{130}Xe^{s}) - (^{i}Xe^{t}/^{130}Xe^{t})}, \qquad (1)$$

where the superscipts t, o and s refer to trapped, observed and spallation respectively. The arithmetic average of the three estimates of the quantity $^{130}Xe^{t}/^{130}Xe^{o}$ from eq. (1) was used to calculate the quantity $^{136}Xe^{t}/^{136}Xe^{o}$ by the formula:

$$^{136}Xe^{t}/^{136}Xe^{o} =$$

$$= \frac{(^{130}Xe^{t}/^{130}Xe^{o})(^{136}Xe^{t}/^{130}Xe^{t})}{(^{136}Xe^{o}/^{130}Xe^{o})} . \qquad (2)$$

Observed $^{i}Xe^{o}/^{136}Xe^{o}$ ratio were converted to $^{i}Xe^{o}/^{136}Xe^{t}$ by dividing by the result of eq. (2). New plots using $^{i}Xe^{o}/^{136}Xe^{t}$ versus $^{126}Xe^{o}/^{136}Xe^{t}$ were constructed and used to calculate the spallation yields of ^{129}Xe, ^{131}Xe, ^{132}Xe, and ^{134}Xe.

The open circles in fig. 1 are the fission corrected points. They are included to demonstrate how the fission correction moves the points along the line. The 1000° point moved down the line due to a value of $^{136}Xe^{t}/^{136}Xe^{o}$ from eq. (2) which was slightly greater than one. Actually two sets of spallation yields were calculated; one using solar wind xenon (as given by Eberhardt et al. [13]) as the trapped component, and the other using atmospheric xenon, Nier [14], as the trapped component. The two sets of results are given in table 3. As can be seen the two sets agree almost exactly – indicating that the calculated yields are not a function of the trapped component assumed. In addition, the ^{124}Xe to ^{130}Xe yields inclusive do not assume a zero spallation yield of ^{136}Xe. However, it was necessary to assume a zero spallation yield for the calculation of the relative yields of ^{131}Xe, ^{132}Xe and ^{134}Xe. The fraction of trapped ^{136}Xe from eq. (2) was used together with

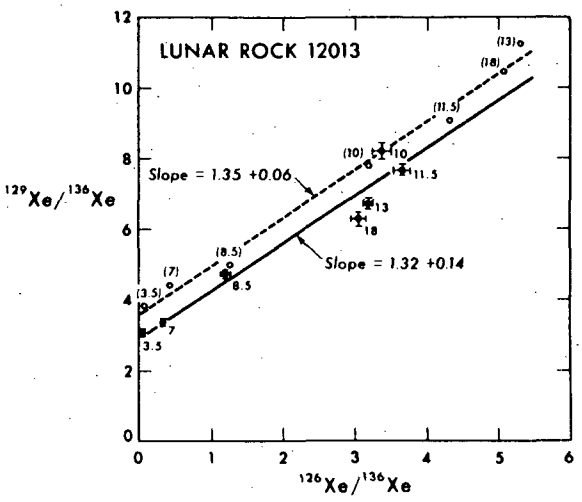

Fig. 2. Correlation at ratios $^{129}Xe/^{136}Xe$ and $^{126}Xe/^{136}Xe$ in lunar rock 12013. The numbers, points and lines have the same meaning as in fig. 1. Slopes at the lines are the ratio of spallation ^{129}Xe to spallation ^{126}Xe. The fission corrected points appear to contain only trapped and spallation xenon with no radiogenic ^{129}Xe.

the relative fission yields of ^{238}U from von Gunten [15] to correct $^{131}Xe^{o}$, $^{132}Xe^{o}$ and $^{134}Xe^{o}$ for fission.

Using the method described in Hohenberg et al. [4] and Wakita and Schmitt's [7] values for the Ba and rare earth concentrations, the cosmic ray production rate of $^{130}Xe^{s}$ (2.5×10^{-12} cm^3/g-my ± 30%) was calculated for our sample of rock 13. Because of the high Ba to rare earth element ratio in rock 13, the calculation indicates that approximately 95% of $^{130}Xe^{s}$ comes from spallation of Ba. The production rate is based on the $^{130}Xe^{c}$ content in the Nuevo Laredo achondrite, as measured by Munk [16]. Dividing the observed concentration of $^{130}Xe^{s}$ ($191 \pm 10 \times 10^{-12}$ cm^3/g) by P^{130} yielded an $^{130}Xe^{s}$ cosmic ray exposure age of 76 ± 23 my. This age is in complete agreement with the exposure ages calculated from the ^{3}He and ^{21}Ne concentrations and is listed in table 3.

3.3. *Decay products of extinct* ^{129}I *and* ^{244}Pu

A search for ^{129}Xe from the decay of extinct ^{129}I and/or $^{136}Xe^{f}$ from the decay of extinct ^{244}Pu

was the main purpose of our analysis of rock 13. No such products of extinct radioactivity were found. Fig. 2 is a plot of $^{129}Xe/^{136}Xe$ versus $^{126}Xe/^{136}Xe$. As in fig. 1, the solid points in fig. 2 are the raw data points and the open circles are the fission corrected data points (assuming solar wind xenon as the trapped component). The solid line is the least-squares fit to the raw data and the dashed line is the fit to the corrected data. Although the fission corrected data do not define as sharp a line as do the ^{124}Xe, ^{128}Xe and ^{130}Xe data, the line does pass through the error bars of each point at the 2σ level [17]. In addition the linearity of the fission corrected ^{129}Xe data, as measured by the uncertainty in the slope, is comparable to the linearity of the fission corrected ^{131}Xe data and these are the two isotopes which show the greatest variation in spallation yields in lunar samples, Reynolds [18]. The somewhat larger errors for the ^{129}Xe and ^{131}Xe spallation yields in table 3 may in fact be due to variation from mineral to mineral in the yield of these two isotopes. In short, there is no evidence for excess ^{129}Xe from the decay of extinct ^{129}I in rock 13.

A simple way to look for $^{136}Xe^{f}$ from the decay of ^{244}Pu is to calculate the U-Xe age. An "age" older than the accepted age of the sample would indicate the presence of excess $^{136}Xe^{f}$, presumably from the decay of ^{244}Pu. The amount of $^{136}Xe^{f}$ in rock 13 is dependent on the trapped xenon assumed. Therefore, two calculations were made. The first, assuming trapped solar wind xenon, gave $^{136}Xe^{f} = (13.5 \pm 6.0) \times 10^{-12}$ cm^3/g. The second calculation, assuming trapped atmospheric xenon, yielded $^{136}Xe^{f} = (7.3 \pm 6.8) \times 10^{-12}$ cm^3/g. Using von Gunten's [15] value for the ^{238}U fission yield of ^{136}Xe (4.58% [19]) and Fleischer and Price's [20] value for the spontaneous fission decay constant of ^{238}U, the U-Xe ages shown in table 3 were calculated. The upper limit of the older age, 4.6 by, is comparable to the Rb-Sr age [2]. Clearly, there is no need to invoke ^{244}Pu to explain the observed concentration of $^{136}Xe^{f}$ in rock 13.

3.4. *Trapped xenon*

Knowledge of the isotopic composition of xenon trapped in lunar rock (independent of that xenon implanted by the solar wind) would be of great interest to the study of the earth-moon system. As our sample of rock 12 was an interior sample which hopefully had not been exposed to the solar wind, an effort was made to determine the isotopic composition of the trapped xenon. Unfortunately the trapped xenon is almost entirely masked by the very large spallation xenon component.

Release patterns were calculated for the trapped and spallation components and are independent of the trapped component assumed. There is a small low temperature release of trapped xenon unaccompanied by spallation xenon which is probably due to a component of absorbed atmospheric xenon picked up during the processing of the sample. Above 700°C a trapped component is released which correlates with the spallation component and is apparently a true "trapped" component.

As discussed earlier, the amount of fission xenon is a function of the trapped component assumed. Therefore, two release patterns were calculated. The assumption of a solar wind trapped component leads to positive amounts of fission xenon at all temperatures except at 1000° where it is only slightly negative. The assumption of an atmospheric trapped component yields large *negative* amounts of fission xenon at 850°C and 1000°C – a physical impossibility. However, the errors in the calculated amounts are very large and the negative points are within experimental error of zero. The major release of fission xenon is in the high temperature fractions – starting in the 1150°C fraction and rising monotonically to the 1800°C fraction. In view of the large errors, the data can only be said to suggest that atmospheric xenon has a higher $^{136}Xe/^{130}Xe$ ratio than the trapped component, i.e. that the trapped xenon in rock 13 *may* have a $^{136}Xe/^{130}Xe$ ratio similar to solar wind xenon.

The suggestion of such a trapped component in rock 13 is admittedly indirect and is subject to a serious objection: the lack of light rare gases as seen in the solar wind. If the 1.4×10^{-10} cm^3/g of trapped ^{132}Xe are due to the solar wind, there should be present $\approx 1 \times 10^{-6}$ cm^3/g of ^{36}Ar and $\approx 2 \times 10^{-5}$ cm^3/g of ^{20}Ne. The total amounts of ^{36}Ar and ^{20}Ne are factors of 20 and 200 respectively lower and are largely due to spallation.

4. Conclusions

In summary, our rare gas data do not support the

suggestion that the Rb-Sr age might be as large as 4.6 by [2] of Apollo sample 12013. There is no evidence of the decay products of extinct ^{129}I or ^{244}Pu. Gas retention ages are consistent with Turner's ^{40}Ar-^{39}Ar age of 3.9 by [9]. The cosmic ray exposure age of rock 13 is approximately 60 my.

Acknowledgments

I thank P.K.Davis for his assistance with computer programming and W.Kaiser, R.Lewis and G.McCrory for their assistance and suggestions. Particularly thanks are due to J.H.Reynolds without whose constant aid and advise this work would have been impossible. This work received partial support from NASA and from AEC and bears AEC code number UCB-34P32-74.

References

[1] The Lunar Sample Preliminary Examination Team, Preliminary examination of lunar samples from Apollo 12, Science 167 (1970) 1325.

[2] Lunatic Asylum, Preliminary results.

[3] Anderson, Earth Planet. Sci. Letters 9 (1970) 94.

[4] C.M.Hohenberg, P.K.Davis, W.A.Kaiser, R.S.Lewis and J.H.Reynolds, Trapped and cosmogenic rare gases from stepwise heating of Apollo 11 samples, Geochim. Cosmochim. Acta, Suppl. I (1970) 1283.

[5] The errors are the statistical error in the extrapolated intercept of the linear fit to the observed ratios and are calculated by:

$$E=\left[\left(\frac{1}{n}+\frac{(\bar{t}-t_0)^2}{\Sigma(t_i-\bar{t})^2}\right)\left(\frac{\Sigma(r_i-a-bt_i)}{n-2}\right)^2\right]^{1/2}$$

where n is the number of measurements, r_i is the isotope ratio, t_i is the time r_i was measured, $\bar{t}$ is the average of the t_i, t_0 is the time the accelerating voltage was turned, and a and b are the intercept and slope respectively of the least-squares fit to the data. This error thus includes both the uncertainty in the fitting parameter, a, and the uncertainty of extrapolation over the time $\bar{t}-t_0$ due to the uncertainty in the parameter b, the slope.

[6] H.Hintenberger, H.W.Weber, H.Voshage, H.Wanke, F. Begeman, and F.Wlotzka, Concentrations and isotopic abundances of rare gas, hydrogen, and nitrogen in lunar material, Geochim. Cosmochim. Acta, Suppl. I (1970) 1269;
L. Schultz, private communication.

[7] H.Wakita and R.A.Schmitt, Earth Planet. Sci. Letters 9 (1970) 169.

[8] O.A.Schaeffer, J.G.Funkhouser and D.D.Bogard, K-Ar ages from the Sea of Tranquillity and the Ocean of Storms, Science (1970) in press.

[9] G.Turner, Earth Planet. Sci. Letters 9 (1970) 177.

[10] D.D.Bogard, J.G.Funkhouser, O.A.Schaeffer and J. Zähringer, Xenon and krypton in lunar material returned by Apollo 11 and Apollo 12, Trans. Amer. Geophys. Union 51 (1970) 345.

[11] K.Marti, G.W.Lugmair and H.C.Urey, Solar wind gases cosmic ray spallation products, and irradiation history of Apollo 11 samples, Geochim. Cosmochim. Acta, Supplement I (1970) 1357.

[12] D.York, Least-squares fitting of a straight line, Can. J. Phys. 44 (1966) 1079.

[13] P.Eberhardt, J.Geiss, H.Graf, N.Grogler, U.Krahenbuhl, H.Schwaller, J.Schwarzmuller and A.Stettler, Trapped solar wind noble gases, exposure age and K/Ar-age in Apollo 11 lunar fine material, Geochim. Cosmochim. Acta, Suppl. I (1970) 1037.

[14] O.A.Nier, A redetermination of the relative abundance of the isotopes of neon, krypton, rubidium, xenon and mercury, Phys. Rev. 79 (1950) 450.

[15] H.R.von Gunten, Distribution of mass in spontaneous and neutron-induced fission, Actinides Rev. 1 (1969) 275.

[16] M.N.Munk, Argon, krypton, and xenon in Angra dos Reis, Nuevo Laredo, and Norton County achondrites: the case for two types of fission xenon in achondrites, Earth Planet. Sci. Letters 3 (1967) 457.

[17] Error bars were not shown on the fission corrected data to keep the figure uncluttered. However, the 2σ error bars can be easily visualized by doubling the 1σ error bars shown on the solid data points and transferring them to the appropriate fission corrected points.

[18] J.H.Reynolds, private communications.

[19] A fission yield of 6% for $^{136}Xe^f$ has often been assumed in the past. Using the value of 6% would lower the calculated age and strengthen the argument.

[20] R.L.Fleischer and P.B.Price, Decay constant for spontaneous fission of ^{238}U, Phys. Rev. 133 (1964) B63.

Proceedings of the Second Lunar Science Conference, Volume 2, pp. 1693–1703.
The M.I.T. Press, 1971.

Stepwise heating analyses of rare gases from pile-irradiated rocks 10044 and 10057

P. K. DAVIS, R. S. LEWIS, and J. H. REYNOLDS
Physics Department, University of California,
Berkeley, California 94720

(Received 23 February 1971; accepted in revised form 5 April 1971)

Abstract—Argon, krypton, and xenon from stepwise heating of two lunar rocks which had been irradiated in a pile (integrated flux 1.35 × 10^{19} slow neutrons/cm^2) were examined mass spectrometrically. The argon data are the basis for the so-called $^{40}Ar/^{39}Ar$ method of K–Ar dating, which gives an age of (4.00 ± 0.07) × 10^9 years for rock 10044 but is not useful for rock 10057, where the argon is very lightly bound. The krypton and xenon results led to release curves for "trapped" and cosmogenic gases plus the gases produced by neutron capture (or fission) in Ba, Br, I, and U. Inferred concentrations for rocks 10044 and 10057, respectively, are: Ba: 84 and 202 ppm; Br: 12.4 and 47 ppb; I: 0.9 and 0.7 ppb; U from krypton: 0.15 and 1.37 ppm; U from xenon (preferred): 0.19 and 0.59 ppm. Despite the fact that we have not recovered the rare gases from sites where they were lightly bound (in later experiments we shall), our inferred trace element compositions are in acceptable agreement with other workers, except for iodine where there are not yet definitive analyses for lunar samples.

INTRODUCTION

AS ONE MEANS at our disposal to increase the scientific return from lunar samples, we have undertaken a rather broad study of rare gases in specimens which have been strongly neutron irradiated in a reactor. Initial objectives were to obtain K–Ar ages by the $^{40}Ar/^{39}Ar$ technique (MERRIHUE and TURNER, 1966), I–Xe ages from release of ^{128}Xe correlated with excess ^{129}Xe from extinct ^{129}I (JEFFERY and REYNOLDS, 1961), and Pu–U–Xe ages from release of xenon from pile-induced fission of ^{235}U correlated with fission xenon from extinct ^{244}Pu (PODOSEK, 1970). We also expected to obtain concentrations of certain trace elements which produce rare gas nuclides by slow neutron absorption (MERRIHUE, 1966). This paper is more nearly a progress report than a definitive study; the program is ongoing with present results indicating rather well what can be obtained and what cannot, as follows. The K–Ar ages are often obtainable with high precision as TURNER (1970a) has already so beautifully demonstrated. The I–Xe and U–Pu–Xe dating techniques are not yet applicable to lunar rocks since we have yet to find a lunar rock which is old enough to exhibit fossil xenon from extinct radioactivities. The trace elements Ba, Br, I, and U are readily measured in the lunar rocks by our technique, even in the presence of complicated preexisting krypton and xenon spectra. Indeed, temperature release curves for the gases from these trace elements can be calculated, as a possible means of distinguishing surficial and other lightly bound fractions of an element from more retentively sited components.

EXPERIMENTAL PRELIMINARIES

The work was focused on the two lunar rocks for which HOHENBERG *et al.* (1970) have obtained complete data for stepwise temperature release of rare gases, rock 10057, which is a fine-grained and high rubidium (type A) basalt, and rock 10044, which is a coarse-grained and low-rubidium (type B) basalt (PAPANASTASSIOU, *et al.*, 1970). Because of the variety of effects involved; we chose a neutron spectrum for the irradiation with a smaller ratio of fast to thermal neutrons than TURNER (1970a) has used. The irradiation was carried out in the pool of the General Electric Test Reactor, Vallecitos Nuclear Center, Pleasanton, California. The nominal integrated fluxes, as supplied by the Vallecitos Center were

thermal ($E < 0.17$ ev) 1.35×10^{19} neutrons/cm^2
epithermal (0.17 ev $< E <$ 0.18 Mev) 0.411×10^{19} neutrons/cm^2
fast ($E >$ 0.18 Mev) 0.0869×10^{19} neutrons/cm^2.

We have not yet run the monitors which can confirm those fluxes. Tentatively we use the nominal values with an assigned error of $\pm 20\%$. The capsule was designed to rotate continuously about a vertical axis parallel to the core of the reactor, but unfortunately the mechanism for rotation failed soon after the irradiation began. As a substitute for continuous rotation under these circumstances, the capsule was rotated 180° midway through the irradiation. Counting of cobalt-doped flux wires packed with the samples indicates that the spatial variations in the total neutron exposure for the samples were no more than 2 to 3%.

The samples were packed in evacuated quartz tubes, but it was not possible to analyze the rare gases which escaped into the gas phase during the neutron irradiation or during the time the samples were stored in the extraction system (and mildly heated, maximum temperature 110° C) prior to the actual run. In subsequent work these "lost" gases are also being analyzed. But in the present report, we must emphasize, the sites in the rocks of very low retentivity for argon, krypton, and xenon have not been sampled.

$^{40}Ar/^{39}Ar$ AGE STUDIES

In favorable rocks the argon data permit reliable K–Ar ages to be determined (MERRIHUE and TURNER, 1966). If during the last part of the release there is a temperature regime where the argon is coming almost entirely from highly retentive sites, the ratio $^{40}Ar/^{39}Ar$ will exhibit a plateau. Both isotopes are coming from potassium sites: The ^{40}Ar was formed there by natural radioactive decay of ^{40}K; the ^{39}Ar was formed there during the pile irradiation by fast neutrons via the (n, p) reaction on ^{39}K. The ratio of the isotopes seen at the plateau is proportional to the $^{40}Ar/^{40}K$ ratio in retentive minerals, a quantity which is a well known function of the age of the minerals. Figure 1 shows $^{40}Ar/^{39}Ar$ ratios from Apollo 11 rocks 10044 and 10057 determined at a progression of temperatures (half hour heatings) and plotted as a function of the cumulative ^{39}Ar release at the end of the heatings. The data for the plot are set out in Table 1. In determining the ordinate we have subtracted small amounts of ^{40}Ar due to combined contributions of solar wind and cosmic-ray spallation (the ratio $^{40}Ar/^{36}Ar$ assumed to be unity in this component); similarly we have subtracted small amounts of ^{39}Ar from the (n, α) reaction on ^{42}Ca, using the monitoring reaction ^{40}Ca (n, α) ^{37}Ar to make this correction. One can see from Table 1 that both corrections are usually small.

For rock 10044, one can obtain a valid date by the method. It exhibits a well-defined plateau, which is almost identical to that found by TURNER (1970a). Note that Turner's points are for the upper midpoints of the rectangles in the implied histogram,

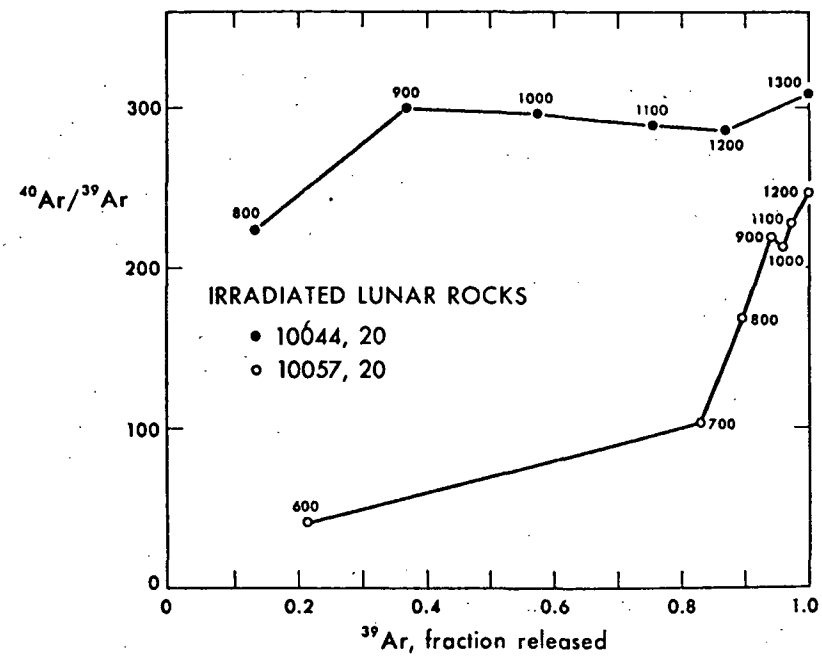

Fig. 1. Comparative release of ^{40}Ar and ^{39}Ar from pile-irradiated lunar rocks. The numbers on the points are release temperatures in degrees Centigrade (progressive half hour heatings). Rock 10044, with a good high temperature plateau, can be precisely dated by the technique. Rock 10057 cannot.

Table 1. Data for $^{40}Ar/^{39}Ar$ dating of lunar rocks.

Heating Temperature °C	Cumulative fractional release of ^{39}Ar after heating	$\left(\frac{^{40}Ar}{^{39}Ar}\right)_{measured}$	$\left(\frac{^{40}Ar}{^{39}Ar}\right)_{corrected}$
	Rock 10044		
800	0.133*	221.3†	223.3‡
900	0.372	293.0	300.9
1000	0.577	288.0	297.3
1100	0.758	281.5	289.7
1200	0.872	254.7	286.5
1300	1.000	203.2	309.4
	Rock 10057		
600	0.214*	41.7†	40.5‡
700	0.830	109.9	103.8
800	0.898	176.5	168.9
900	0.942	217.9	218.9
1000	0.959	214.6	213.7
1100	0.973	213.5	228.9
1200	1.000	200.4	247.2

* Errors in ^{39}Ar increments are 10% of the increments.
† Errors in the measured $^{40}Ar/^{39}Ar$ ratios are 1.5%.
‡ The additional error in the corrected $^{40}Ar/^{39}Ar$ ratios is 14% of the correction. ^{40}Ar has been corrected for cosmogenic and trapped argon. ^{39}Ar has been corrected for production by the (n, α) reaction on ^{42}Ca.

whereas we plot the upper right-hand corner. The difference in method of plotting makes it appear that our sample was less retentive of ^{40}Ar than his, which is not the case (our sample showed 3.2% loss of ^{40}Ar; Turner's showed 7% loss). The maximum fractional variation in the $^{40}Ar/^{39}Ar$ ratios above 800° C in this rock corresponds to a fractional age variation of only 3%, a respect in which our results are identical with Turner's. The age we calculate for rock 10044 is $(4.00 \pm 0.07) \times 10^9$ years, based on a meteorite standard, Karoonda. Karoonda is one of a group of meteorites found to have a common age when dated by the $^{40}Ar/^{39}Ar$ method (PODOSEK 1971). We assume, with PODOSEK, that the most precisely dated meteorite of this group (St. Severin) is 4.6×10^9 years old; in that case, the age of Karoonda inferred from PODOSEK's data is $(4.58 \pm 0.05) \times 10^9$ years. The error in this last quantity is the largest component in the error computed for rock 10044. In addition, any shift in the age of St. Severin will shift the age of rock 10044 essentially the same amount. Our result does not agree well with TURNER's (1970a) value of $(3.74 \pm 0.08) \times 10^9$ years for this rock, but it coincides, within the errors, with the average age of TURNER's other type B rocks from Apollo 11, namely $(3.88 \pm 0.08) \times 10^9$ years. TURNER (1970b) has noted that "plateau ages" obtained for type B rocks from Apollo 11 are systematically older than those for type A. Our datum supports this observation.

Rock 10057, on the other hand, exhibits no plateau whatsoever and cannot be dated by the method. From agreement between the Rb–Sr ages on these two rocks (PAPANASTASSIOU *et al.*, 1970) we would expect $^{40}Ar/^{39}Ar$ ratios in retentive minerals in the two rocks to have the same values within 5%. But note how lightly the ^{39}Ar is bound in rock 10057: 90% of the isotope is released even before the 900° C heating was started. It is clear from our work that the isotope ^{40}Ar is also lightly bound and poorly retained.

The difference between rocks 10044 and 10057 for argon dating could well have been anticipated from the release patterns obtained for unirradiated samples of these rocks and tabulated by HOHENBERG *et al.* (1970). Both rocks show double peaks in their ^{40}Ar release, at ~800° C and ~1200° C. But most of the release in rock 57 is associated with the low temperature peak, whereas virtually all of the release in rock 44 is associated with the high temperature peak. For both rocks the release curves for ^{40}Ar after irradiation (this work and TURNER, 1970a) are different from before. For rock 44 the release curve is shifted down in temperature by about 200 centigrade degrees, without change in shape. For rock 10057 the broad lower temperature release peak is sharpened and shifted down in temperature by 100 to 200 centigrade degrees. The higher temperature peak, of less importance than the other in both irradiated and unirradiated samples, is shifted down in temperature by about 300 centigrade degrees and broadened. Clearly ^{40}Ar release patterns are altered by the neutron irradiation. This does not seem to affect the validity of the method, which, of course, depends only upon effects for the two isotopes, 39 and 40, being the same.

Kr AND Xe RELEASE

Krypton and xenon spectra from irradiated lunar rocks are very complex because of the presence of so many gas components. Fortunately the isotopic compositions

of the various components are known and the number of isotopes exceeds the number of components. In this circumstance, the problem is amenable to analysis. For krypton we have 7 isotopes: the usual stable isotopes plus 10.7 year ^{85}Kr produced in the neutron-induced fission of ^{235}U. There are five possible gas components: spallogenic krypton from cosmic-rays, "trapped" krypton, fissiogenic krypton from n-fission of ^{235}U, monoisotopic ^{83}Kr from *n*-capture in ^{82}Se, and a mixture of ^{80}Kr and ^{82}Kr from *n*-capture in bromine. We use quotation marks in referring to the "trapped" component because this component is probably a mixture of atmospheric contamination and of solar-wind krypton in dust particles adhering to the rock sample; in neither case is the gas trapped in the rock in the usual sense. For xenon we have 9 isotopes and 6 components of known isotopic composition: spallogenic xenon from cosmic rays, "trapped" xenon, fission xenon from *n*-fission of ^{235}U (completely dominating the traces of xenon present from spontaneous fission of ^{238}U), an extra monoisotopic component, ^{136}Xe, from pile-neutron capture in short-lived fissiogenic ^{135}Xe, monoisotopic ^{128}Xe from *n*-capture in iodine, and monoisotopic ^{131}Xe from *n*-capture in barium (in lunar rocks completely dominating ^{131}Xe from *n*-capture in tellurium).

Most of these components are known and constant in composition throughout the release. Where there were uncertainties in composition we adopted a single isotopic composition taken from HOHENBERG *et al.* (1970), but assigned large enough errors to include the possible variations. We refer here to "trapped" xenon where the isotopic composition may be like the atmosphere, or like the solar wind, or in between; and to cosmogenic ^{129}Xe, ^{131}Xe, and ^{132}Xe which showed occasional, sporadic variations in relative abundance during the experiments with the unirradiated samples.

METHOD OF CALCULATION

How best to unravel these spectra and determine the amounts (and errors in the amounts) of each component present in each temperature fraction posed an interesting mathematical problem. We solved the problem to our satisfaction with a least squares method involving matrices which permitted us to use all the data in a simple computational format. We describe the process briefly here as it applies to krypton. Although straightforward, the method appears not to be published and we plan to publish a more adequate account elsewhere. Each of the samples is a mixture of seven isotopes which can be represented by a vector $\vec{A}$ in seven dimensional space. Each of the samples is also a mixture of five components which can be represented by a vector $\vec{C}$ in five dimensional space. The fractional isotopic abundances of the various pure components, written as an array, define a 7 × 5 matrix, **F**, which relates the vectors $\vec{A}$ and $\vec{C}$:

$$\vec{A} = \mathbf{F}\vec{C}.$$

We measure $\vec{A}$ for a sample and seek $\vec{C}$. The best value of $\vec{C}$ is one for which the sum of squares:

$$S = \sum_{j=1}^{7}\left[a_j - \sum_{i=1}^{5} f_{ji}c_i\right]^2$$

is a minimum. The solution to this least squares problem is $\vec{C} = (F'F)^{-1}F'\vec{A}$ where F' is the transpose of F and $(M)^{-1}$ is the inverse of M. The error estimates in $\vec{C}$ are also obtained by a matrix method which utilizes the errors in both the components of $\vec{A}$ and the elements of F. The basic matrix relation used in solving the error problem was

$$(P + \varepsilon Q)^{-1} \rightarrow P^{-1} - \varepsilon P^{-1}QP^{-1} \qquad \text{as } \varepsilon \rightarrow 0.$$

by means of which the errors in the matrix $(F'F)^{-1}F'$ were obtained from the errors in F.

RESULTS AND DISCUSSIONS

The totaled results from all temperature fractions are set out in Table 2. Release curves for the various components are shown as Figs. 2 through 5. The errors plotted in the figures are 1 σ errors with contributions included, as they would propagate through our matrix solutions, from all known sources, *except* the uncertainties in mass spectrometer sensitivity. These last errors affect equally all components of a gas at each release temperature. For krypton this additional source of error is judged to be 25%; for xenon, 20%. The errors in Table 2 are total errors, including the errors in spectrometer sensitivity. The final errors are sometimes quite large, in part because we were generous in assigning errors to the isotopic abundances of those components where a range of values would be possible (see above).

Table 2. Totaled gas components from pile-irradiated lunar rocks.

Component	Amount	Inferred Quantity	Comparison	Reference
		Kr Components		
		Rock 10044		
Kr "trapped"	400 ± 103		1450 ± 450 unirradiated	(1)
$Kr^{80,82}$ *n*-capture Br	292 ± 75	12.4 ± 3.2 ppb Br	190 ppb Br	(2)
Kr cosmogenic	258 ± 72		523 ± 156 unirradiated	(1)
Kr *n*-fission U^{235}	30 ± 14	0.15 ± 0.07 ppm U	0.28 ppm U	(3)
Kr^{83} *n*-capture Se	2 ± 12	134 ± 770 ppb Se	~800 ppb Se (rock 10045)	(4)
		Rock 10057		
Kr "trapped"	1907 ± 486		2060 ± 370 unirradiated	(1)
$Kr^{80,82}$ *n*-capture Br	1105 ± 287	47 ± 12 ppb Br	25.2 ppb Br	(5)
Kr cosmogenic	350 ± 153		326 ± 59 unirradiated	(1)
Kr *n*-fission U^{235}	280 ± 76	1.37 ± 0.37 ppm U	0.80 ppm U	(3)
Kr^{83} *n*-capture Se	16 ± 64	990 ± 3900 ppb Se	~700 ppb Se (rock 10022)	(4)
		Xe Components		
		Rock 10044		
Xe^{131} *n*-capture Ba	2070 ± 415	84 ± 17 ppm Ba	95 ppm Ba	(7)
Xe *n*-fission U^{235}	224 ± 55	0.19 ± 0.05 ppm U	0.28 ppm U	(3)
Xe "trapped"	89 ± 62		52 ± 7 unirradiated	(1)
Xe cosmogenic	85 ± 90		128 ± 9 unirradiated	(1)
Xe^{128} *n*-capture I	13 ± 12	0.93 ± 0.85 ppb I	≥10 ppb I	(2)
		Rock 10057		
Xe^{131} *n*-capture Ba	4939 ± 989	202 ± 40 ppm Ba	208 ppm Ba	(3)
Xe *n*-fission U^{235}	686 ± 139	0.59 ± 0.12 ppm U	0.80 ppm U	(3)
Xe "trapped"	370 ± 83		669 ± 44 unirradiated	(1)
Xe cosmogenic	112 ± 64		296 ± 21 unirradiated	(1)
Xe^{128} *n*-capture I	10.3 ± 7.9	0.74 ± 0.55 ppb I	≥4.7 ppb I (rock 10017)	(6)

Units are 10^{-12} cc STP/g unless otherwise specified. Errors in this table are total errors (~1 σ). References: (1) HOHENBERG *et al.* (1970); (2) REED and JOVANOVIC (1970); (3) WÄNKE *et al.* (1970); (4) HASKIN *et al.* (1970); (5) GANAPATHY *et al.* (1970); (6) REED and JOVANOVIC (1971); (7) TERA *et al.* (1970).

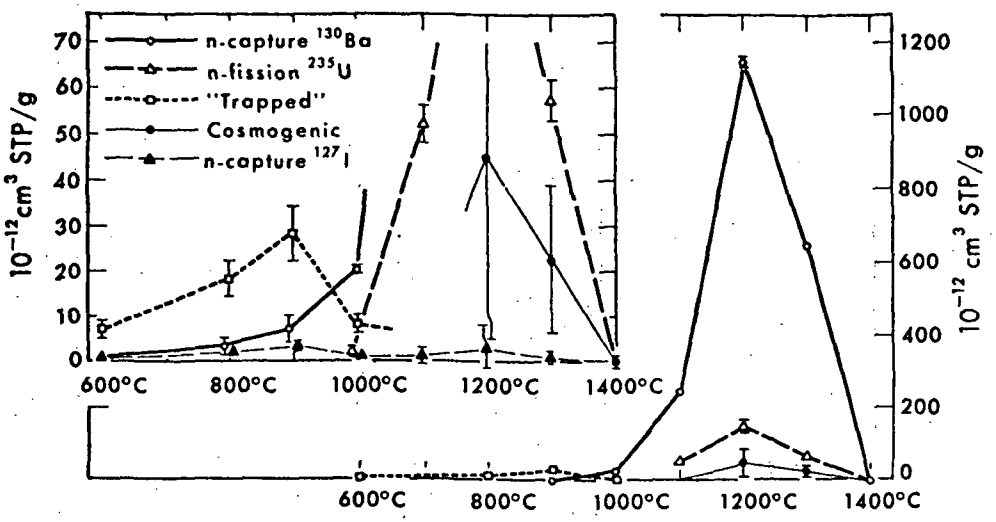

Fig. 2. Release curves for xenon components from pile-irradiated lunar rock 10044. The spectra are dominated by ^{131}Xe from *n*-capture in ^{130}Ba. Errors (1 σ) include all known sources except for variation from one temperature to another in xenon sensitivity ($\pm$20%).

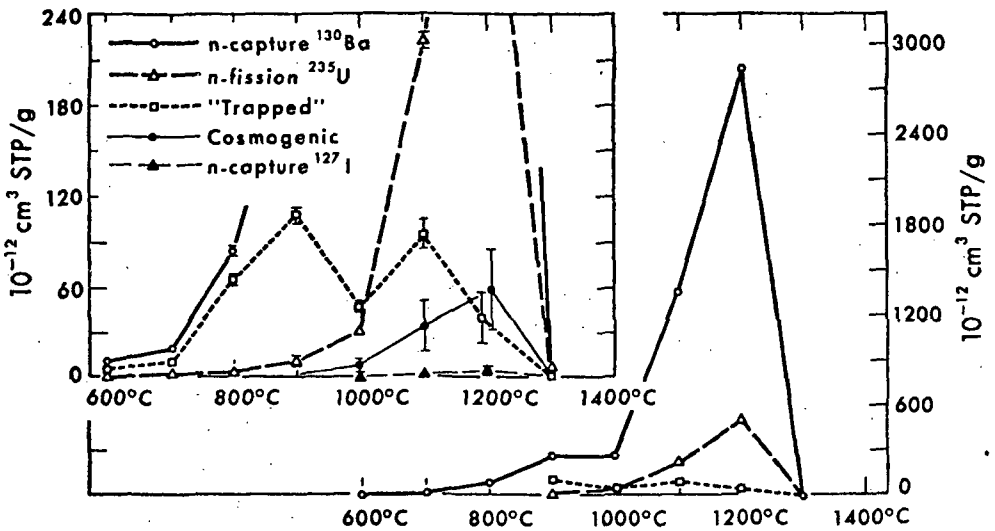

Fig. 3. Release curves for xenon components from pile-irradiated lunar rock 10057. The spectra are dominated by ^{131}Xe from *n*-capture in ^{130}Ba. For comment on errors, see caption for Fig. 2.

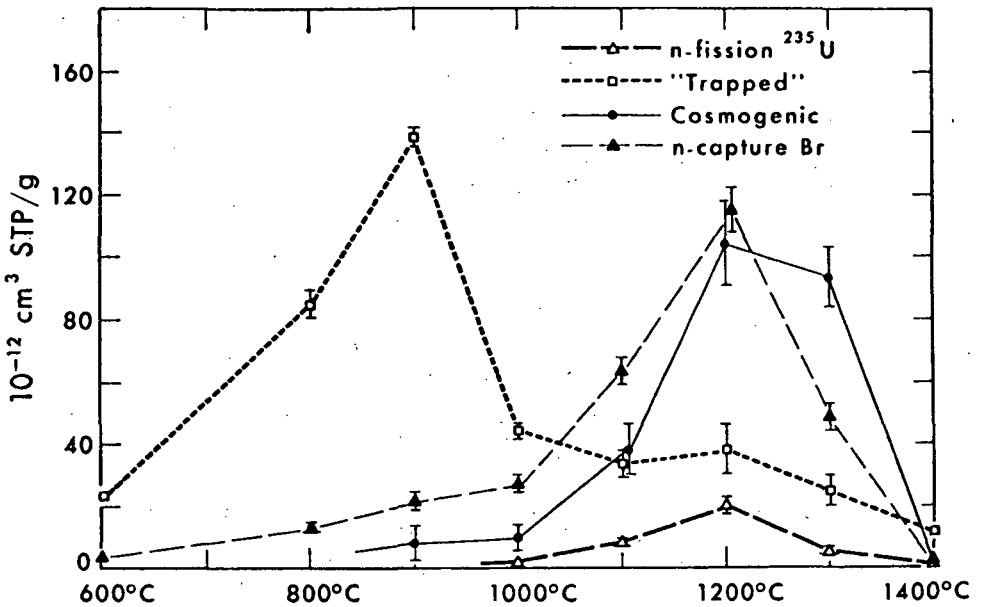

Fig. 4. Release curves for krypton components from pile-irradiated lunar rock 10044. Errors (1 σ) include all known sources except for variation from one temperature to another in krypton sensitivity ($\pm 25\%$).

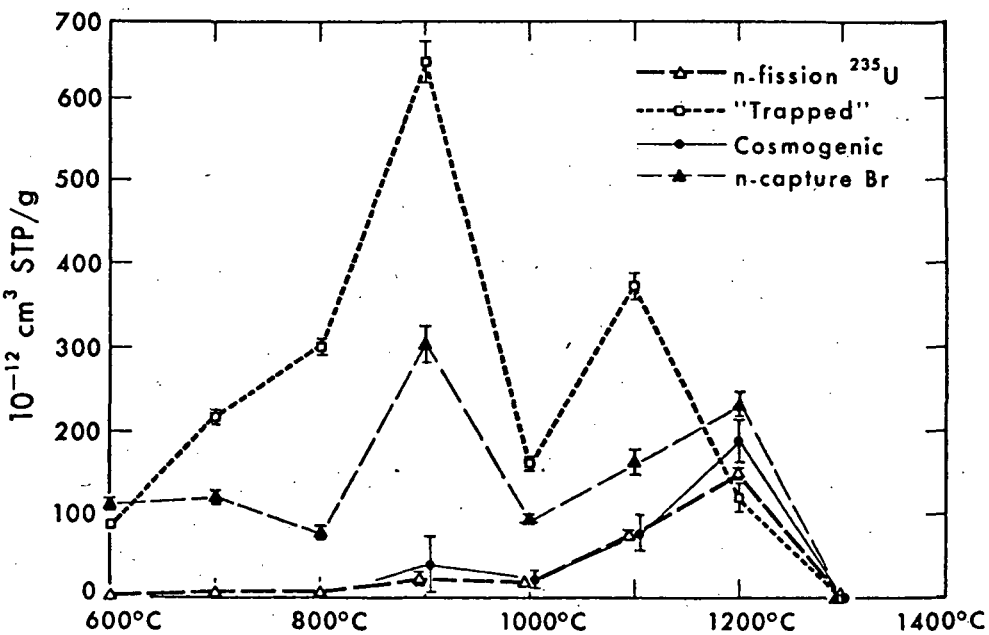

Fig. 5. Release curves for krypton components from pile-irradiated lunar rock 10057. For comment on errors, see caption for Fig. 4.

No serious discrepancies between results in irradiated and unirradiated samples can be noted. There appears to be less "trapped" krypton in 10044 and less "trapped" xenon in 10057 after the irradiation than before, but since the "trapped" gases are probably a mixture of atmospheric contamination and of solar wind gas dissolved in dust particles adhering to the grains, their concentrations would not be expected to be highly reproducible. The substantially larger amounts of "trapped" xenon and krypton in our sample of 10057, relative to the amounts we saw in 10044, was again seen in the irradiated samples and proved that the effect is not instrumental. The release patterns for the "trapped" gases in irradiated rock 10044 differ from those obtained with the unirradiated samples (see Fig. 4, HOHENBERG *et al.*, 1970) but the latter were of such shape as to suggest that most of the "trapped" gases in 10044 are system blanks.

One would not expect the amounts or release patterns for the cosmogenic gases to be altered by the irradiation, and no such effects were seen. An exception was an apparent loss of cosmogenic xenon in irradiated rock 10057. But the effect is statistically of low significance. There is a large 1 σ error (aside from the 20% uncertainty in xenon sensitivity for the mass spectrometer) for cosmogenic xenon in irradiated 10057. At the 2 σ level, the errors would almost overlap.

The release curves in Figs. 2–5 are useful for getting an overall picture of the krypton and xenon in the irradiated rocks. Most striking is the dominance of the xenon by ^{131}Xe from n-capture in ^{130}Ba. The effect is so large as to suggest that neutrons are in some way responsible for the large and variable ^{131}Xe anomaly in the Apollo rocks. Unfortunately the ^{131}Xe anomaly cannot be attributed to capture of natural slow neutrons in the rocks, a process which can be independently monitored in the rocks by the measurement of n-capture in ^{157}Gd (ALBEE *et al.*, 1970; MARTI *et al.*, 1970).

The xenon components generated in the pile have single-peaked release patterns rather similar to the release of the cosmogenic component, except for the component from iodine, which is more diffuse in its release.

For krypton there is no dominant component corresponding to Xe^{131}; the various components tend to be comparable in size. Most of the components generated in the pile have release patterns similar to the cosmogenic release pattern, but again the component from the halogen, now bromine, is released more diffusely. Also we note that the krypton components in 10057 tend to be generally more diffusely released than in 10044. The krypton from n-capture in bromine in 10057 is especially diffusely released, and is almost four times more abundant than its counterpart in 10044.

TRACE ELEMENT ESTIMATES

The concentrations of Ba, U, Br, I, and Se inferred from our rare gas concentrations (see Table 2) depend upon the nominal slow-neutron flux for the irradiation, which we have not yet checked, and upon values for slow neutron cross sections taken from the literature. Some confidence in these parameters is generated by the generally good agreement with radiochemical data for the barium and uranium concentrations we have measured. These elements are lithophile and nonvolatile.

They can thus be expected to be sited away from grain boundaries where the rare gases produced will be reasonably well retained. Such appears to be the case, judging from both our concentrations and release curves.

Our values for selenium are too imprecise to be very useful. It is doubtful if our method will ever give much better selenium values, except in particularly favorable samples.

There are relatively few data for bromine and iodine in the lunar rocks. Bromine has been measured by MORRISON *et al.* (1970, 1971) but in their Apollo 12 report they include this element in a group for which there are analytical problems associated with the determinations. Bromine has been measured in rock 10057 by GANAPATHY *et al.* (1970) at 25.2 ppb and in rock 10044 by REED and JOVANOVIC (1970) at 190 ppb. Our results for the bromine (at reasonably gas-retentive sites) in these rocks are 47 and 12.4 ppb respectively, so that we agree reasonably well with GANAPATHY *et al.* (1970) but poorly with REED and JOVANOVIC. In other comparisons (see GANAPATHY *et al.*, 1970) the bromine values of REED and JOVANOVIC (1970) tend to be high. While rock 10044 is a type B rock and conceivably could differ greatly in its bromine content from Type A rocks, ANDERS *et al.* (1971) recently have reported a low value (29 ppb) from bromine in rock 10047, of Type B. We thus are inclined to question the high value reported by REED and JOVANOVIC (1970). But we really have to reserve judgment until we have studied the "lost" gases from irradiated lunar rocks and have gained some idea of the concentrations of surficial bromine.

The situation with respect to iodine analyses is presently unclear. Here we can compare only our values for "interior" iodine with values of "leachable" iodine given by REED and JOVANOVIC (1970) as lower limits. Obviously we are comparing what may be mutually exclusive results. For rock 10044 their value is ≥ 10 ppb; ours is 0.9 ppb. For type A rocks we had no samples in common, but their value of ≥ 4.7 ppb for rock 10017 can perhaps be compared with our value of 0.7 ppb for rock 10057. The question of the abundance of iodine in lunar samples is clearly still open.

Acknowledgments—This work was supported in part by NASA and the U.S. Atomic Energy Commission. It bears AEC Code No. UCB-34P32-76.

REFERENCES

ALBEE A. L., BURNETT D. S., CHODOS A. A., EUGSTER O. J., HUNEKE J. C., PAPANASTASSIOU D. A., PODOSEK F. A., RUSS G. P., II, SANZ H. G., TERA F., and WASSERBURG G. J. (1970) Ages, irradiation history, and chemical composition of lunar rocks from the Sea of Tranquillity. *Science* **167**, 463–466.

ANDERS E., LAUL J. C., KEAYS R. R., GANAPATHY R., and MORGAN J. W. (1971) Elements depleted on lunar surface: Implications for origin of moon and meteorite influx rate. Second Lunar Science Conference (unpublished proceedings).

GANAPATHY R., KEAYS R. R., LAUL J. C., and ANDERS E. (1970) Trace elements in Apollo 11 lunar rocks: Implications for meteorite influx and origin of moon. *Proc. Apollo 11 Lunar Sci. Conf., Geochim. Cosmochim. Acta* Suppl. 1, Vol. 2, pp. 1117–1142. Pergamon.

HASKIN L. A., ALLEN R. O., HELMKE P. A., PASTER T. P., ANDERSON M. R., KOROTEV R. L., and ZWEIFEL K. A. (1970) Rare earths and other trace elements in Apollo 11 lunar samples. *Proc. Apollo 11 Lunar Sci. Conf., Geochim. Cosmochim. Acta* Suppl. 1, Vol. 2, pp. 1213–1231. Pergamon.

HOHENBERG C. M., DAVIS P. K., KAISER W. A., LEWIS R. S., and REYNOLDS J. H. (1970) Trapped and cosmogenic rare gases from stepwise heating of Apollo 11 samples. *Proc. Apollo 11 Lunar Sci. Conf., Geochim. Cosmochim. Acta* Suppl. 1, Vol. 2, pp. 1283–1309. Pergamon.

JEFFERY P. M. and REYNOLDS J. H. (1961) Origin of excess Xe^{129} in stone meteorites. *J. Geophys. Res.* **66**, 3582–3583.

MARTI K., LUGMAIR G. W., and UREY H. C. (1970) Solar wind gases, cosmic ray spallation products, and the irradiation history. *Science* **167**, 548–550.

MERRIHUE C. M. (1966) Xenon and krypton in the Bruderheim meteorite. *J. Geophys. Res.* **71**, 263–313.

MERRIHUE C. M. and TURNER G. (1966) Potassium-argon dating by activation with fast neutrons. *J. Geophys. Res.* **71**, 2352–2857.

MORRISON G. H., GERARD J. T., KASHUBA A. T., GANGADHARAM E. V., ROTHENBERG A. M., POTTER N. M., and MILLER G. B. (1970) Elemental abundances of lunar soil and rocks. *Proc. Apollo 11 Lunar Sci. Conf., Geochim. Cosmochim. Acta* Suppl. 1, Vol. 2, pp. 1383–1392. Pergamon.

MORRISON G. H., GERARD J. T., POTTER N. M., GANGADHARAM E. V., ROTHENBERG A. M., and BURDO R. A. (1971) Elemental abundances of lunar soil and rocks from Apollo 12. Second Lunar Science Conference (unpublished proceedings).

PAPANASTASSIOU D. A., WASSERBURG G. J., and BURNETT D. S. (1970) Rb–Sr ages of lunar rocks from the Sea of Tranquillity. *Earth Planet. Sci. Lett.* **8**, 1–19.

PODOSEK F. A. (1971) Neutron-activation potassium-argon dating of meteorites. *Geochim. Cosmochim. Acta* **35**, 157–173.

REED G. W., Jr. and JOVANOVIC S. (1970) Halogens, mercury, lithium, and osmium in Apollo 11 samples. *Proc. Apollo 11 Lunar Sci. Conf., Geochim. Cosmochim. Acta* Suppl. 1, Vol. 2, pp. 1487–1492. Pergamon.

REED G. W. and JOVANOVIC S. (1971) The halogens and other trace elements in Apollo 12 soil and rocks; Halides, platinum metals and mercury on surfaces. Second Lunar Science Conference (unpublished proceedings).

TERA F., EUGSTER O., BURNETT D. S. and WASSERBURG G. J. (1970) Comparative study of Li, Na, K, Rb, Cs, Ca, Sr and Ba abundances in achondrites and in Apollo 11 lunar samples. *Proc. Apollo 11 Lunar Sci. Conf., Geochim. Cosmochim. Acta* Suppl. 1, Vol. 2, pp. 1637–1657. Pergamon.

TURNER G. (1970a) Argon–40/argon–39 dating of lunar rock samples. *Science* **167**, 466–468.

TURNER G. (1970b) Argon–40/argon–39 dating of lunar rock samples. *Proc. Apollo 11 Lunar Sci. Conf., Geochim. Cosmochim. Acta* Suppl. 1, Vol. 2, pp. 1665–1684. Pergamon.

WÄNKE H., RIEDER R., BADDENHAUSEN H., SPETTEL B., TESCHKE F., QUIJANO-RICO M., and BALACESCU A. (1970) Major and trace elements in lunar material. *Proc. Apollo 11 Lunar Sci. Conf., Geochim. Cosmochim. Acta* Suppl. 1, Vol. 2, pp. 1719–1727. Pergamon.

Proceedings of the Second Lunar Science Conference, Volume 2, pp. 1627–1641.
The M.I.T. Press, 1971.

Rare gas measurements in three mineral separates of rock 12013,10,31

W. A. KAISER
Department of Physics, University of California, Berkeley, California 94720

(*Received 24 February 1971; accepted in revised form 20 April 1971*)

Abstract—He, Ne, Ar, Kr, and Xe were measured in 3 different mineral separates of 12013,10,31 selected by handpicking and identified by microprobe analysis (WALTER, 1970). About 10 mg of each fraction were available for the rare gas analyses. The rare gas measurements showed clear differences due to different concentrations of K, Ba, rare earth elements (REE) etc. The K–Ar ages were in good agreement with TURNER's (1970) results. The Kr and Xe amounts were predominantly produced by cosmic ray bombardment. The ^{126}Xe-exposure ages varied from 40 × 10^6 y to 47 × 10^6 y). In one sample cosmogenic ^{126}Xe was, by calculation, 98.5% from Ba as a target; in another, this percentage was 76. Thus we could make a good measurement of the cosmogenic Xe spectrum for Ba and a rough estimate of the spectrum for REE. The spectra were generally in agreement with published target data for 730 MeV protons (FUNK *et al.*, 1967; HOHENBERG and ROWE, 1970). No trapped Xe and Kr was found in the separates. No ^{129}Xe coming from in situ decay of ^{129}I was measured. No evidence for or against the ^{244}Pu hypothesis was seen, confirming the results of ALEXANDER (1970) and LUNATIC ASYLUM (1970).

INTRODUCTION

THIS WORK WAS STARTED under the impression that Apollo rock 12013 had a crystallization age of 4.5 × 10^9 y (WASSERBURG, 1970), in which case it should be highly possible to detect traces of extinct radioactivities in lunar material. The extraordinarily high abundances of Ba, REE, U, and nearly all other trace elements reported by the LSPET (1970), pointed to this rock as a unique source for studies. We should have been able to see radiogenic ^{129}Xe coming from decay in situ of ^{129}I and a fissiogenic Xe contribution from ^{244}Pu.

Thus, the situation appeared unusually favorable in 12013. Since ALEXANDER (1970) was investigating a homogenized sample 24 + 37, mostly light material, and the LUNATIC ASYLUM (1970) had measured several bulk pieces, our approach was to make separations, in hopes of achieving in one or the other of the fractions enrichments of the trace elements, especially U. We were successful in this respect as judged by microprobe investigations on representative material, which provided us with mineralogical data we could use to identify our samples with samples measured elsewhere for trace element abundances. Meanwhile several investigations (TURNER, 1970; LUNATIC ASYLUM, 1970; TATSUMOTO, 1970) showed that the actual crystallization age of this rock was closer to 4.0 × 10^9 y, making it doubtful that evidences of extinct radioactivity could be detected.

EXPERIMENTAL TECHNIQUES

Sample 12013,10,31 was an interior chip consisting of a light and a dark phase. We crushed the sample in an agate mortar and separated by sieving particles of a size between 50 and 150 μ, in

order to acquire as many pure crystals (without intergrowths) as possible. Then, we put the whole sample in reagent grade acetone and cleaned it in an ultrasonic-cleaner for 5 min, separating the grains from each other in the process. Afterwards, we sieved the sample again using a special filtering funnel. This consisted of 3 quartz sections, which enabled us to sieve and filter simultaneously. We used a "membrane" filter with a pore size of 0.04 μ to remove the fine particles. The crystals larger than 50 μ were collected on a stainless steel screen. We made separates from this material handpicking under a stereomicroscope according to color. We were able to separate 4 different mineral agglomerates: milky white, clear, black vesicular, and greenish, but we present results for only three of the fractions in this paper in the interests of brevity. (Additional measurements on sample 12013,10,31 including a detailed stepwise temperature analysis of the residual fine material, will be described elsewhere (KAISER, 1971).

The samples were wrapped in Reynolds Al-foil (heavy duty), previously cleaned by polishing with a tissue wipe and ultrasonic agitation in acetone. The Al-foil was always handled with gloves after cleaning. The samples were measured in BMS 4, previously described as system I in HOHENBERG *et al.* (1970), a Pyrex glass-spectrometer with an all-metal-sample system. Separate analyses were made of the gases released by one-hour heating at 700°C and 1550°C (well above the melting point for all samples). The temperature was measured by two thermocouples, which were consistently in good agreement with each other. The temperatures specified (referring to the base of crucible) are correct to within ±15°C. We have made numerous measurements of the blanks. Since the samples weighed only about 10 mg each and were wrapped in about 200 mg of Al-foil, it was important to include the Al-foil in our blanks. Therefore, we ran pure Al-foil of the same kind and amounts as used to wrap our samples under the same temperature and measurement conditions as the samples. The results for the different gases were in good agreement with each other except for Kr. The isotopic compositions found were those of air. Three Al-samples were run (Table 1).

All results are corrected for spectrometer background and for discrimination except for He, where no discrimination-value was available. For He we applied a discrimination factor of 1. (Results of He measurements on an interlaboratory standard sample of the Bruderheim meteorite indicated that this discrimination factor is essentially unity.) The spectrometer background corrections were essentially negligible except in instances to be noted below. The errors listed in the tables include all known sources and are based upon observed reproducibilities of peak-ratios, air-pipette analyses, or blank runs as the case may be. A few of the errors had to be increased further for causes we now note: During this series of runs we had some problems with the ^{20}Ne background, caused by a saturation of the Vac-ion pump of the spectrometer and requiring a somewhat large background correction. The error assigned for this correction was the full value of the background and is certainly too high. The ^{20}Ne values were also corrected for doubly charged ^{40}Ar but this correction was small. We had a high "dirt" background for ^{78}Kr. The error listed in this case includes the full value of this correction.

TRACE ELEMENT ABUNDANCES

Mineralogical data were obtained for each of the three fractions by electron microprobe analysis of a few grains (WALTER, 1970). Mineral agglomerate 31A, a

Table 1. Rare gases in the Al-foil [$\times 10^{-8}$ cc STP/g Al]. The foil is Reynolds Wrap, heavy duty, 0.001" thickness. Except for Kr, we have averaged these separate runs.

T	^4He	^{22}Ne	^{36}Ar	^{83}Kr			^{130}Xe
				Weight			
				132 mg	167 mg	186 mg	
700°C	31.9 ± 3.8	0.013 ± 0.001	0.029 ± 0.001	0.00006	0.00026	0.00027	0.000022 ± 0.000002
1550°C	2.7 ± 0.3	0.005 ± 0.001	0.056 ± 0.003	0.00020	0.00058	0.00023	0.000041 ± 0.000008
Total	34.6 ± 4	0.018 ± 0.002	0.085 ± 0.004	0.00026	0.00084	0.00050	0.000063 ± 0.000010

Table 2. Estimates of trace element abundances for the separates.

	31A Milky white	31B Clear	31C Black vesicular	Remarks
K (%)	4.32 ± 0.78	1.67 ± ?	$\frac{0.57 + 0.48^{g}}{2} = 0.53 \pm 0.07^{i}$	[a] $Y(31A, 31B) = \frac{\bar{Y}(15, 18, 41, 44, 37 + 24)}{Y(\text{chondrites})} \times Y(\text{chondrites})$ $Y(\text{chondrites} = 1.9$ ppm) (WAKITA and SCHMITT, 1970, p. 174, Fig. 3)
Ba (ppm)	6360 ± 970	3450 ± ?	$\frac{895 + 1330^{g}}{2} = 1112 \pm 217^{i}$	[b] Average value for 15, 18, 31, 44, 37 + 24; WAKITA and SCHMITT, 1970, p. 171, Table 1)
Ce (ppm)	96 ± 20	169 ± ?	374 ± ?	[c] $Zr(31A, 31B) = Zr/Hf \times Hf$; $(Zr/Hf)_{\text{Apollo 12 soil}} = 27$; (GOLES *et al.*, 1971)
Eu (ppm)		2.8 ± ?	3.48[g] ± ?	[d] Zr value measured by optical spectroscopy (LSPET, 1970)
Sr (ppm)	145 ± 10	180[f] ± ?	$\frac{157 + 219^{f}}{2} = 190^{i} \pm 31$	[e] $U = \frac{K}{K/U}$; K/U [%/ppm] = 0.19 ± 0.02 (average value of 15, 18, 41, 44, 37 + 24; WAKITA and SCHMITT, 1970, p. 171, Table 1)
Y (ppm)	247[a] ± ?	247[a] ± ?	589[b] ± ?	[f] $Sr(31B) = (Sr/Eu) \times Eu$; $(Sr/Eu)_{\text{light colored phase}} = 64.3$ (HUBBARD *et al.*, 1970, p. 182, Table 1)
Hf (ppm)	20.3[b] ± ?	20.3[b] ± ?	36[g] ± ?	[g] Chemical abundances for 06 (WAKITA and SCHMITT, 1970, p. 171, Table 1, a sample similar to 15—dark (SCHNETZLER *et al.*, 1970))
Zr (ppm)	548[c] ± ?	548[c] ± ?	972[c] ± ?	[h] $Y(31C) = \frac{Y(06)}{Y(\text{chondrites})} \times Y$ (chondrites) (WAKITA and SCHMITT, 1970, p. 174, Fig. 3)
	(2200)[d] ± ?	(2200)[d] ± ?	(2200)[d] ± ?	[i] Average values of 06 (WAKITA and SCHMITT, 1970) and 15—dark (SCHNETZLER *et al.*, 1970)
U (ppm)	22.7[e] ± 4.8	8.8 ± ?	6[g] ± ? 6.6[i] ± 0.9	[j] $U = \frac{K}{K/U}$; K/U [%/ppm] = 0.08 (06) (WAKITA and SCHMITT, 1970, p. 171, Table 1)

Sample 31A corresponds to an average of samples 15, 15A, and 15B (SCHNETZLER *et al.*, 1970). Sample 31B corresponds to sample 8—light (SCHNETZLER *et al.*, 1970). Sample 31C corresponds to sample 15—dark (SCHNETZLER *et al.*, 1970). The errors assigned are $\Delta\bar{x} = \sqrt{\frac{\Sigma(\bar{x} - x_i)^2}{n(n-1)}}$ type.

milky white phase, contained mainly plagioclase (An_{50}) and pyroxene; sample 31B, a clear phase, was mostly plagioclase (An_{80}); sample 31C, a black phase, was mostly low Ca pyroxene with some feldspar and a high abundance of opaque minerals e.g., ilmenite. In a private communication SCHNETZLER (1970) compared our samples with those of SCHNETZLER *et al.* (1970) using both the mineralogical data by WALTER and direct microscopic observation. On this basis he supplied us with the correspondences specified in Table 2. Trace element abundances were then estimated for the three fractions using those correspondences and data of SCHNETZLER *et al.* (1970); WAKITA

Table 3. Rare gases from one-hour heating of separates

	12013,10,31A (8.95) mg Al foil (199.1 mg)			
	700°C	1550°C	Total	700°C
$^3He/^4He$	0.000089 ± 0.0000006[a]	0.000128 ± 0.000003[a]	0.00009 ± 0.0000008[a]	0.00015 ± 0.000004[a]
$^4He[10^{-3}$ cc STP/g]	3.14 ± 0.06	0.15 ± 0.003	3.29 ± 0.06	1.26 ± 0.03
$^{20}Ne/^{22}Ne$	2.64 ± 1.22	0.84 ± 2.22	1.72 ± 1.42	5.28 ± 0.09
$^{21}Ne/^{22}Ne$	0.67 ± 0.01	0.852 ± 0.02	0.77 ± 0.01	0.53 ± 0.01
$^{22}Ne[10^{-8}$ cc STP/g]	2.73 ± 0.10	3.45 ± 0.14	6.18 ± 0.20	3.43 ± 0.13
$^{38}Ar/^{36}Ar$	0.91 ± 0.03	1.15 ± 0.02	1.05 ± 0.02	0.68 ± 0.02
$^{40}Ar/^{36}Ar$	21630 ± 780	22090 ± 440	21890 ± 420	7530 ± 170
$^{36}Ar[10^{-8}$ cc STP/g]	4.31 ± 0.07	5.81 ± 0.1	10.12 ± 0.13	5.24 ± 0.09
$^{40}Ar_r[10^{-4}$ cc STP/g]	9.27 ± 0.37	12.80 ± 0.34	22.07 ± 0.50	3.85 ± 0.07
$^{78}Kr/^{83}Kr$	0.59 ± 1.2	0.10 ± 0.26	0.19 ± 0.25	0.03 ± 0.95
$^{80}Kr/^{83}Kr$	0.33 ± 0.03	0.44 ± 0.02	0.42 ± 0.02	0.38 ± 0.03
$^{82}Kr/^{83}Kr$	0.78 ± 0.09	0.78 ± 0.03	0.78 ± 0.03	0.96 ± 0.07
$^{84}Kr/^{83}Kr$	2.73 ± 0.19	1.06 ± 0.05	1.35 ± 0.05	3.46 ± 0.16
$^{86}Kr/^{83}Kr$	0.72 ± 0.03	0.29 ± 0.01	0.37 ± 0.02	1.07 ± 0.04
$^{83}Kr[10^{-12}$ cc STP/g]	75 ± 3	350 ± 10	425 ± 10	40 ± 2
$^{124}Xe/^{130}Xe$	0.38 ± 0.02	0.41 ± 0.01	0.41 ± 0.01	0.29 ± 0.01
$^{126}Xe/^{130}Xe$	0.67 ± 0.03	0.78 ± 0.02	0.78 ± 0.02	0.50 ± 0.02
$^{128}Xe/^{130}Xe$	1.17 ± 0.05	1.23 ± 0.03	1.23 ± 0.03	0.98 ± 0.04
$^{129}Xe/^{130}Xe$	2.76 ± 0.13	1.62 ± 0.05	1.66 ± 0.05	3.07 ± 0.09
$^{131}Xe/^{130}Xe$	4.81 ± 0.18	4.31 ± 0.12	4.32 ± 0.12	4.22 ± 0.13
$^{132}Xe/^{130}Xe$	2.47 ± 0.09	1.19 ± 0.03	1.24 ± 0.03	3.01 ± 0.13
$^{134}Xe/^{130}Xe$	0.79 ± 0.03	0.24 ± 0.006	0.26 ± 0.01	0.93 ± 0.04
$^{136}Xe/^{130}Xe$	0.68 ± 0.03	0.17 ± 0.004	0.19 ± 0.004	0.83 ± 0.04
$^{130}Xe[10^{-12}$ cc STP/g]	13 ± 0.5	368 ± 10	381 ± 10	10 ± 0.5

and SCHMITT (1970); HUBBARD *et al.* (1970); GOLES *et al.* (1971) (see Table 2 for details).

RESULTS AND DISCUSSION

The results for He, Ne, Ar, Kr, and Xe for separates 31A, 31B, and 31C are presented in Tables 3 to 11.

Helium

All samples investigated had very high amounts of He with low $^3He/^4He$ ratios (Table 3). Sample 31A contained the lowest $^3He/^4He$ ratio observed. The total amount of ^3He was low compared with 31C, the sample with the highest ^3He concentration. Assuming a similar cosmic ray exposure history for all the minerals, this indicates a severe He loss by diffusion in 31A. The correction for trapped ^4He and for cosmogenic ^4He (using a cosmogenic $^3He/^4He$ ratio of 0.0266; KAISER, 1971) could be neglected. Sample 31B showed a $^3He/^4He$ ratio comparable to 31C. However, the total ^3He and ^4He concentrations were the lowest observed. The total ^3He-content is comparable to 31A, but the ^4He content is nearly a factor of 3 lower, understandable because of the low U concentration in 31B. The total ^3He and ^4He contents in 31C were the highest observed. This sample, mostly pyroxene, showed higher retentivity against diffusive loss of He than the two plagioclase fractions 31A and 31B.

Neon

Most of the Ne measured in the separates was cosmogenic (Table 4). Two kinds

from rock 12013. Errors given are total errors (1σ).

12013,10,31B (9.99 mg) 1550°C	Al-foil (245.7 mg) Total	700°C	12013,10,31C (9.26 mg) 1550°C	Al-foil (243.8 mg) Total
0.00036 ± 0.000007[a]	0.000161 ± 0.0000007[a]	0.00014 ± 0.000001[a]	0.00017 ± 0.000012[a]	0.000146 ± 0.000001[a]
0.05 ± 0.001	1.31 ± 0.03	3.37 ± 0.06	0.33 ± 0.006	3.70 ± 0.06
1.23 ± 0.24	3.83 ± 0.26	3.52 ± 0.11	1.07 ± 0.05	2.15 ± 0.06
0.865 ± 0.023	0.65 ± 0.01	0.66 ± 0.02	0.855 ± 0.04	0.77 ± 0.02
1.91 ± 0.07	5.34 ± 0.15	3.70 ± 0.15	4.66 ± 0.20	8.36 ± 0.25
1.08 ± 0.02	0.89 ± 0.02	0.65 ± 0.02	1.05 ± 0.03	0.88 ± 0.02
12000 ± 220	9830 ± 140	5100 ± 160	3210 ± 90	4030 ± 80
5.56 ± 0.10	10.80 ± 0.13	3.70 ± 0.06	4.77 ± 0.08	8.47 ± 0.01
6.63 ± 0.12	10.48 ± 0.14	1.82 ± 0.07	1.49 ± 0.05	3.31 ± 0.09
0.11 ± 0.28	0.11 ± 0.28	1.00 ± 2.2	0.14 ± 0.29	0.24 ± 0.30
0.44 ± 0.02	0.44 ± 0.02	0.38 ± 0.06	0.46 ± 0.03	0.45 ± 0.02
0.78 ± 0.03	0.80 ± 0.03	1.32 ± 0.11	0.82 ± 0.04	0.88 ± 0.04
1.23 ± 0.03	1.50 ± 0.03	3.07 ± 0.24	1.10 ± 0.05	1.34 ± 0.05
0.29 ± 0.008	0.39 ± 0.01	0.96 ± 0.08	0.26 ± 0.01	0.34 ± 0.02
293 ± 8	333 ± 8	42 ± 3	300 ± 12	342 ± 13
0.39 ± 0.02	0.39 ± 0.02	0.17 ± 0.02	0.51 ± 0.03	0.49 ± 0.03
0.71 ± 0.05	0.70 ± 0.05	0.33 ± 0.03	0.83 ± 0.04	0.80 ± 0.04
1.23 ± 0.09	1.22 ± 0.08	0.89 ± 0.08	1.39 ± 0.08	1.36 ± 0.07
1.65 ± 0.12	1.72 ± 0.12	5.02 ± 0.25	2.17 ± 0.13	2.36 ± 0.13
4.39 ± 0.32	4.39 ± 0.32	5.05 ± 0.26	4.36 ± 0.25	4.41 ± 0.24
1.46 ± 0.13	1.53 ± 0.13	4.88 ± 0.28	1.72 ± 0.09	1.93 ± 0.09
0.23 ± 0.02	0.26 ± 0.02	1.89 ± 0.09	0.59 ± 0.03	0.68 ± 0.03
0.13 ± 0.01	0.16 ± 0.01	1.63 ± 0.08	0.53 ± 0.03	0.61 ± 0.03
236 ± 13	246 ± 13	7 ± 0.3	93 ± 4	100 ± 4

[a] The $^3He/^4He$ ratios are not discrimination corrected.
We applied the discrimination factor 1.

of trapped Neon were present: Ne coming from the Al-foil and an additional component, probably a surface correlated air contamination. The separation of trapped and cosmogenic components was based only on the $^{21}Ne/^{22}Ne$ ratio. The cosmogenic $^{21}Ne/^{22}Ne$ value used was 0.865, the highest value observed in rock 12013,10,31 (31B) which is in good agreement with values found in other lunar samples and in meteorites. Cosmogenic ^{21}Ne measured in 31A and 31B was low compared to 31C, further supporting the observation that these samples have suffered diffusive loss of the light rare gases.

Argon

The Ar was dominated by large amounts of radiogenic ^{40}Ar due to the high K-concentration in this rock. The ^{36}Ar and ^{38}Ar were mainly cosmogenic (Table 5). The correction for cosmogenic ^{40}Ar was small because according to LÄMMERZAHL and ZÄHRINGER (1966) the cosmogenic $^{40}Ar/^{38}Ar$ ratio is less than 0.2. A "pure" cosmogenic ratio ($^{38}Ar/^{36}Ar = 1.52$) was taken from the 1200°C fraction in rock 10044 (HOHENBERG *et al.*, 1970). The trapped $^{38}Ar/^{36}Ar$ ratio chosen was that for air. Sample 31A had the highest $^{40}Ar/^{36}Ar$ ratio measured (21890); 31C, the lowest (4030). The total ^{36}Ar amount was comparable in all the separates. The fraction of ^{36}Ar which is cosmogenic (X) was calculated by means of the formula

$$(^{38}Ar/^{36}Ar)_m = (^{38}Ar/^{36}Ar)_{cosm}X + (1 - X)(^{38}Ar/^{36}Ar)_{air}.$$

Table 4. Trapped and cosmogenic ^{22}Ne in the separates. Units are 10^{-8} cc STP/g.

Sample	700°C cosm.	700°C trapped	1550°C cosm.	1550°C trapped	Total cosm.	Total trapped
31A	2.09 ± 0.10	0.64 ± 0.05	3.4 ± 0.15	0.05 ± 0.09	5.49 ± 0.17	0.69 ± 0.1 (0.40)[a]
31B	2.06 ± 0.10	1.37 ± 0.07	1.91 ± 0.07	≡0	3.97 ± 0.12	1.37 ± 0.07 (0.45)[a]
31C	2.78 ± 0.13	0.92 ± 0.10	4.61 ± 0.27	0.05 ± 0.21	7.39 ± 0.30	0.97 ± 0.23 (0.47)[a]

[a] Total concentrations of $\frac{^{22}Ne}{\text{gram of sample}}$ attributed to Al-foil.

Table 5. Trapped and cosmogenic ^{36}Ar in the separates. Units are 10^{-8} cc STP/g.

Sample	700°C cosm.	700°C trapped	1550°C cosm.	1550°C trapped	Total cosm.	Total trapped
31A	2.52 ± 0.12	1.79 ± 0.12	4.52 ± 0.13	1.29 ± 0.11	7.04 ± 0.18	3.08 ± 0.16 (1.89)[a]
31B	2.10 ± 0.08	3.14 ± 0.09	4.03 ± 0.12	1.53 ± 0.10	6.13 ± 0.14	4.67 ± 0.14 (2.10)[a]
31C	1.40 ± 0.07	2.30 ± 0.08	3.34 ± 0.13	1.43 ± 0.12	4.74 ± 0.15	3.73 ± 0.14 (2.24)[a]

[a] Total concentrations of $\frac{^{36}Ar}{\text{gram of sample}}$ attributed to Al-foil.

The Al-foil did not account for all the trapped Ar suggesting again that there was some adsorbed air.

Xenon

Xe results will be discussed first because the treatment of the Kr results are dependent upon them. Xe was predominantly cosmogenic in all the samples. Trapped Xe and Xe produced in decay by spontaneous fission of the U–Pu system were present. *Trapped* Xe. ALEXANDER (1970) and LUNATIC ASYLUM (1970) reported a trapped Xe component the composition of which could not be established because of the dominant cosmogenic Xe in rock 12013. The isotopic composition of this trapped component can make a large difference in determining the cosmogenic yields for the higher masses and the yield of Xe produced in fission. Because of the small weight of sample involved, it was important to have good data for blanks, including Al-foil. We assume for the moment that the trapped Xe component is atmospheric in composition; we shall see if this leads to consistent results. The ^{130}Xe concentrations were quite different in the three separates (Table 3) but the ^{130}Xe amounts in the Al-foil per gram of sample were nearly the same because the samples had similar weights and the amount of Al-foil used was roughly the same. Thus, the percentage of Al-trapped Xe in the total ^{130}Xe was quite different from one sample to another. For the 1550°C gas fractions these percentages, based on the foil measurements, were 2.5, 4.3, and 11.6 in fractions A, B, and C. The *maximum* possible (terminal) percentages of trapped ^{130}Xe—assuming that all ^{136}Xe was trapped, i.e., neglecting the fission contribution for this isotope—were 8, 5, and 25.

The comparison between the percentage value of trapped ^{130}Xe due to the Al-foil and the terminal percentage value is especially interesting in the case of 31B. The predicted ^{130}Xe-percentage value of the Al-foil experiment almost agreed with the terminal percentage value, showing that little trapped Xe beyond that contributed by the Al-foil was present. This led us to the conclusion that no trapped Xe component

other than the Al-trapped Xe was in the separates. The trapped Xe in the 700°C fractions of the separates, obtained from a two component plot ($^{124}Xe/^{130}Xe$ vs. $^{126}Xe/^{130}Xe$—see HOHENBERG *et al.*, 1970, p. 1298; the pure cosmogenic point was computed as described below) was in fair agreement with the Xe-amounts measured in the 700°C fraction of the Al-foil supporting this conclusion. Since an assumption of atmospheric composition for the trapped Xe component has thus led to consistent results, we see no need to invoke another trapped component of different isotopic composition.

Cosmogenic Xe. The measured xenon was primarily cosmogenic in all the samples of 12013,10,31 investigated (Tables 3 and 6). This is in agreement with ALEXANDER (1970) and LUNATIC ASYLUM (1970). The cosmogenic Xe amounts were obtained by subtracting the trapped and fission contributions: First we subtracted the trapped Xe due to the Al-foil; then we subtracted a component from U-fission assuming all the remaining ^{136}Xe to be from such a source. Sample 31A contained an extremely high abundance of Ba (6360 ppm). The REE concentration (Ce = 96 ppm) was low, and, therefore, the cosmogenic ^{126}Xe present was 98.5% from Ba isotopes, based on spallation systematics (RUDSTAM, 1966, as used by HOHENBERG *et al.*, 1967). The cosmogenic Xe in 31B is also mostly from Ba (95.6%). Thus, these samples give an essentially pure cosmogenic Xe spectrum from Ba in rock 12013 (Fig. 1, Tables 7a and 7b). The cosmogenic yields are based on the 1550°C fractions only. The cosmogenic Xe

Table 6. Cosmogenic and trapped ^{130}Xe [$\times 10^{-12}$ cc STP/g]. See text for the method used to calculate these components.

Sample	700°C		1550°C		Total	
	cosm.	trapped	cosm.	trapped	cosm.	trapped
31A	11 ± 1	2 ± 0.5	359 ± 10	9 ± 2	370 ± 10	11 ± 2
31B	7 ± 0.5	3 ± 3	226 ± 13	10 ± 2	233 ± 13	13 ± 4
31C	2 ± 0.5	5 ± 1.5	82 ± 5	11 ± 2	84 ± 5	16 ± 5

Table 7a. Isotopic composition of cosmogenic Xe in the separates.

Sample	124	126	128	129	130	131	132	134
31A	0.42 ± 0.01	0.80 ± 0.02	1.25 ± 0.03	1.49 ± 0.06	1.00 ± 0.00	4.28 ± 0.13	0.99 ± 0.05	0.08 ± 0.02
31B	0.41 ± 0.03	0.74 ± 0.06	1.26 ± 0.09	1.44 ± 0.13	1.00 ± 0.00	4.36 ± 0.33	1.21 ± 0.14	0.09 ± 0.03
31C	0.58 ± 0.04	0.95 ± 0.06	1.52 ± 0.10	1.60 ± 0.22	1.00 ± 0.00	4.22 ± 0.33	0.88 ± 0.19	0.06 ± 0.07

Table 7b. Isotopic composition of cosmogenic Xe from Ba and REE.

Ba:	124	126	128	129	130	131	132	134
Ba[a]	0.54 ± 0.05	1.00 ± 0.00	1.63 ± 0.15	1.91 ± 0.18	1.30 ± 0.09	5.62 ± 0.54	1.44 ± 0.26	0.11 ± 0.03
$BaCl_2$[b]	0.72 ± 0.02	1.00 ± 0.00	1.14 ± 0.04	1.12 ± 0.04	0.72 ± 0.03	1.31 ± 0.06	0.55 ± 0.04	0.05 ± 0.10
REE[c]	0.83 ± 0.29	1.00 ± 0.00	1.50 ± 0.79	0.96 ± 1.17	0.25 ± 0.38	0.71 ± 2.50	≤1.2	≤0.29
$CeCl_3$[d]	0.83 ± 0.02	1.00 ± 0.00	1.08 ± 0.04	1.08 ± 0.09	0.24 ± 0.10	1.15 ± 0.10	0.22 ± 0.17	0.0015 ± 0.0015

[a] Inferred from samples 31A and 31B.
[b] FUNK *et al.* (1967).
[c] Inferred from samples 31A, 31B, and 31C.
[d] HOHENBERG and ROWE (1970).

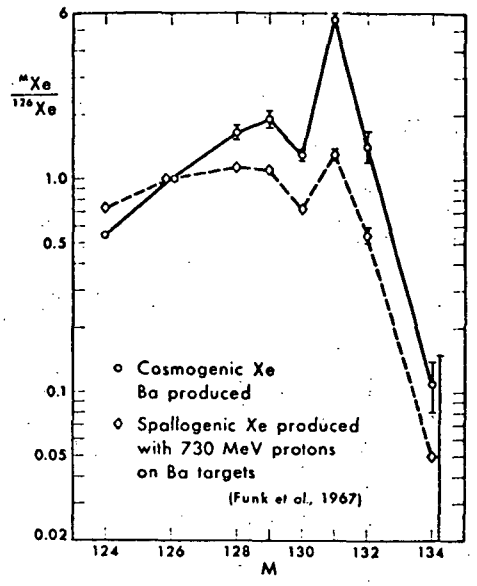

Fig. 1. Spectrum of cosmogenic Xe from lunar Ba inferred from separates 31A and 31B. It is compared to the spectrum of Xe produced by 730 MeV protons in a Ba target (FUNK *et al.*, 1967).

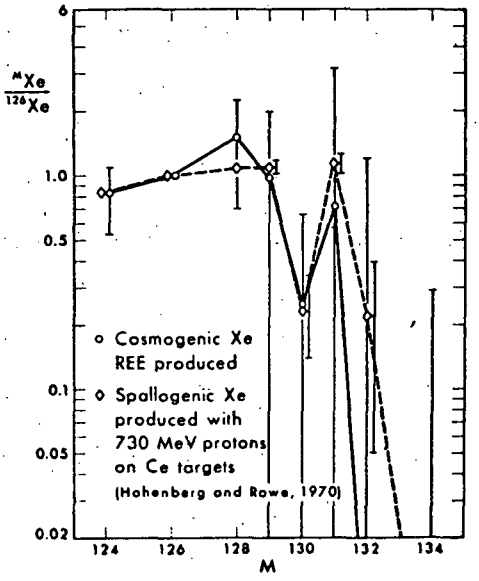

Fig. 2. Spectrum of cosmogenic Xe from lunar REE obtained by subtraction of Xe from separates in rock 12013. It is compared to the spectrum of Xe produced by 730 MeV protons in a Ce target (HOHENBERG and ROWE, 1970).

spectrum obtained in 31C is different from 31A and 31B. The $^{129}Xe/^{126}Xe$ and $^{131}Xe/^{126}Xe$ yields are lower. The ^{126}Xe produced in this sample contained, unlike the other separates, a significant portion (24%) of cosmogenic ^{126}Xe from REE targets according to RUDSTAM calculations. This made it possible to estimate the cosmogenic Xe spectrum from REE targets in this rock (Fig. 2, Table 7b). The spectrum is marked by a high $^{124}Xe/^{126}Xe$, and by low $^{129}Xe/^{126}Xe$, $^{130}Xe/^{126}Xe$, and $^{131}Xe/^{126}Xe$ ratios. The $^{132}Xe/^{126}Xe$ and $^{134}Xe/^{126}Xe$ ratios seem to be very low. The errors listed are based on the Xe measurements only. No errors for the chemical abundances were taken into account. We also plotted the spallation spectra obtained by bombardment of Ba targets (FUNK *et al.*, 1967) and Ce targets (HOHENBERG and ROWE, 1970) with 730 MeV protons. The spallation spectrum for Ce agrees well with the cosmogenic spectrum for REE.

The spallation spectrum for Ba disagrees with the cosmogenic Ba spectrum. The spectra (except for mass 131) could be brought into fair agreement by rotating the spallation spectrum counterclockwise around the intersection point at mass 126. But this is generally what would be expected for particles of lower energy than the somewhat high value of 730 MeV used in the target experiment, since high energy protons accentuate the spallation yields at masses far removed from the target. The discrepancy at mass 131 is of course augmented by the now famous ^{131}Xe anomaly in lunar rocks.

Fissiogenic Xe. All the sample of 12013,10,31 contained Xe produced by spontaneous fission decay of the U–Pu system. However, because of the dominance of and the uncertainties in the cosmogenic yields for Xe it was impossible to determine the isotopic composition of fission Xe in any of the samples studied. Thus, we used the Xe spectrum for spontaneous fission decay of ^{238}U (WETHERILL, 1953). The amounts of fission ^{136}Xe were obtained by subtracting the ^{136}Xe due to the Al-foil from the total ^{136}Xe and assuming all the remaining ^{136}Xe to be fissiogenic (Table 8).

Krypton

Trapped Kr. The Kr measurements for the Al-foil were not as consistent as the results obtained for the other rare gases. Three experiments with Al-foil (two temperatures each, namely 700°C and 1550°C) led to discordant results for this gas (Table 1). We have no explanation for the nonreproducibility in Al-trapped Krypton. The procedure for separating trapped, cosmogenic, and fission Kr was necessarily changed from that used for Xe. The fission corrections, which were small for the 1550°C and negligible otherwise, were based on the fission Xenon found. We used the fission yields for spontaneous fission of ^{238}U measured by WETHERILL (1953). The remaining ^{86}Kr was

Table 8. Fissiogenic ^{86}Kr and ^{136}Xe [$\times 10^{-12}$ cc STP/g].

Sample	Xenon 700°C	Xenon 1550°C	Xenon Total	Krypton Total
31A	5 ± 1	44 ± 4	49 ± 4	6 ± 4.5
31B	1 ± 1	8 ± 2	9 ± 2	1 ± 2
31C	1 ± 1	26 ± 5	27 ± 5	4 ± 4

assumed to be trapped (i.e., $^{86}Kr_{cosm} = 0$). Results of the calculations (Tables 8–10) were cosmogenic Kr spectra and concentrations for trapped and cosmogenic Krypton. The Kr is mostly cosmogenic as illustrated by sample 31C where at most 17% of the 300×10^{-12} cc STP/g ^{83}Kr of the 1550°C fraction could be trapped, based on the ^{86}Kr content. This 17% trapped ^{83}Kr corresponds to a ^{83}Kr value of 1.9×10^{-12} cc STP/g Al-foil for the 1550°C fraction, a value lower than measured in any of the foils. The trapped ^{83}Kr percentage values for the other separates were 31B = 19% (2.3×10^{-12} cc STP/g Al-foil in 1550°C) 31A = 19% (3.0×10^{-12} cc STP ^{83}Kr/g Al-foil in 1550°C). The amounts of trapped ^{83}Kr in the 700°C fractions of the separates were, if attributed to the Al-foil in the range of concentrations found at 700°C in the experiments with the foil (Tables 1 and 9).

Cosmogenic Kr. Cosmogenic Kr, as obtained by subtracting trapped and fission contributions, was more abundant in the 1550°C fractions and we therefore adopt the cosmogenic spectra obtained for those fractions (Table 10). Using these spectra, we were able to deduce the concentrations of cosmogenic Kr in the 700°C fractions by means of the ratio $^{84}Kr/^{83}Kr$.

AGES

Radiogenic ages

The K–Ar ages of 31A, 31B, and 31C were nominally 3.8×10^9 y, 4.1×10^9 y, and 4.1×10^9 y, respectively (Table 11). These values are in very good agreement with each other within the errors assigned, and with the results obtained by TURNER (1970), LUNATIC ASYLUM (1970), and TATSUMOTO (1970). We also confirm TURNER's (1970) result that neither the light phase nor the dark phase had suffered diffusive loss of ^{40}Ar. We note that the K–Ar ages obtained on 31A, 31B, and 31C confirm the estimated chemical compositions. The ^{4}He–U–Th ages are lower in the plagioclases 31A and 31B. The ages, both of which were 0.7×10^9 y, indicate an equally severe diffusive loss of He in both samples. This leads to similar ^{4}He–U–Th ages despite different U concentrations. A ^{4}He–U–Th age of 2.3×10^9 y was found in 31C. This particular ^{4}He–U–Th age was in good agreement with values reported by ALEXANDER (1970) and LUNATIC ASYLUM (1970).

Table 9. Cosmogenic and trapped ^{83}Kr [$\times 10^{-12}$ cc STP/g].

Sample	700°C cosm.	700°C trapped	1550°C cosm.	1550°C trapped	Total cosm.	Total trapped
31A	34 ± 8	41 ± 7	287 ± 8	63 ± 3	321 ± 11	104 ± 8
31B	23 ± 4	17 ± 4	237 ± 7	56 ± 2	260 ± 8	73 ± 5
31C	24 ± 8	18 ± 8	251 ± 13	49 ± 2	275 ± 15	67 ± 8

Table 10. Isotopic composition of cosmogenic Kr in the separates.

Sample	78	80	82	83	84
31A	0.12 ± 0.24	0.49 ± 0.02	0.73 ± 0.04	1.00 ± 0.00	0.20 ± 0.05
31B	0.13 ± 0.28	0.50 ± 0.02	0.73 ± 0.03	1.00 ± 0.00	0.35 ± 0.03
31C	0.15 ± 0.29	0.51 ± 0.03	0.79 ± 0.05	1.00 ± 0.00	0.34 ± 0.04

Table 11. Ages.

	31A Milky-white	31B Clear	31C Black
Measured rare gas components			
$^3He_{cosm}$ ($\times 10^{-8}$ cc STP/g)	29.6 ± 0.5	21.1 ± 0.5	54.2 ± 0.9
$^4He_{rad}$ ($\times 10^{-3}$ cc STP/g)	3.29 ± 0.06	1.31 ± 0.03	3.71 ± 0.06
$^{21}Ne_{cosm}$ ($\times 10^{-8}$ cc STP/g)	4.75 ± 0.15	3.43 ± 0.10	6.39 ± 0.26
$^{40}Ar_{rad}$ ($\times 10^{-4}$ cc STP/g)	22.1 ± 0.5	10.48 ± 0.14	3.31 ± 0.09
$^{83}Kr_{cosm}$ ($\times 10^{-12}$ cc STP/g)	320 ± 11	260 ± 8	275 ± 15
$^{126}Xe_{cosm}$ ($\times 10^{-12}$ cc STP/g)	296 ± 11	173 ± 17	80 ± 5
$^{136}Xe_{sf}$ ($\times 10^{-12}$ cc STP/g)	49 ± 4	9 ± 2	27 ± 5
Inferred ages			
^{4}He–U–Th age ($\times 10^9$ y)	0.7 ± 0.1	0.7 ± 0.1	2.3 ± 0.4
^{40}Ar–^{40}K age ($\times 10^9$ y)	3.8 ± 0.4	4.1 ± ?	4.1 ± 0.3
$^{136}Xe_{sf}$–^{244}Pu–^{238}U age ($\times 10^9$ y)	4.0 + 0.2 − 0.8	2.2 ± ?	4.3 + 0.1 − 0.15
^{3}He-exposure age ($\times 10^6$ y)	30 ± 0.5	21 ± 0.5	54 ± 1
^{21}Ne-exposure age ($\times 10^6$ y)	32 ± 1.5	23 ± 1	43 ± 2
^{83}Kr-exposure age ($\times 10^6$ y)	215 ± 66(102 ± 32)[a]	180 ± 55(85 ± 26)[a]	107 ± 34(73 ± 23)[a]
^{126}Xe-exposure age ($\times 10^6$ y)	40 ± 13	41 ± 13	47 ± 16

[a] This value is based on spectroscopic data for Zr (LSPET, 1970).

Exposure ages

The plagioclases (31A and 31B) had lower ^{3}He concentrations than the pyroxene (31C). Assuming a production rate of 1×10^{-8} cc STP ^{3}He/g 10^6 y (KIRSTEN *et al.*, 1970) these amounts lead to ^{3}He exposure ages of 30×10^6, 21×10^6, and 54×10^6 y, respectively. Together with the low ^{4}He–Th–U ages for 31A and 31B, this indicates a diffusive loss of He in the plagioclases (Table 11). The ^{21}Ne amounts show essentially the same pattern. The plagioclases (31A and 31B) have lower cosmogenic ^{21}Ne concentrations than 31C. Using 0.15×10^{-8} cc STP ^{21}Ne/g 10^6 y (KIRSTEN *et al.*, 1970) as the production rate, we arrive at exposure ages of 32×10^6 y, 23×10^6 y, and 43×10^6 y (31C), respectively. We want to note here, that the assumption of a universal production rate for Ne is certainly an oversimplification (KAISER, 1971). But even taking chemical effects into account would not change the point we intend to express here: 31A and 31B both suffered diffusive loss of Ne.

The cosmogenic ^{126}Xe concentrations were significantly different in the separates. Despite this, the exposure ages based on ^{126}Xe, are in good agreement. They range from 40×10^6 y in 31A to 47×10^6 y in 31C. The samples are strongly enriched in Ba and REE, the target elements for cosmogenic-produced Xe. The production rates used (assuming a 2π geometry) were

$$1.07 \times 10^{-15} \text{ cc STP } ^{126}\text{Xe}/10^{-6} \text{ g Ba } 10^6 \text{ y},$$

and

$$1.01 \times 10^{-15} \text{ cc STP } ^{126}\text{Xe}/10^{-6} \text{ g Ce } 10^6 \text{ y (REE)}$$

These values were obtained from the achondrite Nuevo Laredo (MUNK, 1967) and RUDSTAM calculations for Pasamonte (HOHENBERG *et al.*, 1967) assuming an exposure age 16×10^6 y for Nuevo Laredo (HEYMANN *et al.*, 1968). These exposure ages are the most trustworthy ones we obtained for rock 12013. This fact is not evident in view of

the large errors assigned, but they are due almost entirely to the 30% error in $^{128}Xe_{cosm}$ for the Nuevo Laredo meteorite.

The ^{83}Kr exposure ages are questionable. The essential elements are Sr, Y, and Zr. The production rates used were

$$3.56 \times 10^{-15} \text{ cc STP } ^{83}Kr/10^{-6} \text{ g Sr } 10^{6} \text{ y},$$
$$1.76 \times 10^{-15} \text{ cc STP } ^{83}Kr/10^{-6} \text{ Y } 10^{6} \text{ y}$$

(Y value for Nuevo Laredo was estimated by SCHMITT (1970) and GOLES (1970) to be 23 ppm.)

$$0.98 \times 10^{-15} \text{ cc STP } ^{83}Kr/10^{-6} \text{ g Zr } 10^{6} \text{ y}$$

and were based on Nuevo Laredo (MUNK, 1967) and Pasamonte calculations (HOHENBERG *et al.*, 1967) as before. The exposure ages obtained were much higher than the ^{126}Xe exposure ages and ranged from 107×10^6 y in 31C to 215×10^6 y in 31A.

There are two ways of explaining the high Kr exposure ages: either the production rates used were wrong or the chemical abundances were underestimated. Therefore, we checked our production rates on lunar rock 10017, studied by MARTI *et al.* (1970). This rock has a ^{81}Kr–^{83}Kr exposure age of 509×10^6 y. The ^{83}Kr exposure age obtained using MARTI's ^{83}Kr concentration value, the chemical values for Sr, Y, and Zr (WAKITA *et al.*, 1970) and the production rates previously stated was 473×10^6 y. Therefore, we believe that the chemical abundances—especially the Zr values—used for the calculations are underestimated. The Zr values are very uncertain. None of the investigators working with samples of 12013 remeasured Zr, although one of them inferred a value substantially lower than the 2200 ppm reported by LSPET (1970). However, using the LSPET Zr value in the calculations, the ^{83}Kr exposure ages become lower and more nearly agree with the ^{126}Xe exposure ages (listed in Table 11 in brackets). Thus, our results support the Zr value reported by LSPET (1970).

Unfortunately, the samples studied were too small and the background for ^{81}Kr too high to perform ^{81}Kr–^{83}Kr exposure age determinations.

^{136}Xe–^{244}Pu–^{238}U *ages*

Sample 31A showed the highest fissiogenic Xe concentration and highest U concentration. The resulting ^{136}Xe–Pu–U age was 4.0×10^9 y and was in agreement with the K–Ar age of 3.8×10^9 y (Table 11). A ^{136}Xe spontaneous fission yield of 6% was used for ^{238}U as well as ^{244}Pu. The spontaneous fission half lives applied were taken from FLEISCHER and PRICE (1964) for ^{238}U, and from FIELDS *et al.* (1966) for ^{244}Pu. A $^{244}Pu/^{238}U$ ratio of 0.015 at the time of the formation of the solar system (4.6×10^9 y ago) was assumed (PODOSEK, 1970; LUNATIC ASYLUM, 1970). But, one gets the same age (to three significant figures) for assumed $^{244}Pu/^{238}U$ ratios of 0.0 and 0.047 (HOHENBERG, 1970). If the U and fissiogenic ^{136}Xe data are taken at face value for 31C unreasonably old ages and contributions to fission Xe from ^{244}Pu are required.

But a much more likely explanation for the data is that the U-value was underestimated. Use of the fissiogenic ^{136}Xe data and the crystallization age of TURNER

(1970) leads to a K–U ratio = 0.06 (%/ppm) for the dark colored phase. There would be negligible ^{136}Xe from ^{244}Pu decay for these values.

Conclusions

We confirm, in essence, the results reported by Alexander (1970) and Lunatic Asylum (1970), that no ^{129}Xe coming from in situ decay of ^{129}I is present. Also, no real evidence for fission Xe originating from ^{244}Pu was established. The K–Ar ages are in good agreement with results obtained by Turner (1970) and with the Rb–Sr ages (Lunatic Asylum, 1970), for distinct mineral phases. Because of pronounced chemical differences among the different fractions, we were able to derive cosmogenic Xe spectra from Ba targets and REE targets in this moon sample. The ^{126}Xe exposure ages confirm the data reported by Alexander (1970) and the Lunatic Asylum (1970). We did not find any indications of trapped Kr and Xe components in the separates. Instead, we could attribute all the trapped Kr and Xe to the Al-foil in which the samples were wrapped.

The ^{83}Kr exposure ages were very high and in disagreement with each other, suggesting much higher Zr concentrations than inferred by Wakita and Schmitt (1970) and supporting the value by LSPET (1970).

Acknowledgments—The author is particularly pleased to acknowledge the inspiring advice and helpful criticism of John H. Reynolds. I also benefited from Paul K. Davis for his assistance in writing the computer programs used. I wish to thank E. C. Alexander, R. S. Lewis, G. McCrory, and D. Overskei for many encouraging discussions and M. C. Malin for taking some of the Al data. This work was supported in part by NASA and by the U.S. Atomic Energy Commission and bears AEC Code UCB–34P32–77.

References

Alexander E. C. (1970) Rare gases from stepwise heating of lunar rock 12013. *Earth Planet. Sci. Lett.* **9**, 201–208.

Bochsler P., Eberhardt P., Geiss J., Graf H., Grögler N., Krähenbühl U., Mörgeli M., Schwaller H., and Stettler A. (1971) Potassium–argon ages, exposure ages and radiation history of lunar rocks. Second Lunar Science Conference (unpublished proceedings).

Drake M. J., McCallum I. S., McKay G. A., and Weill D. F. (1970) Mineralogy and petrology of Apollo 12 sample no. 12013: a progress report. *Earth Planet. Sci. Lett.* **9**, 103–124.

Eberhardt P., Geiss J., Graf H., Grögler N., Krähenbühl U., Schwaller H., Schwarzmüller J., and Stettler A. (1970) Correlation between rock type and irradiation history of Apollo 11 igneous rocks. *Earth Planet. Sci. Lett.* **10**, 67–72.

Eugster O., Eberhardt P., and Geiss J. (1967) The isotopic composition of krypton in unequilibrated and gas rich chondrites. *Earth Planet. Sci. Lett.* **2**, 385–393.

Fields P. R., Friedman A. M., Milsted J., Lerner J., Stevens C. M., Metta D., and Sabine W. K. (1966) The decay properties of plutonium 244 and comments on its existence in nature. *Nature* **212**, 131–134.

Fleischer R. L., and Price P. B. (1964) Decay constant for spontaneous fission of ^{238}U. *Phys. Rev.* **B63**.

Funk H., Podosek F., and Rowe M. W. (1967) Spallation yields of krypton and xenon from irradiation of strontium and barium with 730 MeV protons. *Earth Planet. Sci. Lett.* **3**, 193–196.

Gay P., Brown M. G., and Rickson K. O. (1970) Mineralogical studies of lunar rock 12013,10. *Earth Planet. Sci. Lett.* **9**, 124–127.

GOLES G. (1970) Private communication.

GOLES G., DUNCAN A. R., OSAWA M., MARTIN M. R., BEYER R. L., LINDSTROM D. J., and RANDLE K. (1971) Analyses of Apollo 12 specimens and a mixing model for Apollo 12 "soils." Second Lunar Science Conference (unpublished proceedings).

HEYMANN D., MAZOR E., and ANDERS E. (1968) Ages of calcium-rich achondrites, I. Eucrites. *Geochim. Cosmochim. Acta* **32**, 1241–1268.

HOHENBERG C. M., MUNK M. N., and REYNOLDS J. H. (1967) Spallation and fissiogenic xenon and krypton from stepwise heating of the Pasamonte achondrite; the case of extinct plutonium 244 in meteorites; relative ages of chondrites and achondrites. *J. Geophys. Res.* **72**, 3139–3176.

HOHENBERG C. M., and ROWE M. W. (1970) Spallation yields of xenon from irradiation of Cs, Ce, Nd, Dy, and a rare earth mixture with 730 MeV protons. *J. Geophys. Res.* **75**, 4205–4209.

HOHENBERG C. M., DAVIS P. K., KAISER W. A., LEWIS R. S., and REYNOLDS J. H. (1970) Trapped and cosmogenic rare gases from stepwise heating of Apollo 11 samples. *Proc. Apollo 11 Lunar Sci. Conf., Geochim. Cosmochim. Acta* Suppl. 1, Vol. 2, pp. 1283–1309. Pergamon.

HOHENBERG C. M. (1970) Radioisotopes and the history of nucleosynthesis in the galaxy. *Science* **166**, 212–215.

HUBBARD N. J., GAST P. W., and WIESMANN H. (1970) Rare earth, alkaline and alkali metal and $^{87/86}Sr$ data for subsamples of lunar sample 12013. *Earth Planet. Sci. Lett.* **9**, 181–185.

KAISER W. A. (1971) Unpublished data.

KIRSTEN T., MÜLLER O., STEINBRUNN F., and ZÄHRINGER J. (1970) Study of distribution and variation of rare gases in lunar material by a microprobe technique. *Proc. Apollo 11 Lunar Sci. Conf., Geochim. Cosmochim. Acta* Suppl. 1, Vol. 2, pp. 1331–1343. Pergamon.

LÄMMERZAHL P., and ZÄHRINGER J. (1966) K–Ar–Altersbestimmungen an Eisenmeteoriten II: Spallogenes ^{40}Ar and ^{40}Ar–^{38}Ar Bestrahlungsalter. *Geochim. Cosmochim. Acta* **30**, 1059–1075.

LSPET (Lunar Sample Preliminary Examination Team) (1970) Preliminary examination of the lunar samples from Apollo 12. *Science* **167**, 1325–1339.

LUNATIC ASYLUM (1970) Mineralogic studies of lunar rock 12013. *Earth Planet. Sci. Lett.* **9**, 137–164.

MARTI K., LUGMAIR G. W., and UREY H. C. (1970) Solar wind gases, cosmic ray spallation products, and irradiation history of Apollo 11 samples. *Proc. Apollo 11 Lunar Sci. Conf., Geochim. Cosmochim. Acta* Suppl. 1, Vol. 2, pp. 1357–1367. Pergamon.

MARTI K., and LUGMAIR G. W. (1971) Kr^{81}–Kr and K–Ar^{40} ages, cosmic-ray spallation products, and neutron effects in Apollo 11 and Apollo 12 lunar samples. Second Lunar Science Conference (unpublished proceedings).

MORRISON G. H., GERARD J. T., KASHUBA A. T., GANGADHARAM E. V., ROTHENBERG A. M., POTTER N. M., and MILLER G. B. (1970) Multielement analysis of lunar soil and rocks. *Science* **167**, 505–507.

MUNK M. N. (1967) Argon, krypton, and xenon in Angra dos Reis, Nuevo Laredo, and Norton County achondrites. *Earth Planet. Sci. Lett.* **3**, 457–465.

NIER O. A. (1950) A redetermination of the relative abundance of the isotopes of neon, krypton, rubidium, xenon, and mercury. *Phys. Rev.* **79**, 450–454.

PODOSEK F. A. (1970) The abundance of ^{244}Pu in the early solar system. *Earth Planet. Sci. Lett.* **8**, 183–187.

RUDSTAM G. (1966) Systematics of spallation yields. *Z. Naturforsch.* **21a**, 1027–1041.

SCHMITT R. A. (1970) Private communication.

SCHNETZLER C. C., PHILPOTTS J. A., and BOTTINO M. L. (1970) Li, K, Rb, Sr, Ba, and rare earth concentrations, and Rb–Sr age of lunar rock 12013. *Earth Planet. Sci. Lett.* **9**, 185–193.

SCHNETZLER C. C. (1970) Private communication.

TATSUMOTO M. (1970) U–Th–Pb age of Apollo rock 12013. *Earth Planet. Sci. Lett.* **9**, 193–201.

TURNER G. (1970) ^{40}Ar–^{39}Ar age determination of lunar rock 12013. *Earth Planet. Sci. Lett.* **9**, 177–181.

WAKITA H., and SCHMITT R. A. (1970) Elemental abundances in seven fragments from lunar rock 12013. *Earth Planet. Sci. Lett.* **9**, 164–169.

WAKITA H., SCHMITT R. A., and REY P. (1970) Elemental abundances of major, minor, and trace

elements in Apollo 11 lunar rocks, soil, and core samples. *Proc. Apollo 11 Lunar Sci. Conf., Geochim. Cosmochim. Acta* Suppl. 1, Vol. 2, pp. 1685–1717. Pergamon.

WALTER L. S. (1970) Unpublished data.

WASSERBURG G. J. (1970) COSPAR, Leningrad Russia.

WETHERILL G. W. (1953) Spontaneous fission yields from uranium and thorium. *Phys. Rev.* **92**, 907–912.

YORK D. (1966) Least squares fitting of a straight line. *Can. J. Phys.* **44**, 1079–1084.

Proceedings of the Second Lunar Science Conference, Volume 2, pp. 1643–1650.
The M.I.T. Press, 1971.

Spallogenic Ne, Kr, and Xe from a depth study of 12002

E. C. ALEXANDER, JR.
Department of Physics, University of California, Berkeley, California 94720

(*Received 22 February 1971; accepted in revised form 30 March 1971*)

Abstract—Isotopic abundances and concentrations of neon, krypton, and xenon were measured in the top, middle, and bottom of rock 12002. The rare gases are mainly spallation produced and *no* evidence of a depth variation was detected in the relative isotopic yields. Apparent depth variations do exist in the concentration of xenon and krypton. The rare gas data along with the results of other workers are used to construct a three stage model of the irradiation history of 12002. The model is as follows: Stage 1. A long (~100 m.y.) irradiation at greater than one meter burial. Stage 2. A shorter (20 to 50 m.y.) irradiation at a shallow burial of 0 to 10 cm. Stage 3. A very short (2 to 5 m.y.) surface residence period. Stages 2 and 3 may not be separate stages but may reflect a noncatastrophic continuous movement of 12002 to the surface.

INTRODUCTION

THE SPALLATION YIELDS of stable rare gas isotopes in lunar rocks were some of the more enigmatic results reported at the Apollo 11 Lunar Science Conference. The high and variable yield of ^{131c}Xe was particularly puzzling. A number of authors (ALBEE *et al.*, 1970; FUNKHOUSER *et al.*, 1970; HINTENBERGER *et al.*, 1970; HOHENBERG *et al.*, 1970; MARTI *et al.*, 1970; PEPIN *et al.*, 1970; BOGARD *et al.*, 1971) have offered possible explanations which fall into two broad categories. The two-fold variation in the ^{131c}Xe spallation yield could be due to: (1) differences in chemical abundances of target elements and/or (2) differences in the effective irradiation energy spectrum integrated by each rock due to varying shielding histories. A companion paper (ALEXANDER *et al.*, 1971) discusses the effects of chemical differences between the minerals of rock 12013 on the spallation yields. In this paper we present the results of a study of self-shielding effects on the spallation yields within rock 12002.

EXPERIMENTAL TECHNIQUES

Rare gas mass spectroscopy was used to measure both the concentration and isotopic abundance of the rare gas isotopes. The rare gases were extracted from ~250 mg samples in three temperature steps. The glass extraction system has been previously described as System 2 (HOHENBERG *et al.*, 1970). Experimental procedures and data reduction were essentially unchanged from those described for System 2.

SAMPLE DESCRIPTION

We received three pieces of Apollo rock 12002. The samples were 12002,80, 12002,83, and 12002,88—the top, "middle," and bottom of pieces 12002,28 respectively. Piece 12002,28 was column B3, an approximately 1.5 × 1.5 × 6.5 cm bar extending through rock 12002 (see the Apollo 12 Lunar Receiving Laboratory Orientation Drawings of Lunar Rock No. 12002). The top 1 to 2 mm of sample 12002,

80 and the bottom 3 to 4 mm of sample 12002,88 were removed to eliminate the surface solar wind component; i.e., the bottom of the top piece and the top of the bottom piece were analyzed. Sample 12002,83 was completely interior.

RESULTS

After the analysis of 12002 was completed, it was discovered that the He and Ar data were obtained in a region of nonlinearity in the mass spectrometer and are erroneous. Therefore, the discussion will be confined to the Ne, Kr, and Xe data which were not affected by the nonlinearity. Neon and krypton data are given in Table 1 and xenon data are given in Table 2. The errors listed for the isotope ratios are one standard deviation (1 σ) in the fit of the observed ratios to the drift line. The ^{40}Ar peak was monitored during the Ne analyses and was used to correct the ^{20}Ne data for $^{40}Ar^{+2}$ contamination. The correction was greater than 1% only in the ~700°C

Table 1. Neon and krypton from lunar rock 12002

	12002,80 (210.8 mg)			
Temp. °C	~700	1000	1800	~700
21/20	0.755 ± 0.017	0.997 ± 0.004	1.009 ± 0.003	0.799 ± 0.036
22/20	0.959 ± 0.020	1.145 ± 0.005	1.148 ± 0.005	0.968 ± 0.043
$[^{20}Ne]^*$ × 10^{-8} cc/gm	0.52	8.53	9.31	0.59
Blank ^{20}Ne × 10^{-8} cc/gm			0.47	
78/84	0.00 ± 0.02	0.15 ± 0.02	0.18 ± 0.01	0.01 ± 0.02
80/84	0.076 ± 0.006	0.49 ± 0.02	0.58 ± 0.02	0.10 ± 0.01
82/84	0.24 ± 0.01	0.84 ± 0.02	0.96 ± 0.03	0.26 ± 0.02
83/84	0.26 ± 0.01	1.08 ± 0.04	1.30 ± 0.05	0.27 ± 0.02
86/84	0.307 ± 0.006	0.188 ± 0.009	0.131 ± 0.005	0.307 ± 0.010
$[^{84}Kr]^*$ × 10^{-12} cc/gm	15.2	24.5	41.5	11.1†
Blank ^{84}Kr × 10^{-12} cc/gm			20.3	

12002,83 (292.6 mg)		12002,88 (251.8 mg)		
1000	1800	~700	1050	1800
1.028 ± 0.003	1.048 ± 0.002	0.790 ± 0.033	1.031 ± 0.003	1.048 ± 0.002
1.167 ± 0.002	1.167 ± 0.004	0.981 ± 0.038	1.138 ± 0.004	1.144 ± 0.002
8.75	10.2	0.79	9.27	10.1
	0.15			0.22
0.13 ± 0.01	0.17 ± 0.01	0.02 ± 0.01	0.14 ± 0.01	0.13 ± 0.02
0.48 ± 0.02	0.50 ± 0.01	0.061 ± 0.006	0.45 ± 0.01	0.39 ± 0.01
0.82 ± 0.04	0.86 ± 0.02	0.21 ± 0.01	0.76 ± 0.03	0.73 ± 0.02
1.00 ± 0.05	1.15 ± 0.02	0.23 ± 0.01	0.97 ± 0.04	0.91 ± 0.02
0.199 ± 0.008	0.173 ± 0.007	0.285 ± 0.015	0.193 ± 0.005	0.171 ± 0.005
19.9†	37.2†	19.1	27.9	30.7
	8.3†			15.3

* The concentrations of ^{20}Ne and ^{84}Kr were determined using the "peak height" method and are reproducible to about ±10%.

† The concentrations of krypton in sample 12002,83 may be in error by ±30% due to erratic sensitivities in the associated calibration runs. The krypton data have been corrected for background as discussed in the text.

Table 2. Xenon from lunar rock 12002

Sample	12002,80			
Temp. °C	~700	1000	1800	~700
124/132	0.0268 ± 0.0020	0.396 ± 0.016	0.370 ± 0.009	0.0307 ± 0.0017
126/132	0.0237 ± 0.0046	0.729 ± 0.019	0.642 ± 0.022	0.0397 ± 0.0016
128/132	0.122 ± 0.010	1.154 ± 0.033	1.045 ± 0.030	0.119 ± 0.009
129/132	1.028 ± 0.042	1.550 ± 0.039	1.410 ± 0.034	0.995 ± 0.022
130/132	0.165 ± 0.011	0.768 ± 0.014	0.713 ± 0.012	0.167 ± 0.005
131/132	0.905 ± 0.027	4.591 ± 0.107	4.222 ± 0.089	0.904 ± 0.015
134/132	0.385 ± 0.020	0.284 ± 0.007	0.366 ± 0.007	0.428 ± 0.018
136/132	0.346 ± 0.008	0.214 ± 0.003	0.270 ± 0.005	0.363 ± 0.009
$[^{132}Xe]^*$ × 10^{-12} cc/gm	1.4	6.4	5.3	0.9
Blank ^{132}Xe × 10^{-12} cc/gm			0.8	

12002,83		12002,88		
1000	1800	~700	1050	1800
0.408 ± 0.010	0.358 ± 0.007	0.0251 ± 0.0027	0.435 ± 0.011	0.317 ± 0.010
0.729 ± 0.016	0.623 ± 0.008	0.0279 ± 0.0017	0.744 ± 0.013	0.570 ± 0.006
1.126 ± 0.023	0.976 ± 0.016	0.117 ± 0.007	1.167 ± 0.036	0.886 ± 0.020
1.547 ± 0.027	1.414 ± 0.027	1.063 ± 0.026	1.549 ± 0.019	1.361 ± 0.011
0.752 ± 0.018	0.685 ± 0.017	0.178 ± 0.005	0.775 ± 0.018	0.632 ± 0.014
4.470 ± 0.098	3.934 ± 0.072	0.927 ± 0.022	4.652 ± 0.120	3.823 ± 0.049
0.291 ± 0.003	0.352 ± 0.014	0.382 ± 0.011	0.310 ± 0.006	0.360 ± 0.016
0.208 ± 0.010	0.270 ± 0.005	0.332 ± 0.011	0.213 ± 0.004	0.262 ± 0.012
4.9	4.5	1.2	5.6	3.1
	0.4			0.8

* The concentrations of ^{132}Xe were determined using the "peak height" method and are reproducible to ±10%.

fractions. The maximum correction was 38% for the ~700°C fraction of 12002,80. The light isotopes of krypton have been corrected for background (as measured in the spectrometer immediately before the krypton was admitted), and the error shown includes the added uncertainty due to the background correction. None of the data were corrected for blanks. Data for an 1800°C blank run before each sample are included in the tables.

The data in Tables 1 and 2 are typical of those previously reported for lunar crystalline rocks. The rare gases are almost completely due to spallation, and there is no evidence of a trapped or "solar wind" component. The small amount of non-spallation gas is probably due to blank contamination.

A search for a depth effect in the relative ^{131c}Xe yield was the main purpose of our analysis of 12002. Figure 1 is a plot of $^{131}Xe/^{136}Xe$ vs. $^{126}Xe/^{136}Xe$ in the manner described by ALEXANDER (1970). A small fission correction was applied to the data (see the previous reference for details). In a plot such as Fig. 1 the data will form a linear array if the heating experiment samples different mixtures of uniform spallation and trapped components. The slope of the plot is then the relative spallation yield $^{131c}Xe/^{126c}Xe$. The data in Fig. 1 define a line well within the error limits. If there were a depth variation in the ^{131c}Xe yield, the data would form two or more lines or scatter badly. Therefore, to a depth of 6.5 cm in rock 12002 and to the error limits of the

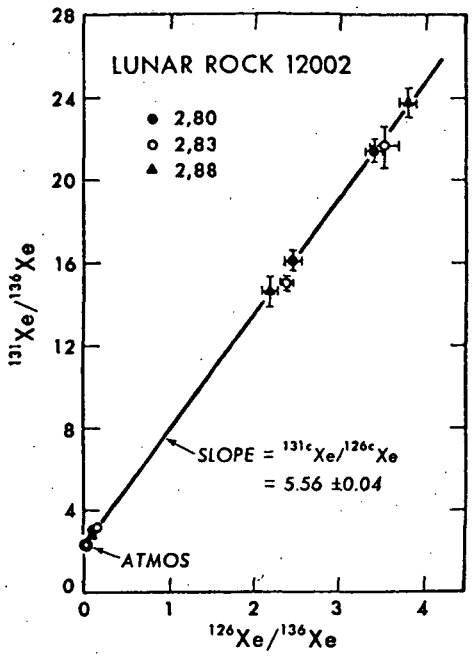

Fig. 1. Correlation of $^{131}Xe/^{136}Xe$ vs. $^{126}Xe/^{136}Xe$ for lunar rock 12002. Data have been corrected for spontaneous fission of ^{238}U in the manner described by ALEXANDER (1970). The line is the least-squares fit of the data using the method of YORK (1966). The regression line was forced through the atmospheric value. The well-defined line demonstrates the absence of a depth variation in the spallation yield of ^{131c}Xe relative to ^{126c}Xe.

Table 3. Relative spallation yields of xenon and krypton.*

Xenon isotopes	124	126	128	129	130	131	132	134	136
	56.3 ± 0.6	≡100	150.4 ± 0.9	121 ± 0.5	91.1 ± 0.6	556 ± 0.4	46 ± 4	7.0 ± 0.7	≡0.0
Krypton isotopes		78	80	82	83	84	86		
		21 ± 1	65 ± 2	≡100	134 ± 2	61 ± 3	≡0.0		

* The relative yields listed in this table are the slopes of the least-squares fits to data in Fig. 1 and in similar figures constructed for the other isotopes.

experiment (a few percent) there is *no* depth variation in the yield of ^{131c}Xe relative to the other spallation xenon isotopes.

Plots similar to Fig. 1 were constructed for all of the xenon and krypton (normalized to ^{86}Kr) isotopes. No evidence of depth variations were found in the relative yields of any xenon or krypton isotopes. Table 3 contains the relative spallation yields for xenon and krypton isotopes as calculated from the slopes of Fig. 1 and similar plots. Although there are no depth effects in the relative isotopic yields, apparent depth variations do exist in the concentration of spallation gases. Figure 2 is a plot of the relative concentrations of ^{130c}Xe, ^{83c}Kr, and ^{21c}Ne as a function of depth. Both

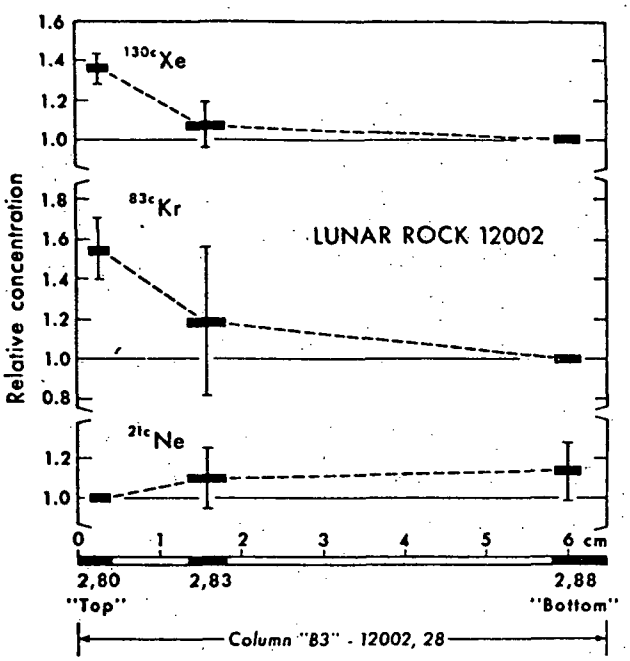

Fig. 2. Relative concentration of ^{130c}Xe, ^{83c}Kr, and ^{21c}Ne in column "B3" of lunar rock 12002. Shaded areas in the horizontal cm scale give the positions of the samples within column B3.

the ^{130c}Xe and the ^{83c}Kr decrease with depth. In contrast, the ^{21c}Ne appears to increase slightly with depth although it could be uniform within the experimental error.

Using the method described by HOHENBERG *et al.* (1970), which is based on the spallation xenon content of the Nuevo Laredo meteorite, and the Ba and REE concentrations of HUBBARD *et al.* (1971), we calculate a production rate of 7.0×10^{-14} cc ^{130c}Xe/gm/m.y. $\pm$ 30% in rock 12002. As the concentration of ^{130c}Xe varies with depth, the apparent "^{130c}Xe exposure age" also varies from 105 $\pm$ 32 m.y. at the top to 77 $\pm$ 25 m.y. at the bottom. Using a production rate of 0.12×10^{-8} cc ^{21c}Ne/gm/m.y. we calculate a "^{21c}Ne exposure age" of 161 $\pm$ 20 m.y.

DISCUSSION

The lack of a depth variation in the yield of ^{131c}Xe relative to the other xenon isotopes appears to argue against the specific suggestion of HOHENBERG *et al.* (1970) that the high ^{131c}Xe yield might be a surface effect. Mechanisms involving solar flare protons (ALBEE *et al.*, 1970; BOGARD *et al.*, 1971) also predict a strong surface effect in the ^{131c}Xe yield (as the range of solar flare protons is only a few mm) and are not supported by our results. Unfortunately, the irradiation history of 12002 is particularly unfavorable for observing surface effects.

The irradiation history of 12002 is complicated, and at least a three stage model is necessary to accommodate observations of other workers to the results of this work. The model can be summarized as follows:

Stage 1. A long irradiation under at least one meter (~350 to 400 gm/cm²) of regolith. This stage lasted at least on the order of 100 m.y. but could have been much longer if 12002 was buried deeper. The Gd isotope observation of ALBEE *et al.* (1971) that 12002 accumulated most of its neutron flux in a very shielded location necessitates this stage.

Stage 2. A shorter irradiation at a slightly shielded (0 to ~10 cm) depth for from 20 to 50 m.y. The tracks of the heavy cosmic rays (BHANDARI *et al.*, 1971 and ALBEE *et al.*, 1971) and the $^{3c}He/2^{3}H$ exposure ages of D'AMICO *et al.* (1971) document this stage. (The first and second stages could easily have occurred in the opposite order.)

Stage 3. A very short irradiation (compared to the total irradiation) on the actual lunar surface. BHANDARI *et al.* (1971) calculate ~2 m.y. for the length of Stage 3. D'AMICO *et al.* (1971) calculate 8.8 ± 6.5 m.y. and by combining the ^{3}H profile of D'AMICO *et al.* (1971) with the ^{3}He profile of MARTI and LUGMAIR (1971) we calculate ~2.6% of the total irradiation, or ~3 m.y., as the length of the surface irradiation. A short surface residence time is compatible with the observation of FINKEL *et al.* (1971) and others that 12002 did not tumble once it reached the surface.

Possible variations in the ^{131c}Xe yield due to surface irradiations may simply be masked by the longer irradiations at depth. The larger question of whether differences of shielding from galactic cosmic rays cause the variation in the ^{131c}Xe yield (EBERHARDT *et al.*, 1970 and MARTI and LUGMAIR, 1971) is not answered by the results from 12002. The scale of any energy effects from galactic cosmic rays is expected to be decimeters to meters and rock 12002 is too small to monitor such variations.

The ^{21c}Ne and ^{130c}Xe exposure ages of 161 ± 20 m.y. and 77 ± 25 to 105 ± 32 m.y. respectively can be compared to MARTI and LUGMAIR's (1971) Kr^{81}–Kr age of 94 ± 6 m.y. and to the $^{3c}He/2^{3}H$ ages of from 63 ± 5 to 144 ± 10 m.y. and the $^{38c}Ar/(^{37}Ar + {}^{39}Ar)$ ages of from 125 ± 15 to 155 ± 15 m.y. of D'AMICO *et al.* (1971). In view of the complex history of rock 12002, however, the "exposure ages" based on meteoritic production rates are of doubtful physical meaning.

The variations in the ^{130c}Xe and ^{83c}Kr concentrations in Fig. 2 might reflect variations in the abundances of the target trace elements within 12002 or they might be an artifact due to variations in the sensitivity of the spectrometer. However, it is possible that the concentration gradient is real and nontrivial, in which case it reflects the flux gradient in Stage 2 of the above model. Stage 3 is simply not long enough to establish concentration gradients as large as were observed. However, if the gradient were established in Stage 2, then rock 12002 had the same orientation in Stages 2 and 3. It is unlikely that a catastrophic event would have moved the rock without changing its orientation. Therefore, the model might be modified to a two stage model. Namely, a deeply buried Stage 1 followed by a catastrophic movement to a shallow burial under fine regolith in Stage 2. The covering regolith was then slowly, gently, and continuously removed over a span of tens of millions of years by the mechanism of GOLD (1971) or by some other method. Finally rock 12002 reached the surface some two to five m.y. ago.

It is unfortunate for the ^{131c}Xe anomaly question that rock 12002 has such a short surface residence time and complex history. Depth studies on future large lunar rocks will hopefully yield much less ambiguous results.

Acknowledgments—I wish to acknowledge Professor J. H. Reynolds for his many helpful suggestions and critical evaluation; P. K. Davis for his assistance in programming the data reduction, and Dr. W. A. Kaiser, R. L. Lewis, G. McCrory, M. Malin, and D. Overskei for their aid and suggestions. This work was supported in part by NASA and the AEC, it bears AEC Code No. UCB-34P32-78.

References

Albee A. L., Burnett D. S., Chodos A. A., Eugster O. J., Huneke J. C., Papanastassiou D. A., Podosek F. A., Russ G. P., II, Santz H. G., Tera F., and Wasserburg G. J. (1970) Ages, irradiation history, and chemical composition of lunar rocks from the Sea of Tranquillity. *Science* **167**, 463–466.

Albee A. L., Burnett D. S., Chodos A. A., Haines E. L., Huneke J. C., Papanastassiou D. A., Podosek F. A., Russ G. P., Tera F., and Wasserburg G. J. (1971) The irradiation history of lunar samples. Second Lunar Science Conference (unpublished proceedings).

Alexander E. C., Jr. (1970) Rare gases from a stepwise heating of lunar rock 12013. *Earth Planet. Sci. Lett.* **9**, 201–207.

Alexander E. C., Jr., Davis P. K., Kaiser W. A., Lewis R. S., and Reynolds J. H. (1971) Further rare gas studies in rock 12013. Second Lunar Science Conference (unpublished proceedings).

Bhandari N., Bhat S., Lal D., Rajagopalan G., Tamhane A. S., and Venkatavaradan V. S. (1971) Fossil track studies in lunar materials, I: High resolution time averaged (millions of years) data on chemical composition and energy spectrum of cosmic ray nuclei of $Z = 22$–28 at 1 A.U. Second Lunar Science Conference (unpublished proceedings).

Bogard D. D., Funkhouser J. G., Schaeffer O. A., and Zähringer J. (1971) Noble gas abundances in lunar material. Cosmic ray spallation products and radiation ages from the Sea of Tranquillity and the Ocean of Storms. *J. Geophys. Res.* **76**, 2757–2779.

D'Amico J., Defelice J., Fireman E. L., Jones C., and Spannagel G. (1971) Tritium and argon radioactivities and their depth variations in Apollo 12 samples. Second Lunar Science Conference (unpublished proceedings).

Eberhardt P., Geiss J., Graf H., Grögler N., Krähenbühl U., Schwaller H., Schwarzmüller J., and Stettler A. (1970) Correlation between rock type and irradiation history of Apollo 11 igneous rocks. *Earth Planet. Sci. Lett.* **10**, 67–72.

Finkel R. C., Arnold J. R., Reedy R. C., Fruchter J. S., Loosli H. H., Evans J. C., Shedlovsky J. P., Imamura M., and Delany A. C. (1971) Depth variation of cosmogenic nuclides in a lunar surface rock. Second Lunar Science Conference (unpublished proceedings).

Funkhouser J. G., Shaeffer O. A., Bogard D. D., and Zähringer J. (1970) Gas analysis of the lunar surface. *Science* **167**, 561–563.

Gold T. (1971) Evolution of mare surface. Second Lunar Science Conference (unpublished proceedings).

Hintenberger H., Weber H. W., Voshage H., Wänke H., Begeman F., and Wlotzka F. (1970) Concentrations and isotopic abundances of the rare gases, hydrogen and nitrogen in Apollo 11 lunar matter. *Proc. Apollo 11 Lunar Sci. Conf., Geochim. Cosmochim. Acta* Suppl. 1, Vol. 2, pp. 1269–1282. Pergamon.

Hohenberg C. M., Davis P. K., Kaiser W. A., Lewis R. S., and Reynolds J. H. (1970) Trapped and cosmogenic rare gases from stepwise heating of Apollo 11 samples. *Proc. Apollo 11 Lunar Sci. Conf., Geochim. Cosmochim. Acta* Suppl. 1, Vol. 2, pp. 1283–1309. Pergamon.

Hubbard N. J., Gast P. W., and Meyer C. (1971) The origin of the lunar soil based on REE, K, Rb, Ba, Sr, P, and $Sr^{87/86}$ data. Second Lunar Science Conference (unpublished proceedings).

MARTI K., LUGMAIR G. W., and UREY H. C. (1970) Solar wind gases, cosmic-ray spallation products and the irradiation history of Apollo 11 samples. *Proc. Apollo 11 Lunar Sci. Conf., Geochim. Cosmochim. Acta* Suppl. 1, Vol. 2, pp. 1357–1367. Pergamon.

MARTI K., and LUGMAIR G. W. (1971) Kr^{81}–Kr and K–Ar^{40} ages, cosmic-ray spallation products and neutron effects in Apollo 11 and Apollo 12 lunar samples. Second Lunar Science Conference (unpublished proceedings).

PEPIN R. O., NYQUIST L. E., PHINNEY D., and BLACK D. C. (1970) Rare gases in Apollo 11 Lunar Material. *Proc. Apollo 11 Lunar Sci. Conf., Geochim. Cosmochim. Acta* Suppl. 1, Vol. 2, pp. 1435–1454. Pergamon.

YORK D. (1966) Least-square fitting of a straight line. *Can. J. Phys.* 44, 1079.